Thermodynamic Modelling of Asphaltene Phase Equilibria using PC-SAFT Equation of State

by

Nurzhan Seitmaganbetov

2020

Thesis submitted to the School of Mining and Geosciences of Nazarbayev University in Partial Fulfillment of the Requirements for the Degree of
Master of Science in Petroleum Engineering

Nazarbayev University
April 2020

ACKNOWLEDGEMENTS

I want to express my deepest gratitude and heartfelt appreciation to my supervisor, Dr. Ali Shafiei, for his support, motivation, and efficient guidance throughout the process of researching and writing this thesis. I wish to express my sincere appreciation to my co-supervisor Dr. Nima Rezaei (Memorial University of Newfoundland, Canada) for his invaluable advice and comments and for providing useful scientific materials. This work would not have been possible without their persistent help and involvement.

I want to thank Dr. Peyman Pourafshary and Dr. Lei Wang for reviewing my thesis and for their constructive comments. Furthermore, I wish to pay my special regards to all of the members of the SMG faculty and staff for their constant willingness to help and for the knowledge given to me over the past two years in a variety of subjects. I sincerely appreciate the invaluable assistance that all of you provided during my study.

This work was part of the Collaborative Research Collaborative Research (CRP) grant entitled: “A comprehensive study on asphaltene characterization and screening asphaltene deposition inhibitors for Kazakhstan crude oils.” I wish to acknowledge the financial support I received from this grant.

I want to thank Nazarbayev University for the opportunity to pursue my Master's degree in Petroleum Engineering. For two years of study, the University provided me with all the conditions for productive work in a friendly and comfortable environment with access to various scientific resources and a well-equipped workspace. It was a privilege to gain knowledge and conduct my research within the walls of Nazarbayev University.

I also thank my fellow students and friends for their support and constant readiness to help. I enjoyed every day that I spent with you all during our incredible journey. And last but not least, I express my deepest gratitude and love to my dear mother for her moral support, constant patience, and unfailing faith in me throughout my years of study. Thank you all!

ORIGINALITY STATEMENT

I, Nurzhan Seitmaganbetov, hereby declare that this submission is my own work and to the best of my knowledge it contains no materials previously published or written by another person, or substantial proportions of material which have been accepted for the award of any other degree or diploma at Nazarbayev University or any other educational institution, except where due acknowledgement is made in the thesis.

Any contribution made to the research by others, with whom I have worked at NU or elsewhere is explicitly acknowledged in the thesis.

I also declare that the intellectual content of this thesis is the product of my own work, except to the extent that assistance from others in the project's design and conception or in style, presentation and linguistic expression is acknowledged.

Signed on 15.04.2020

_____

NOMENCLATURE

Acronyms and Abbreviations

A+R	=	Aromatics+Resins pseudo-component
AOP	=	Asphaltene Onset Pressure
API	=	American Petroleum Institute
ASTM	=	American Society for Testing and Materials
BIP	=	Binary interaction parameter
BP	=	Bubble-Point Pressure
CPA EoS	=	Cubic-plus-Association EoS
CPU	=	Central Processing Unit
DHSV	=	Downhole Safety Valve
EOR	=	Enhanced Oil Recovery
EoS	=	Equation of State
FVF	=	Formation Volume Factor
GOR	=	Gas-Oil Ratio
HPLC	=	High-Pressure Liquid Chromatography
LJ	=	Lennard-Jones
LLE	=	Liquid-Liquid Equilibrium
MAPE	=	Mean Absolute Percentage Error
MMP	=	Minimum Miscibility Pressure
MW	=	Molecular Weight
NIR	=	Near-Infrared Region
PC-SAFT	=	Perturbed-Chain Statistical Associating Fluid Theory
PNA	=	Polynuclear Aromatic Hydrocarbon
PR EoS	=	Peng-Robinson EoS
PVT	=	Pressure-Volume-Temperature

S+A+R	=	Saturates+Aromatics+Resins pseudo-component
SARA	=	Saturates-Aromatics-Resins-Asphaltenes
SCN	=	Single Carbon Number
SRK EoS	=	Soave modification of Redlich-Kwong EoS
STO	=	Stock-Tank Oil
VLE	=	Vapour-Liquid Equilibrium
VLLE	=	Vapour-Liquid-Liquid Equilibrium
VR-SAFT	=	Variable-Range Statistical Associating Fluid Theory

Symbols

K_c	=	Tuning parameter for viscosity modelling
N_{AV}	=	Avogadro number (=$6.022140857 \times 10^{23}$)
a^{assoc}	=	Part of residual Helmholtz energy per mole of molecules due to association [mol^{-1}]
a^{chain}	=	Part of residual Helmholtz energy per mole of molecules due to covalent chain formation [mol^{-1}]
a_o	=	Helmholtz energy per mole of segments [mol^{-1}]
a^{res}	=	Residual Helmholtz energy per mole of molecules [mol^{-1}]
a^{seg}	=	Part of residual Helmholtz energy per mole of molecules due to segment-segment interactions [mol^{-1}]
d	=	Temperature-dependent diameter of a segment in the chain [Å]
k_{BT}	=	Boltzmann constant ($= 1.381 \times 10^{-23}$ J/K)
m	=	Number of segments in chain
P	=	Pressure [psi or Pa]
R	=	Universal gas constant ($= 8.314$ J × $K^{-1}mol^{-1}$)
T	=	Temperature [°F or °K]
T_R	=	Reduced temperature (=$k_{BT}T/\epsilon$)
X	=	Molar fraction [mol/mol]
Z	=	Compressibility factor [vol/vol]

K	=	Equilibrium constant [fraction]
Nc	=	Total number of components in mixture

Greek letters

η_a, η_r	=	Scaling parameters of viscosity model [μP]
σ	=	Temperature-independent diameter of segments [Å]
φ	=	Fugacity coefficient
γ	=	Tuning aromaticity parameter for A+R pseudo-component tuning
λ	=	Tuning parameter for S+A+R parameter tuning (similar to γ)
β	=	Molar amount fraction [mol/mol]
η	=	Reduced density (=$\frac{\pi}{6}\ N_{AV} d^3 m$)
μ	=	Dynamic viscosity [cP or μP]
ρ	=	Number density of molecules [$Å^{-3}$]
ϵ	=	Well depth of a potential (dispersion energy) [J]

ABSTRACT

Asphaltenes are the heaviest fraction of crude oil that has the potential to cause significant flow assurance and safety risks. The assessment of the tendency of asphaltenes to precipitate can allow early life planning of suitable prevention measures. The thermodynamic modelling of multiphase equilibrium is a viable and cheap tool for understanding crude oils phase behavior under the changing production conditions. The Perturbed-Chain Statistical Associating Fluid Theory (PC-SAFT) Equation of State is one of the most widespread choices for the modelling of asphaltene phase behavior that present in the literature. One of the drawbacks of thermodynamic models is that performing complex modelling of phase equilibria can require experimental data that is not available and can be computationally challenging. This work aims to modify the existing methodologies to reduce the number of necessary experimental data and to achieve superior computational efficiency. Additionally, the ability of PC-SAFT EoS to predict density and viscosity of crude oil was evaluated. The work uses functions and scripts for equilibrium calculations written in MATLAB software in order to perform thermodynamic modelling. Two methods were applied for the asphaltene equilibria modelling, namely "SARA-based" method (from the literature) and the modified "SARA-based" method, that is suggested by this work. Three crude oils were selected for the asphaltene modelling and one for density and viscosity modelling. The results of modelling by both methods showed that PC-SAFT EoS could accurately model asphaltene onset pressures at higher temperatures but deviate from experimental data at lower temperatures. The modified method was able to reproduce the results of "SARA-based" method and showed the increase in computational efficiency of the modelling and in crude oil characterization procedure. The modified method requires less amount of experimental data to perform the modelling and can be used as a viable alternative when full SARA analysis is not available. P-T diagrams and contour maps of asphaltene precipitation were constructed for crude oils. A good match was achieved between predicted and experimental crude oil density and dynamic viscosity values below and above the bubble point pressure. Additionally, the ability of PC-SAFT EoS to calculate a number of PVT parameters was demonstrated.

TABLE OF CONTENTS

LIST OF FIGURES

LIST OF TABLES

1 INTRODUCTION

This chapter includes a statement of the problem of the thesis, presents the objectives of the work, indicates its relevance to the industry and briefly describes methodology adapted to achieve stated goals. The last section contains information about the thesis structure and a brief description of the content of each chapter.

1.1 Statement of the problem

Asphaltene fraction is the heaviest, polar and complex part of crude oil. It is defined in terms of solubility and does not have specific molecular structure or weight [1]. The asphaltene precipitation and the consequent deposition is the serious flow assurance problem that can put under the risk entire viability of the project and cause severe financial and safety damage. Asphaltene deposits can cause damage to:

- Reservoir rock – blockage of pores and permeability reduction, need for the near-wellbore area stimulation.
- Well tubing, manifolds, separators, gathering and transportation pipelines – partial (decrease in the effective diameter of a pipe) or complete blockage of tubing. Need for the remedial actions (toluene/xylene wash, thermal methods, and mechanical methods).
- Downhole and surface equipment – DHSVs, blowout preventers, separators, logging equipment, pumps, and gauges. Need for the equipment repair.

It was shown in the literature that the low asphaltene concentration is no guarantee of the absence of such problems [2]. Because of the severity of the asphaltene deposition damage, it is highly essential to have a tool for early risk assessment of such a problem. The assessment of asphaltene deposition risks can allow early life planning of suitable production conditions, selection of the proper equipment and the development of adequate remedial procedures. The precipitation of the dense asphaltene-rich phase is the necessary condition for the consequent deposition of asphaltenes on the surface of pipes or in pores of the reservoir rock. The alteration of temperature, pressure and oil composition can trigger the process. These properties are always changing during the life of a field.

1.2 Relevance to the industry

Remedial actions are of high cost itself, and financial damage is worsened by the increased non-producing time and lost production. Sometimes, remedial actions are not practical and should be repeated with unreasonably high frequency [3]. Acid stimulation, in particular, can worsen the situation by enhancing the precipitation of heavy asphaltene fraction [4].

It is usually not economically feasible to regularly conduct costly high pressure-high temperature experiments and fluid samplings. The thermodynamic model of multiphase equilibrium is an excellent tool for understanding reservoir fluid phase behaviour under the changing production conditions, including the assessment of the probability of the asphaltene problem appearance throughout the life of a field [5].

PC-SAFT EoS is the engineering tool that throughout almost 20 years of usage shown the ability to accurately model phase behaviour of complex crude oil systems, especially the modelling of asphaltene precipitation [5]. For the modelling of bubble-point, vapor-liquid flash, viscosity, and liquid density the compositional analysis of STO and flashed gas, GOR and a few experimental points is enough to give results with reasonable accuracy [6]. For the modelling of asphaltene precipitation, additionally, SARA analysis and several points of AOPs are required [7].

1.3 Aims and objectives

The work aims to to modify the PC-SAFT modelling method to achieve improved computational efficiency and reduce the number of experimental data that is required. Specific objectives of this work include:

- To evaluate the ability of PC-SAFT EoS in the modelling of behavior of complex heterogeneous systems of crude oils with asphaltene precipitation tendencies by evaluating the MAPE between modelled and experimental data of AOPs and BPs of crude oil.
- To modify the asphaltene modelling methodology and check its modelling capabilities in comparison with the “SARA-based” method.
- To evaluate the computational efficiency of the modified method by calculating the percentage decrease of CPU time in comparison with the old method.

- To evaluate the ability of PC-SAFT EoS to perform predictions of density and viscosity of crude oil by evaluating the MAPE between model predictions and experimental data of respective parameters.

1.4 Research methodology

The aims of the research are achieved by firstly characterizing crude oil data by the PC-SAFT characterization methodologies from the literature ("SARA-based" method) and then introduce the modification to simplify the procedure. The scripts and formulas were written in the MATLAB R2019b software in order to perform multiphase equilibrium calculations, automize the PC-SAFT model tuning processes and predict the PVT parameters of the crude oil of interest. Using MATLAB scripts, the P-T phase diagram of crude oil was constructed, and PVT parameters that were evaluated include liquid densities, formation volume factors of gas and oil and liberated gas compositions.

1.5 Thesis organization

The thesis is organized in the five chapters. Chapter 1 includes the problem statement, relevance to industry, objectives and methodology of the research work. A brief description of the thesis structure is given. Chapter 2 consist of a literature review of asphaltene fraction properties and phase behaviour, flow assurance problems associated with asphaltenes, as well as the thermodynamic modelling of asphaltene precipitation. The chapter gives a background of PC-SAFT EoS and reviews its past usages in the asphaltene modelling. Chapter 3 describes the methodology of the present work. It consists of the description of PC-SAFT crude oil characterization methods, the assumptions of a model, necessary experimental data list, as well as MATLAB equilibrium calculation algorithms. Chapter 4 presents the results and discussions. Several graphs and tables are presented to demonstrate the results of the constructed models. Chapter 5 is dedicated to the conclusions and recommendations for future research.

2 LITERATURE REVIEW

This chapter presents the literature review of the asphaltene fraction thermodynamic modeling. The first section gives an overview of the asphaltene fractions, its parameters, as well as its relations to other crude oil fractions. The second section contains information about the phase behavior of asphaltene-crude oil systems and factors affecting their stability. The third section gives insights about the flow assurance problems that asphaltene precipitation can cause. The fourth section is about the methods of thermodynamic modeling and the background of SAFT EoS. Finally, the fifth section contains the background of PC-SAFT EoS and the review of its usage in the asphaltene precipitation modeling.

2.1 Introduction to Asphaltenes

Asphaltenes are the heaviest parts of crude oil that remain as solid residua during the common distillation process of crude oil refining. They don't boil as other fractions of crude and instead leave foamed and swelled solid at the bottom of a distillation column. They are the complex and most polarizable fraction of crude oil and don't have a certain melting point [1]. The point, at which asphaltenes will start to precipitate from crude oil is commonly referred to as the AOP.

The asphaltene fraction is usually defined as the solubility class. That is, asphaltenes cannot be defined by a particular compound or distinct chemical formula. The general definition is that they are fraction of crude oil that will not dissolve in light normal alkanes (such as heptane or pentane) but are soluble in aromatic hydrocarbons (such as toluene, benzene or xylene). Figure 2 shows the simplified model of crude oil fractionation.

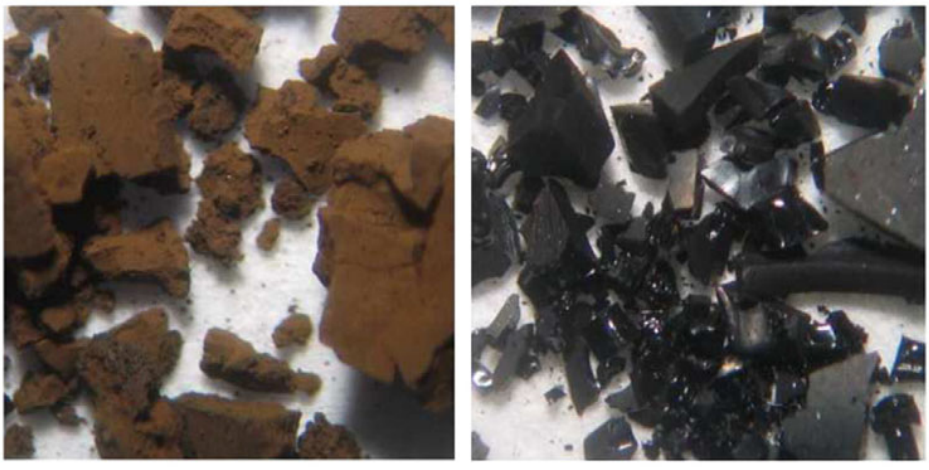

Figure 1 - Asphaltenes extracted using two different precipitants [8].

Such broad definition that covers a wide spectrum of hydrocarbon and non-hydrocarbon compounds results the uncertainty and disputes in the determination of various parameters, such as molecular weight, elemental composition, molecular structure, phase behavior etc. Because asphaltenes are the solubility class, they are polydisperse by definition and contain a variety of molecules (hydrocarbons and impurities) which concentrations vary depending on specific crude and a method of investigation [5].

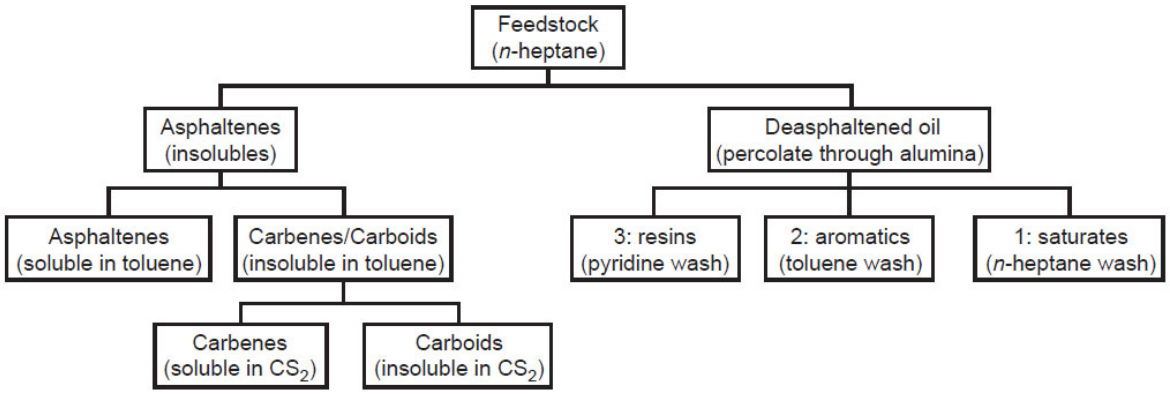

Figure 2 - Simplified petroleum fractionation model [1].

The most common method of separation of asphaltenes from crude oil in laboratories is called SARA. As the name implies, crude oil is fractionated into four different fractions. Asphaltene fraction is separated according to the IP-143 standard [9], using titration by normal alkane at a dilution ratio of 40:1 (40 cm^3 of alkane per 1 g of oil). Remaining fractions (commonly called maltene fraction) separated from the supernatant using HPLC.

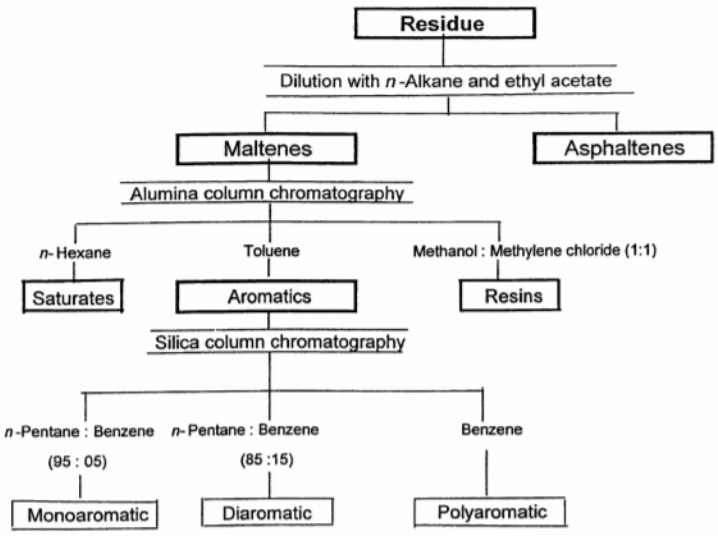

Figure 3 - SARA separation scheme [10]

Several authors investigated the effect of a type and amount of precipitant to the asphaltene yield. Fahim et al. [11] in their experiments on Kuwait crude used four different materials (*n*-alkanes) at different temperatures. Results demonstrate that the highest precipitation amount is achieved by the usage of the lightest solvent *n*-hexane. Figure 4 and Figure 5 show the results of the solvent type effect with a constant and varying dilution (solvent-to-crude) ratio.

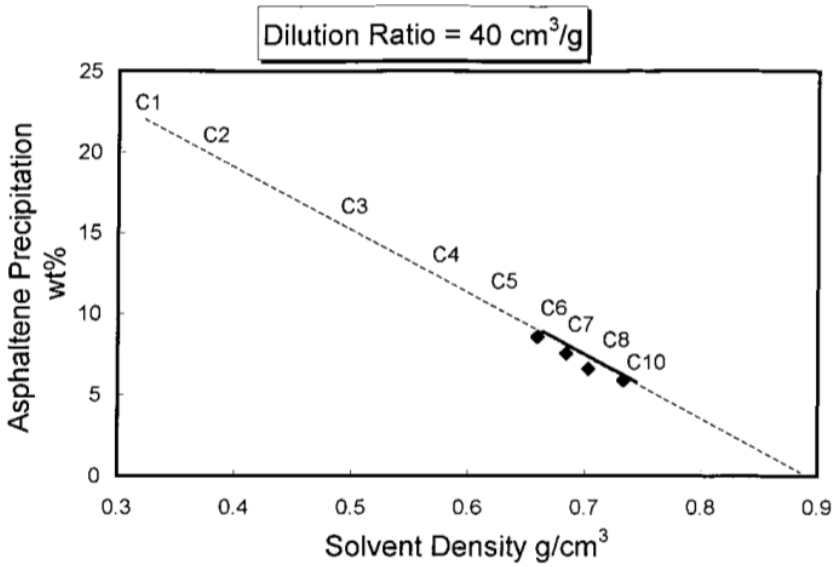

Figure 4 - Effect of solvent at the constant dilution ratio [11].

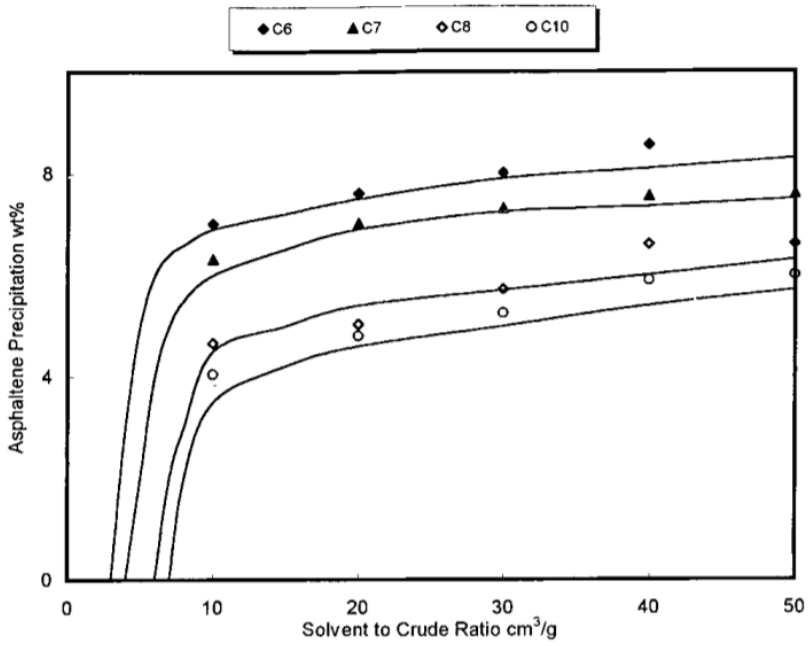

Figure 5 - Effect of solvent type with varying dilution ratio [11].

Furthermore, the type of solvent also has an influence on the size of asphaltene particles. Experimental results by Leontaritis et al. [12] using Waters gel permeation chromatogram shows the distribution of molecular weights of asphaltene particles as a function of *n*-alkane used. The authors tested two different crudes (with API gravity of 21.13 and 30.21). For both of them, the heavier solvent is used, the more of the larger particles in precipitated asphaltenes was observed [13].

2.1.1 Molecular weight

Molecular weight is by far the most dubious parameter and the subject of ongoing discussions. The assessment of asphaltene molecular weight is challenging because they are prone to aggregation, thus resulting in higher weights [11]. Moreover, it was shown that asphaltenes form small clusters, nanoaggregates, even at low concentrations and in the solution with good asphaltene solvents – about 100 mg/L of nanoaggregates was observed in the solution of toluene at 25ºC [14]. The structures, similar to nanoaggregates (named "nanocolloids") was also observed in reservoir crude at about 100ºC [15]. Furthermore, in the case of improperly selected dilution ratio or the type of precipitant, the joint asphaltene-resin precipitation is always a possibility.

All of the above-mentioned factors can lead to scattering of results in the range from 800 g/mol to 11000 g/mol [16] or higher. Speight [1] mentions that the molecular weight of asphaltenes that are precipitated using highly polar solvents is generally in the range of 1500-2500 g/mol.

Barrera et al. [17] have done experiments to determine molecular weight and density variations from 4 crudes – 3 Canadian bitumen samples and one Arabian medium crude. The molecular weight measurements were performed using the vapour pressure osmometer with reported measurement repeatability of ±15% for all samples [17]. The results showed that for 60 kg/m^3 (at 50°C) toluene, the molecular weight of asphaltene fraction ranges from 4000 g/mol to 11000 g/mol.

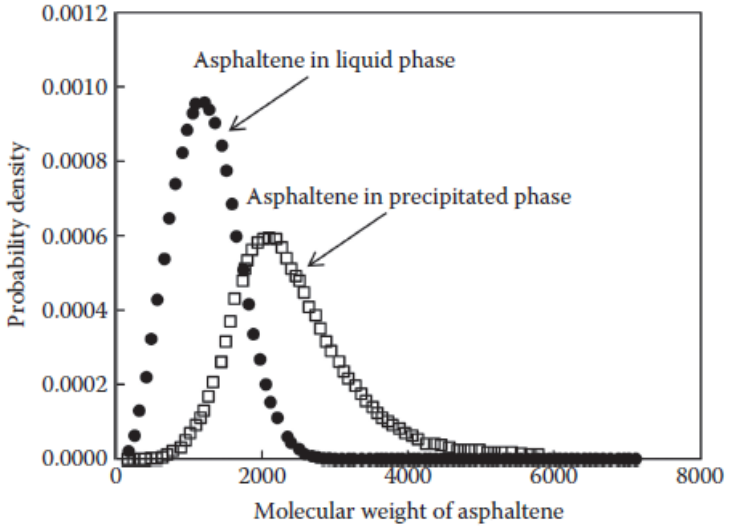

Figure 6 - Typical distribution of asphaltene molecular weight in liquid phase and in the precipitated state [5].

2.1.2 Elemental composition

Speight [1] mentions that the composition of asphaltenes which were extracted using more than 40 volumes of *n*-pentane usually shows the little variance in H/C ratios, about 1.5 – 0.5. On the other hand, concentrations of impurities vary more substantially. Oxygen and sulfur vary in the range of 0.3-4.9 % and 0.3-10.3 % respectively. Nitrogen demonstrated smaller scattering with 0.6-3.3 %. Asphaltenes contain also several types of metals, such as nickel, iron, and vanadium [1]. Oliveira et al. [2] performed characterization of asphaltenes by extracting them through propane addition. Experiments were conducted to 12.7 API degree Brazilian crude. The authors used different oil/propane ratios (1:1.9, 1:4, 1:6, 1:10) to separate crude into solid and liquid phases. Both of these phases were further divided into SARA components. Precipitated solids were considered as asphaltenes and separated from the solution using filter membranes and Soxhlet apparatus. The SARA analysis of solid and liquid phases indicated that asphaltenes are present in both of them. It means that even at high propane ratios, some asphaltenes haven't precipitated. At 1:1.9 ratio analysis shows 0.3 wt% of asphaltene fraction in the liquid phase. This value goes up to 0.5 at the lowest (1/10) ratio case.

Compositional analysis of the asphaltenes was performed by combustion and chromatography using a CHNS analyzer. The results showed 2.1 % of Nitrogen, 1.2 % of Sulfur and 1.18 H/C ratio. Another elemental characterization was performed by the same authors, this time on Arabian crude using the same tools. The separation was carried out by standard IP-143 procedure. Results showed 1.4 % of N, 7.9 % of S, and 1.0905 H/C ratio. Oxygen concentration was estimated by mass difference as 0.7 %.

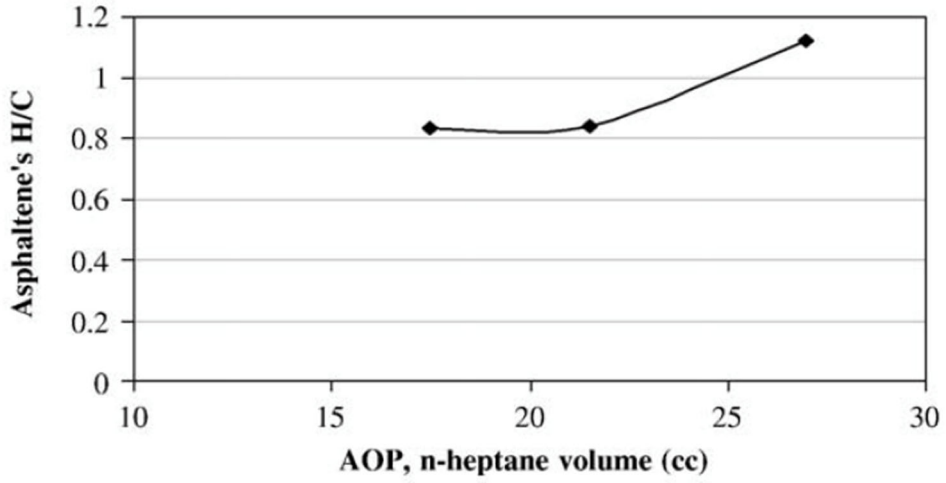

Figure 7 - The relationship between asphaltene onset point and H/C ratio [18].

Fahim et al. [11] also performed an elemental analysis of precipitated asphaltenes from Kuwait crude. The results show the C and H content as 79.65 % and 8.31 % respectively. Impurities have the values as follows – N (0.768 %), O (3.79 %) and S (7.48 %). All shown values for elemental composition from three experiments lay in ranges mentioned by Speight [1].

2.1.3 Molecular Structure

There are several models that were developed in order to describe the structure of asphaltenes. They fall into two main groups, namely “archipelago” and “island” (also known as “continental”) structures [2] (Figure 8). Archipelago structure considers the core of a molecule consisting of aromatic rings bounded by aliphatic chains and stabilized by the aliphatic chains at the shell. The chains have a length from 5 to 7 carbon atoms in length [19]. Island model considers the core of a molecule to consist of aromatic rings (usually 6-7 rings) only [2]. One of the most accepted models of asphaltene molecular structure is the Yen-Mullins model (Figure 9) which falls in the group of “island” models [20]. Asphaltene molecule is considered as one large poly-aromatic hydrocarbon (PNA) surrounded by aliphatic chains. The advantage of this model is that it clearly demonstrates the sequence of the formation of asphaltene clusters.

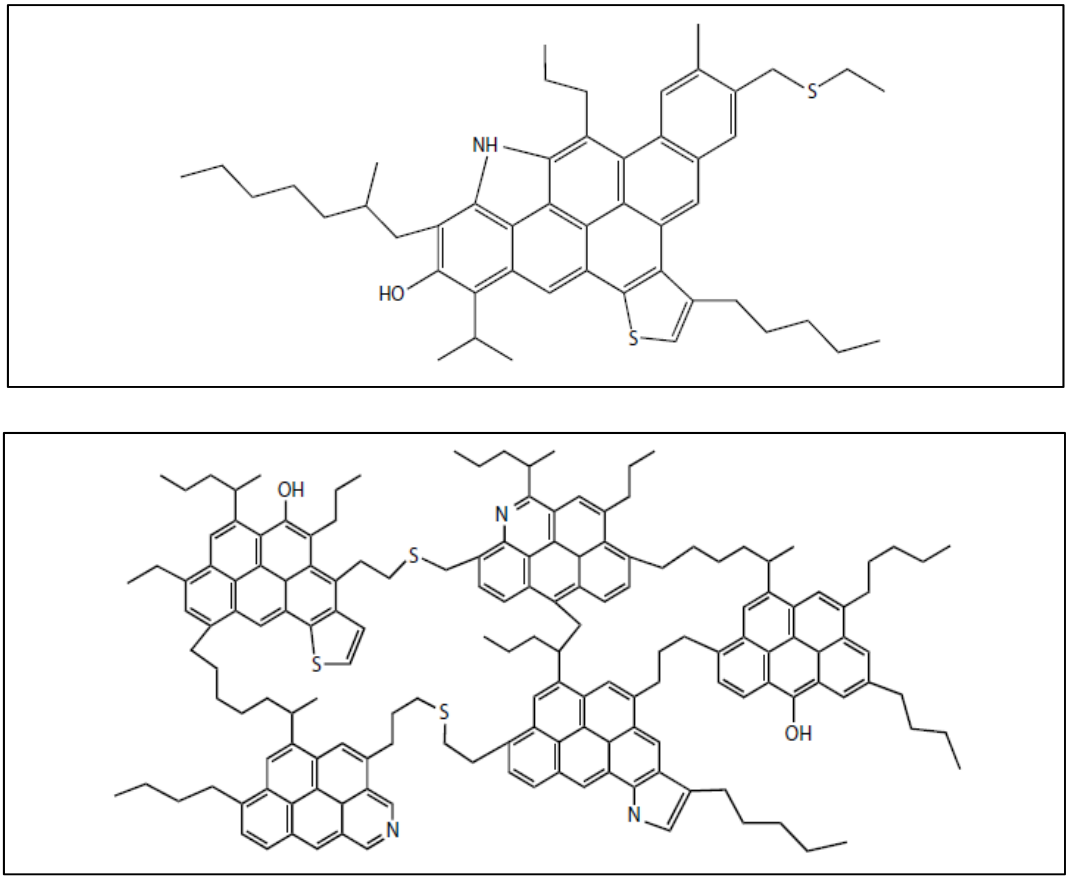

Figure 8 - Typical structure of the island (at the top) and the archipelago model (at the bottom) [2]

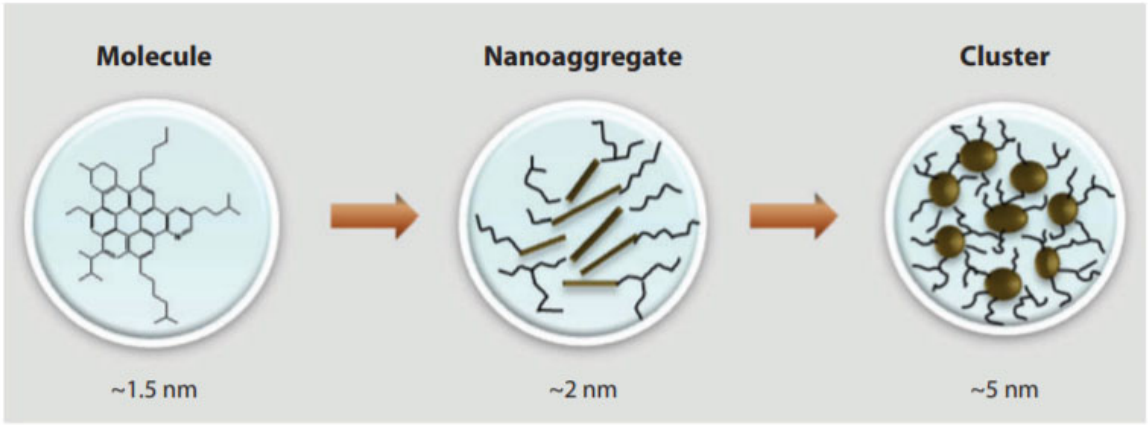

Figure 9 - The modified Yen (Yen-Mullins) model. Asphaltene molecules (PNA) form nanoaggregates surrounded by aliphatic chains. Nanoaggregates then form the larger clusters [21]

2.1.4 Asphaltenes and Resins

Resins are, in contrast to asphaltenes, soluble in n-pentane and n-heptane, but, similarly with asphaltenes, insoluble in liquid-state propane [1]. They are considered as “relatives” to asphaltenes, with lesser weight, polarity and longer aliphatic chains attached to aromatic rings compared to heavier asphaltenes [22].

There are several works that mention the role of resins in asphaltene aggregation. In the frame of the colloidal theory of thermodynamic modeling of asphaltene precipitation, resins are believed to be beneficial to the stability of asphaltene fraction in crude oil [23]. Leontaritis et al. [12] define resins as compounds that act as peptizing agents and help to prevent precipitation of asphaltenes by preserving them in suspension. Layers of resins around the asphaltene core will act as stabilizers, by repulsion of other resin molecules in other aggregates and overcoming attraction forces between asphaltene molecules.

In contrast to that view, Mullins et al. [15] presented the experimental analysis of downhole medium crude oil samples using a visible NIR spectrometer. As was mentioned before, asphaltene nanoaggregates were found in that samples (which contain resins), which are identical to ones found in the solution of toluene (without resins). Asphaltene nanoaggregates have demonstrated no growth after initial formation, and the increase of asphaltene concentration only elevated the number of nanoaggregates, but not their size. Authors conclude that the concept of resins as natural surfactants to asphaltenes is probably fallacious. The nano-filtration experiment results on Athabasca bitumen and Maya crude also showed that asphaltenes do not manifest associative behavior with other SARA components, including resins [24].

As can be seen, the number of precipitated asphaltenes, as well as their composition and physical properties substantially vary depending on the individual properties of the crude tested, pressure and temperature conditions of experiments and the method of experiments itself. Because of this, it is highly important to treat every field individually. Otherwise, the assessment of asphaltene precipitation risks and the selection of preventing/removal methods can be inaccurate and misleading.

2.2 Phase Behavior of Asphaltene Fraction

For the purpose of precipitation modeling, it is crucial to clearly understand the phase behavior of asphaltene fraction at changing PVT conditions. Precipitation of the asphaltene-rich phase is the primary requirement for consequent deposition and the appearance of asphaltene-related problems. Generally, the factors that affect the stability of the asphaltene phase in crude oil systems are the change in temperature, pressure and oil composition.

2.2.1 Pressure-temperature effect

The pressure dependency of the asphaltene concentration is demonstrated in Figure 10. At the starting point of a production system, crude oil is in the reservoir at almost isothermal

conditions. The asphaltene fraction is stable at high pressures and starts to precipitate at certain pressure above bubble point known as the *upper AOP.* The phase amount of the asphaltene-rich phase will increase and finally will reach its maximum at the bubble-point pressure.

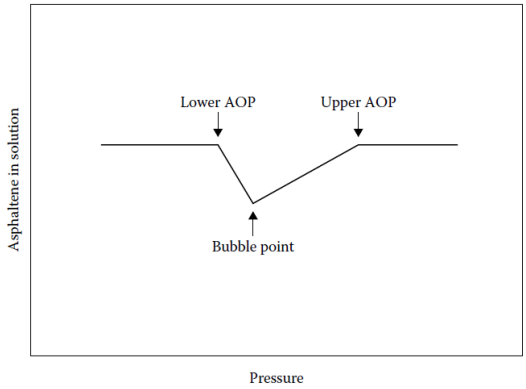

Figure 10 - Schematic of the pressure dependency of the asphaltene concentration in crude oil [16]

At the bubble point, the first bubble of gas will liberate from crude. This means that the composition of crude now is also a variable. Since the liberating gas components (such as N_2, CO_2, and light alkanes) are the poor solvents for asphaltenes, the stability of an asphaltene-crude system rises [25]. The phase amount of asphaltene fraction reduces with a pressure decline. Pressure will eventually reach the *lower AOP* and all asphaltenes will be reintegrated into the crude. In Figure 11 can be seen the effect of temperature at the laboratory experiments of asphaltene precipitation [11]. Figure 12 demonstrates P-T diagram of asphaltene phase behavior modelled by PC-SAFT EoS [5].

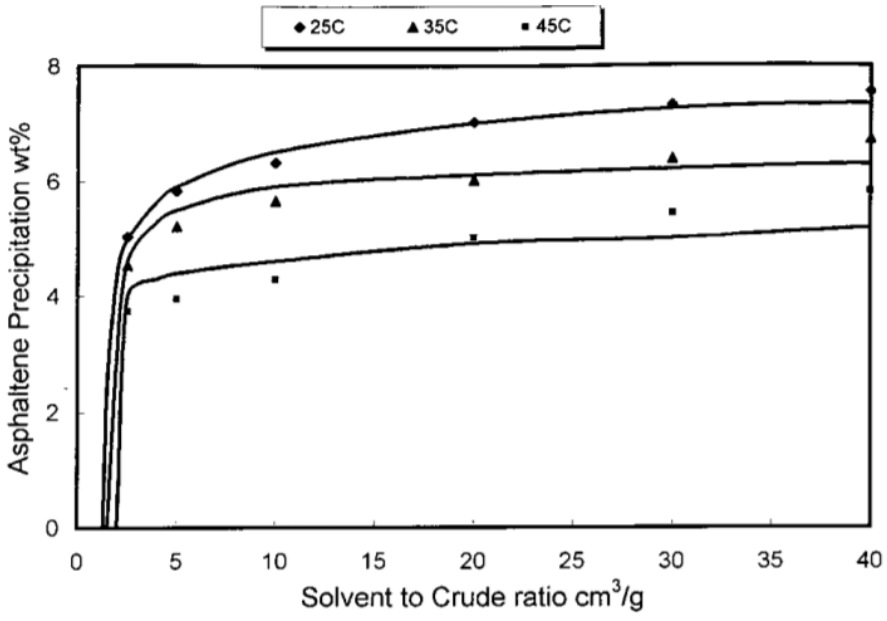

Figure 11 - Results of asphaltene precipitation experiments at different temperatures [11].

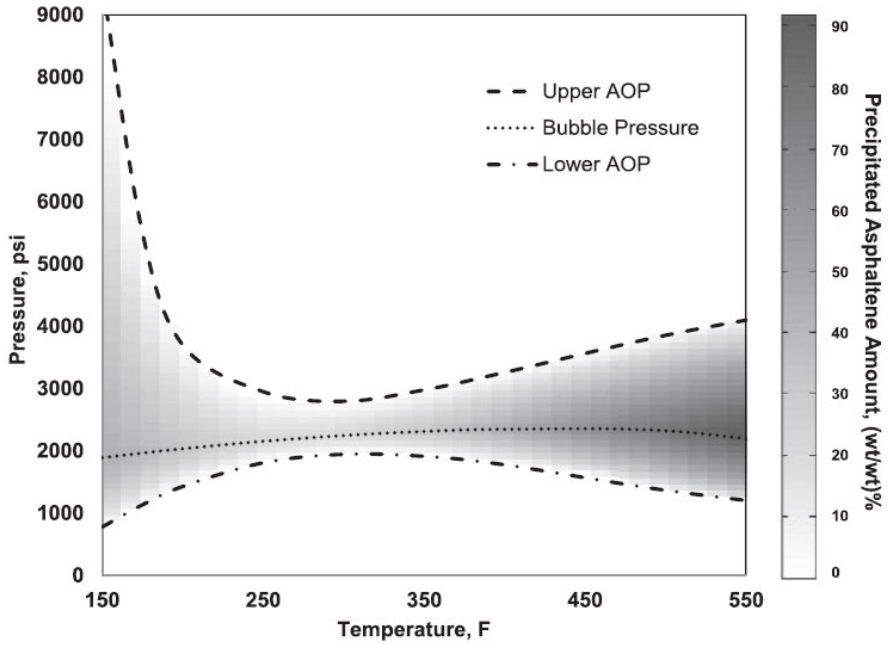

Figure 12 - P-T diagram of asphaltene precipitation modeled by PC-SAFT EoS [26].

2.2.2 Alteration by miscible gas injection EOR

Asphaltene related problems were reported when crude oil composition was altered as a consequence of miscible gas injection EOR [27] [28] since most of the injected gas types (ex. carbon dioxide, natural gas etc.) are bad solvents for asphaltene fraction and can cause a risk of enhancing the precipitation [29]. Particularly, Thomas et al. [3] reported major problems during miscible flooding in Alberta, Canada. The state of the production in some wells required to treat them with solvents every 16 hours to keep them producing. Jamaluddin et al. [30] conducted light transmittance experiments at reservoir fluid under the injection of different concentrations of nitrogen. The results can be seen in Figure 13. The asphaltene onset pressure (here - OAP) almost tripled its value at the maximum (20 mole %) injected concentration. The negative effect of CO_2 and rich gas injections were also noted during a number of laboratory experiments under both standard and reservoir conditions [31] [32] [33].

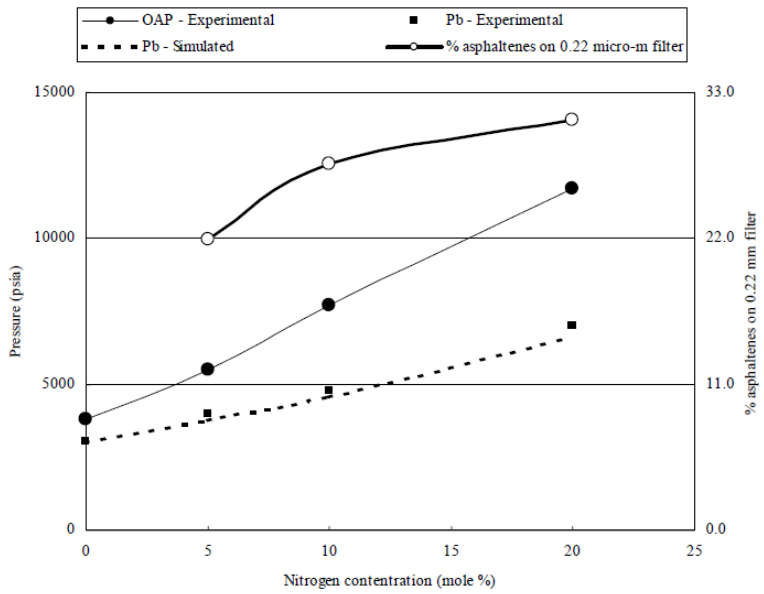

Figure 13 - The effect of nitrogen injection [30]

Particularly, Soroush et al. [34] studied the effect of both miscible and immiscible CO_2 flooding on the permeability reduction. The authors used crude oil samples from southern Iran oilfield and conducted core flood experiments at the reservoir conditions. Results show that asphaltene concentration is higher during immiscible CO_2 flooding case since crude oil composition is not altered by the injected gas. At the pressures near the MMP the asphaltene content in produced oil has drastically declined, meaning the increased amount of precipitated asphaltene fraction. The results are demonstrated in Figure 14.

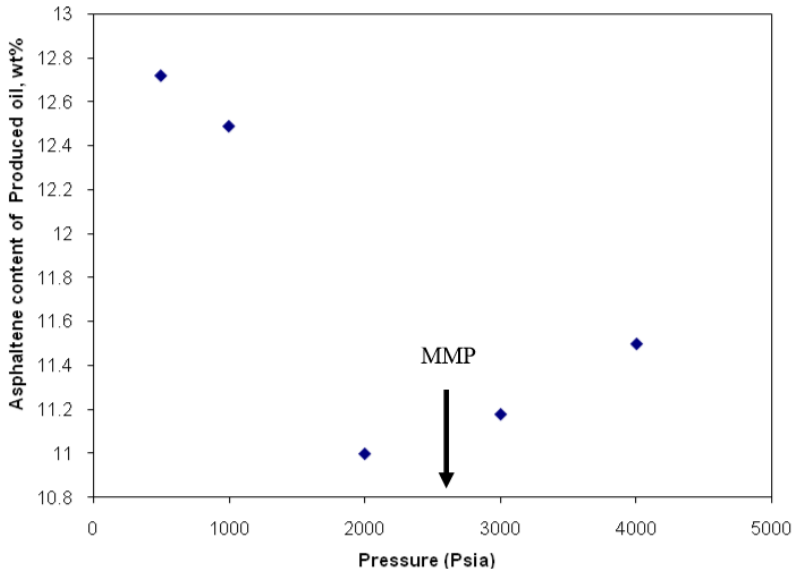

Figure 14 - Asphaltene content in the produced oil after CO_2 injection [34].

2.2.3 Asphaltene concentration

The low concentration of asphaltenes itself is not a guarantee of the absence of flow assurance problems. The crude with asphaltene concentration as high as 17-20 wt% has shown no problems at all [2], but it is constantly reported in the literature that crudes with lower concentrations (0.15 – 4 wt%) demonstrated tendency to precipitate [35] [36] [30] [37] [7]. For example, Hassi Messaoud Field in Algeria [38] faced asphaltene plugging problems since the first day of productions, despite having only 0.06 wt% of asphaltene fraction concentration [5].

2.2.4 Paraffin concentration

High paraffin content can cause spontaneous flocculation and aggregation [39]. Aromatics, natural solvents for asphaltenes, are denser than paraffins (poor solvents). Because of this, generally, lighter crudes (with high alkane content) are more inclined to have asphaltene precipitation than heavier (with more aromatic content) crudes [16].

Yanes et al. [40] in their work evaluated the effect of long-chained paraffin on asphaltene precipitation. They used three Brazilian crudes and asphaltene precipitation was induced by the addition of n-heptane. Crudes were characterized and asphaltene/paraffin content was evaluated prior to the experiments.

Experiments include the addition of two commercial paraffin – *n*-hexadecane (melting point 18°C) and docosane (melting point 42-45°C) and paraffin pool (ASTM-D87, melting point 53-57°C) into crude oil at different concentrations (2,4,10 wt%) [40]. Then, the solution was mixed and homogenized.

The results (in Figure 15) showed the decrease of asphaltene onset point (in terms of wt% of n-C_7 necessary to induce precipitation) with an increase of paraffin content added. The magnitude of change in asphaltene onset were found to be almost similar in the case of lighter *n*-hexadecane and heavier, more long-chained paraffin pool. Authors describe this by the similarities in solubility parameters of paraffin used [40].

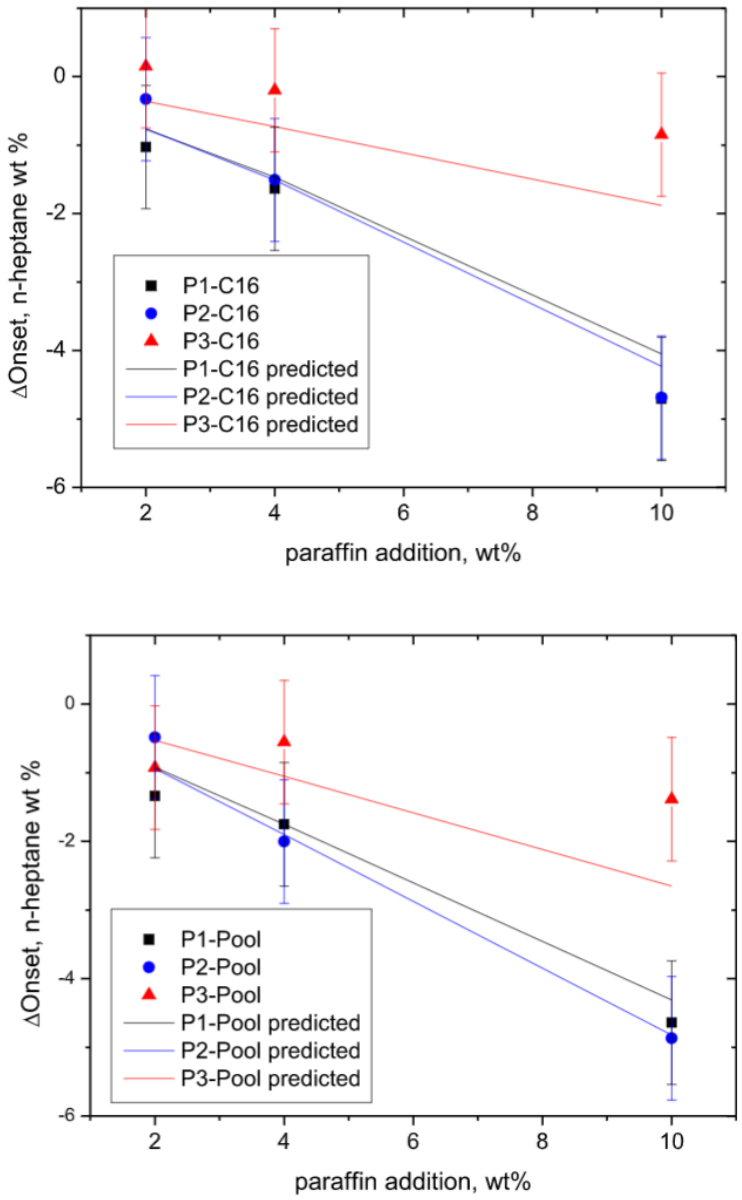

Figure 15 - Effect of the addition of C16 and paraffin pool to the onset point of asphaltene precipitation [40]

2.3 Asphaltene related flow assurance problems

Asphaltene deposition is the well-known source of flow assurance risks and problems in the reservoir rock, production wells, surface facilities and production lines [4]. As was described, change in pressure, temperature, composition and production rate can trigger the process. Such kind of problems can take place in various types of conditions and all over the globe [5]. As was mentioned before, even crudes with little asphaltene content are subject to severe depositional damage. This damage is due to:

- Production decline (or cease) and related financial losses (blockage of rock pores by deposits and reduced permeability in near wellbore area, reduced effective diameter of

pipes and tubings, complete plugging of well tubings, chokes, separators, gathering and transportation pipelines etc.)

- Financial losses due to the need for remedial operations (xylene/toluene wash, mechanical removal, thermal methods etc.) These losses are both for the cost of operations and for the lost production cause of the non-producing time.
- Equipment damage and related safety risks/financial losses (plugging of safety valves, X-mass trees, pump failures, logging tool damage etc.)

Leontaritis et al. [28] summarize the experiences from the number of fields, such as of the Prinos field in Nothern Aegean Sea, where the asphaltene deposition occurred from the early days in both tubing and surface equipment, causing the risk to the economic viability of the project. Creek [41] states that the remediation of asphaltene flow assurance problems can cost from 0.5MM USD to 3MM USD and financial losses due to the lost production can reach up to 1.2MM USD per day. This section will give insights about asphaltene caused damage in reservoir, tubings and surface facilities.

2.3.1 Reservoir damage

Asphaltenes were recorded to substantially reduce the permeability of reservoir rocks by blocking pores. Water to oil-wet wettability change is also claimed as one of the mechanisms of damage, as well as the increase in viscosity of fluids by the creation of emulsions.

Wettability change effects were described by Kaminsky et al. [42] that conducted experiments using low-solubility asphaltenes. Authors report that asphaltenes rupture the water firm at the surface of the reservoir rock within a few hours. However, the destruction of the firm is not enough condition to alter wettability. Following direct deposition of asphaltene material and formation of the multilayered firm is the requirement for drastic irreversible wettability change from strongly water wet to strongly oil-wet.

Piro et al. [43] through static and dynamic experiments studied the effect of asphaltene adsorption in the reservoir rock. Authors claim that adsorption phenomena may contribute to formation of damage caused by asphaltenes. Experiments were conducted using crude and dolomite core sample from Northern Italy field that was experiencing severe asphaltene-caused formation damage. Asphaltene separation was conducted according to IP-143 standard.

Results of this work showed that during dynamic flow condition asphaltene concentration was unable to reach saturation conditions (a condition in which inlet concentration of asphaltene equals outlet concentration) even after 30-35 hours of core

flooding. Authors conclude that dynamic asphaltene adsorption is a continuous process and amount of asphaltene remaining increases with the time of flow [43].

Shedid et al. [44] performed a dynamic flow test to measure formation damage by simultaneous asphaltene and sulfur deposition. They have used four core samples from the Satah oilfield in UAE with different permeabilities at a constant flow rate. Asphaltene and sulfur concentrations are 0.81 wt% and 1.13 wt% respectively. The results presented in the Table 1 below. KFD stands for permeability damage factor and equals the difference between initial and final permeabilities divided into initial permeability.

Table 1 - Permeability reduction caused by asphaltene-sulfur deposition [44]

Vp (cm^3)	Porosity (%)	Initial oil permeability (mD)	Final oil permeability (mD)	KFD (%)
8.89	14.19	2.11	1.31	37.91
8.74	19.14	6.28	5.33	15.13
10.25	20.30	14.75	13.16	10.77
10.65	20.53	20.03	19.17	4.29

Authors also measured the effect of concentration of sulfur and asphaltenes on the viscosity of crude oil at changing temperature conditions. The higher concentrations cause viscosity to increase, while the higher temperature has the opposite effect. It corresponds to the effect of temperature on asphaltene precipitation described above. The main drawbacks of this work are the inability to distinguish and quantitatively evaluate the effects of sulfur and asphaltenes separately.

Madhi et al. [45] through fitting the experimental data to a mathematical model give insight about the mechanism of permeability reduction cause of asphaltene deposition and the effect of injection of inhibitor slug between two crude injections into the core. The main mechanism of permeability alteration is asphaltene cake formation on the surface of grains. This effect reduces the pore throat thus resulting in a decrease in permeability. Figure 16-a and Figure 16-b shows the formation of such a cake. Figure 16-c and Figure 16-d demonstrate the effect of asphaltene inhibitor stabilization. Figure 16-e demonstrate inhibitor molecules that left after the removal of dissociated asphaltenes. Figure 16-f and Figure 16-g shows the effect of inhibitor during the second flood.

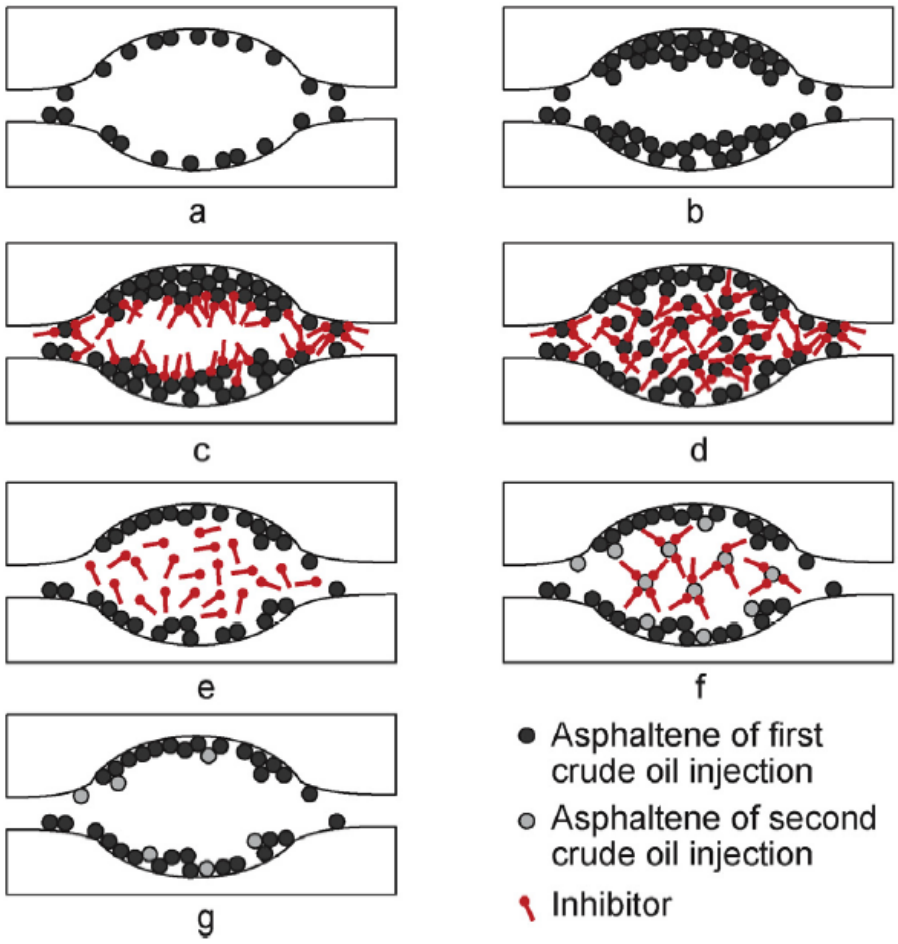

Figure 16 - Schematic of effect of asphaltene deposition and inhibitor in porous media [45].

2.3.2 Production system damage

Thomas et al. [3] presented multiple field cases where the asphaltene deposition caused severe decline in production. The well in southwestern Mexico was initially producing 4700 bbl/day of oil. Almost a year after, asphaltene deposited in tubing and caused production decline to 436 bbl/day. Another well in the same region was reported to be totally plugged up to X-mass tree with asphaltene deposits. The asphaltene deposition was also the case in transportation systems. The pipeline from Mexico experienced plugging, that required pigging to be performed every 2-3 months.

Previously mentioned Hassi Messaoud oilfield in Algeria experienced the building of deposits (83.4% asphaltene) in wells. It was reported that some wells lost almost 20-25% of their wellhead pressure in less than a month, causing tangible production losses [38]. It is worth to mention that the crude in this case was light (42.3 API degree) and with very low asphaltene content. Another example was reported in famous giant Ghawar oilfield, where 10 wells faced restricted flow regime in tubings due to asphaltene precipitation [46].

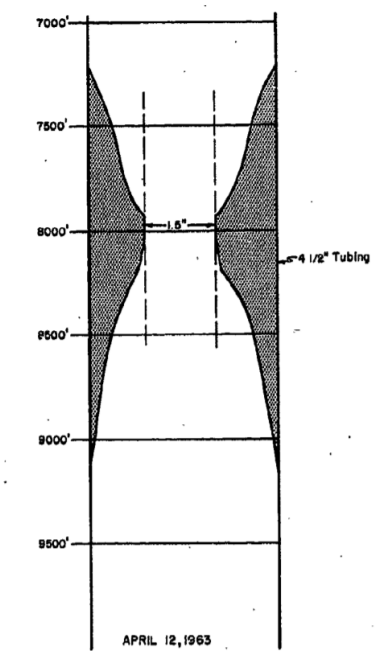

Figure 17 - The profile of asphaltene deposit plugging in the well tubing, Hassi Messaoud Field, Algeria [38].

Several notable cases were observed in the Ula Field located in the North Sea [47]. Crude oil was light (38.98 API gravity degrees) with relatively small asphaltene fraction content (0.57 wt%). The asphaltene depositions were found in DHSV, which caused problems in opening them by applying standard values of hydrostatic pressure. Furthermore, in another wells, deposits damaged logging tools during wireline operations. Large amount of deposited asphaltene fraction was found in two main separators (Figure 18).

Figure 18 - Asphaltene debris that was removed from the separator [47].

2.4 Thermodynamic Modelling of Asphaltene Precipitation

Thermodynamic modeling of asphaltene precipitation is a relatively cheap and useful tool that can be extremely helpful in understanding of the phase behavior of crude in the changing temperature, pressure and composition conditions. There are two main approaches to thermodynamic modeling of asphaltene fraction, namely the colloidal approach and the solubility approach.

The colloidal approach considers asphaltenes as solids in crude oil system, which are stabilized by the presence of resins. Leontaritis et al. [12], in their thermodynamic "colloidal" model, considered that layers of resins around the solid asphaltene core act as stabilizers (natural dispersants), by repulsion of other resin molecules in other aggregates and overcoming attraction forces between asphaltene molecules. The precipitation occurs when the volume of resins that cover asphaltene cores fall lower than the critical resin fraction – the minimum volume of resins that is necessary for asphaltene fraction stability in solution [5]. Victorov et al. [48] presented the thermodynamic "micellization" model. They considered asphaltene molecules existing in micelles with resins on the shells. The absence of resins will initiate precipitation of asphaltene monomers (the only fraction that is allowed to precipitate) due to their low solubility in crude oil. Crude oil was described using PR EoS. Later, this micellization model was further developed by Pan et al. [49] that modeled precipitation as liquid-liquid equilibrium and assumed the incipient phase to consist only from resins and asphaltenes.

Since this approach was developed in analogy with the behavior of surfactants, it is widely used in asphaltene inhibitors/dispersants modeling. For example, Al-Sahhaf et al. [50] in their test of different asphaltene precipitation inhibitors have used the model by Victorov et al. [48] to support experimental results. The main drive for asphaltene aggregation and inhibition is acid-base and π-π aromatic interactions, not considering hydrogen bonding. The model suggests that chemicals stabilize the aggregated asphaltene micelles (they migrate to shells of micelles and attach by their polar heads containing acidic group to the core of micelle) and prevent precipitation similar to resins, while alkane groups destabilize them and induce the process. Authors note that according to a model, in the beginning, inhibitors are dissolved in the continuous oil phase. Then some of the particles, due to their polarity, migrate to shells of micelles. Consequently, the model assumes that the asphaltene core is covered by resins and added inhibitor particles.

Solubility approach considers asphaltenes as particles that are dissolved in crude oil, and interactions between them and other crude oil fractions are driven by relatively weak van

der Waals forces (particularly, London dispersion forces) and not polar interactions. Polar interactions are governing the formation of self-associated nanoaggregates, which were shown to form even in the solution with highly aromatic components, such as toluene. Asphaltenes will start to precipitate when the solubility of crude oil declines below a certain value. The equilibrium in the system is modeled either as liquid-liquid (crude oil – asphaltene rich lean phase) or solid-liquid.

Solubility models can be divided into two distinctive categories [5]:

- Solubility theories, which consider crude oil bulk phase as the one pseudo-pure component and equilibrium is modeled as the binary mixture of crude oil-asphaltenes (Regular solution theory, Hirschberg method, etc.).
- Equation-of-State based approach – the bulk phase is not treated as a single component, but rather a certain number of pure and pseudo components (Cubic EoS, SAFT EoS and their modifications).

2.4.1 SAFT Equation of State

The SAFT Equation of State [51] [52] [53] was developed by in an attempt to increase accuracy of the modelling of the phase equilibria of strongly polar/associating fluids. The theory believes that associative behaviour of molecules has a profound effect on the phase behaviour of mixtures because associated clusters have different molecular properties as compared to monomers. These deviations, if unaccounted, can cause profound errors in predicted fluid properties.

In the scope of petroleum systems, especially in asphaltene equilibria modelling, an assumption of non-associating behaviour is often implemented. Moreover, it is noted that “the SAFT parameters are well-behaved and suggest predictable trends with macroscopic properties” [54]. These factors lead to a substantial decrease in the computational time and in the amount of experimental data necessary to conduct modelling. The SAFT was especially useful in accurately predicting conditions of the asphaltene precipitation phenomena – a requirement for the deposition and subsequent flow assurance problems.

Overall, SAFT and its multiple variations proved, throughout three decades of usage, their ability to predict the phase behaviour of complex and heterogeneous mixtures for various purposes – from polymer solutions behaviour and PVT parameter prediction to description of asphaltene and wax precipitation processes.

The SAFT EoS usually is presented in terms of residual Helmholtz free energy (i.e. subtracting ideal gas energy). The residual Helmholtz energy is the characterization of intermolecular forces since molecules of an ideal gas exert no such forces on each other.

In order to model the fluid of interest, the EoS considers a specific reference fluid consisting of hard-spheres that have only repulsive forces between each other. This reference fluid is assumed to roughly describe the fluid of interest and model, then corrected by introducing corrections (perturbations) to account for other intermolecular interactions:

$$a^{res} = a^{seg} + a^{chain} + a^{assoc} \quad \textbf{(1)}$$

Where a^{res} is the total residual Helmholtz energy per mole of molecules, a^{seg} represents the contribution of the segment formation (reference fluid), a^{chain} is for the covalently bonded chain formation, and the term a^{assoc} is to account for the associative interactions (perturbations). Spheres interact firstly through covalent bonds with the formation of chains. Then chains interact through specific association sites to form chainlike or treelike clusters by association bonds (such as hydrogen or coordination bonds). Also, attractive interactions (such as Van-der-Waals forces) exist between spheres.

Chapman et al. [51] modelled the fluid of interest as consisting of a mixture of LJ spheres. This version is sometimes referred to as "SAFT-0" or "original SAFT". As will be shown later, other intermolecular potentials can be used instead of Lennard-Jones potential. The term for mixtures in SAFT-0 is defined as follows:

$$a^{seg} = a_o^{seg} \sum_i X_i m_i \quad \textbf{(2)}$$

$$a_o^{seg} = a_o^{hs} + a_o^{disp} \quad \textbf{(3)}$$

$$\frac{a_o^{hs}}{RT} = \frac{4\eta - 3\eta^2}{(1-\eta)^2} \quad \textbf{(4)}$$

$$a_o^{disp} = \frac{\epsilon R}{k_{BT}} \left(a_{o1}^{disp} + \frac{a_{o1}^{disp}}{T_R}\right) \quad \textbf{(5)}$$

Where X_i and m_i represent the molar fraction and the number of segments per molecule of a component *i*, ϵ/k_{BT} is a segment-segment interaction energy, *R* is the universal gas constant and η is a reduced density. That is, in the first place, we have a reference fluid – a mixture of hard-spheres, which Helmholtz energy term (a^{hs}) accounts for repulsive forces. The first perturbation (a^{disp}) adds attractive interactions that exist between segments. Chapman et al. [51] suggested that hard-sphere reference can be expressed by equations of Carnahan et al. [55] and

dispersion term for Lennard-Jones spheres can be calculated using correlations from Cotterman et al. [56] for dense-fluids. Simplified versions of theory [52] [57] treated dispersion forces as a contribution by mean-field van der Waals approximation. It has shown an adequate level of accuracy in the modelling of fluids with strong association forces [58] where the effect of dispersion forces is weak.

The other two perturbations are to add accuracy to a model in comparison with a fluid consisting of just hard-sphere monomers. The perturbation (a^{chain}) accounts for the chain formation from equal size segments. Chain molecules that have (m) number of segments formed by covalent bonding. Each segment (i.e. LJ sphere) in the chain has the same temperature-independent diameter (σ). This diameter next corrected to the effect of temperature by introducing *temperature-dependent segment diameter* (d) according to Barker and Henderson [59] theory using expressions from Cotterman et al. [56] through the well depth of Lennard-Jones potential. The term for mixtures is defined as follows:

$$\frac{a^{chain}}{RT} = \sum X_i (1 - m_i) \ln(g_{ii}(d_{ii})^{hs}) \tag{6}$$

$$d_i = \sigma_i \, f_{CT}\left(\frac{k_{BT}T}{\epsilon_i}, m_i\right) \tag{7}$$

$$f_{CT}\left(\frac{k_{BT}T}{\epsilon_i}, m_i\right) = \frac{1 + \frac{0.2977\, k_{BT}T}{\epsilon_i}}{1 + \frac{0.33163\, k_{BT}T}{\epsilon_i} + f(m_i)\left(\frac{k_{BT}T}{\epsilon_i}\right)^2} \tag{8}$$

$$f(m_i) = 0.0010477 + 0.025337\,(m_i - 1)/m_i \tag{9}$$

T is a temperature expressed here and in the following equations in Kelvins. The term then estimated using segment radial distribution function for hard-spheres ($g(d)^{hs}$) from Carnahan et al. [55]. Radial distribution function take part in the calculation of both chain and association terms. This function from statistical mechanics is a probability of like (subscript ii – for chain term) or unlike (subscript ij – for association term) segments to be located at a defined distance (d) from each other in a given system. Any assumptions made in the estimation of the function have a profound effect on the accuracy of modelling [60], and it is one of the expressions that differ in modifications:

$$g(d)^{seg} \approx g(d)^{hs} = \frac{2 - \eta}{2(1 - \eta)^3} \tag{10}$$

The process of evaluation of the chain term considers that all segments in the chain are bonded by all of their available sites. However, if a fluid of interest is associating, then segments can have other sites to form associating bonds. This consideration simply shows that the association is not allowed to interrupt chain molecule formation. Chapman et al. [51] examined EoS modelling capabilities for nonassociative chains with a chain length up to m=8 (*n*-octane).

Generally, to describe non-associating fluid, three SAFT parameters are necessary for each pure component - temperature-independent segment diameter (σ), the number of segments per molecule (m) and segment-segment interaction energy (ϵ/k_{BT}).

The association bonds act on short distances and strongly depend on the number and orientation of association sites of molecules. Association term (a^{assoc}) represents the Helmholtz energy of such bonds. If a fluid of interest is non-associating, then this term is usually ignored. All of the given equations are given originally in pure component form and then converted for mixtures. SAFT-0 uses van der Waals one fluid theory ("one-fluid rule"). Most of the modifications follow the same rule, except for the VR-SAFT.

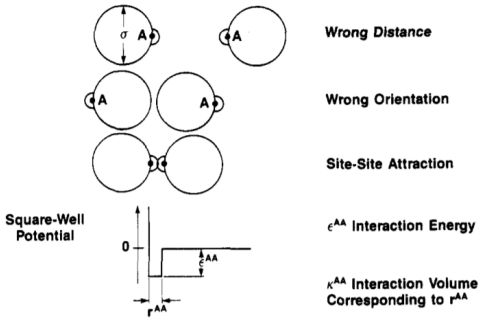

Figure 19 - Square-well potential associative interactions of hard-spheres [51].

The first-order theory considers energy change due to the bonding of two molecules, not accounting for the presence of other molecules [60]. This assumption leads to a series of limitations in SAFT modelling [53] [51]. The angle between different bonding sites in one molecule is not considered, and those sites form bonds independently, without interference from other sites when located close to each other. In the frames of a model, the existence of double bonds is not possible. In the situation when one site of one molecule formed the bond with the site of another molecule, the third molecule will be repulsed and cannot bond to these sites. Finally, one site cannot bond to two sites at the same time. The direct consequence of such limitation is that the model cannot recognize isomers and other configurations of chain molecules and treat them all the same. Furthermore, no ring-like clusters can be formed.

These limitations were addressed in numerous modifications of original SAFT EoS. Modifications, in general, vary on:

- How the reference fluid (i.e. segment term) is estimated
- What intermolecular potential is used to estimate attractive term
- What expression used for the radial distribution function
- How temperature-dependent diameter related to the temperature-independent diameter

Since the appearance, SAFT EoS was substantially developed and modified for multiple cases and purposes. Regarding asphaltenes, it was noted [61] that different versions generally give comparable results. PC-SAFT remains the most applied version to model asphaltene precipitation due to its presence in thermodynamic software such as Multiflash, VLXE, and PVTSim.

2.4.2 PC-SAFT Equation of State

The PC-SAFT EoS was developed by Gross and Sadowski [62]. Unlike other modifications, reference here is a chain fluid – repulsive hard spheres form chains, and then dispersion and association forces are added to the system. Thus, perturbations accounting for attractive interactions are applied to hard-chain molecules and are a function of chain length (m), hence the name "perturbed-chain" SAFT. The reference fluid hard-chain term (a^{hc}) is described as:

$$\frac{a^{hc}}{RT} = \left(\frac{a_o^{hs}}{RT}\right)\sum_i X_i m_i \; - \sum_i X_i (m_i - 1)\ln g_{ii}(d_{ii}) \tag{11}$$

Hard-sphere term calculated using the expression from Mansoori et al. [63]:

$$\left(\frac{a_o^{hs}}{RT}\right) = \frac{1}{\zeta_0}\left[\frac{3\zeta_1\zeta_2}{(1-\zeta_3)} + \frac{\zeta_2^3}{\zeta_3(1-\zeta_3)^2} + \left(\frac{\zeta_2^3}{\zeta_3^2} - \zeta_0\right)\ln(1-\zeta_3)\right] \tag{12}$$

$$\zeta_n = \frac{\pi}{6}\rho\sum_i X_i m_i d_i^n \quad n \in \{0,1,2,3\} \tag{13}$$

The general form of chain term is identical to original SAFT:

$$\frac{a^{chain}}{RT} = \sum_i X_i (m_i - 1)\ln g_{ii}(d_{ii}) \tag{14}$$

However, the radial distribution function is defined differently, by expression from Boublik [64]. For pair of unlike segments:

$$g_{ij}(d_{ij}) = \frac{1}{(1-\zeta_3)} + \left(\frac{d_i d_j}{d_i + d_j}\right)\frac{3}{(1-\zeta_3)^2} + \left(\frac{d_i d_j}{d_i + d_j}\right)^2 \frac{2\zeta_2^2}{(1-\zeta_3)^3} \quad \textbf{(15)}$$

Another difference is the temperature-dependent segment diameter (*d*) which was defined through the square-well potential model by Chen and Kreglewski [65] as follows:

$$d_i = \sigma_i \left[1 - 0.12 \exp\left(-\frac{3\epsilon_i}{k_{BT}T}\right)\right] \quad \textbf{(16)}$$

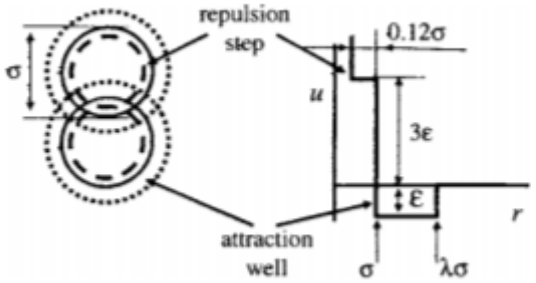

Figure 20 - Chen and Kreglewski potential [66]

Ting et al. [67] [25] conducted a study on prediction of density, bubble point and asphaltene precipitation envelope for recombined oil (STO+Separator gas) in reservoir conditions and for model oil (toluene+asphaltenes). As a result, a method of lumping crude to pseudo-components was introduced, and an assumption of non-associating behaviour of the crude oil- asphaltenes system was made. Later the continuation of the previous work [68] demonstrated the adequacy of using PC-SAFT for asphaltene precipitation modelling under gas injection was demonstrated. Methane and N_2 were shown to be strong precipitants. The study of asphaltene precipitation under gas injection (methane, ethane, N_2, CO_2) was conducted for a recombined oil (from Ting et al. [67]), model oil and experimental results for reservoir fluid from literature. Additionally, CO_2 injection can have a positive or negative effect on asphaltene stability depending on certain temperature threshold (lower – stabilize crude, higher – induce precipitation) [69]. This behaviour was explained through a change in the solubility parameter.

Furthermore, the study [70] of the effect of oil-based mud contamination and compositional change due to gas addition on asphaltene stability was conducted on a number of crude oils with an account for the polydispersity of asphaltenes. Oil-based mud showed to decrease onset and bubble point due to decrease in GOR. Largest in molecular weight asphaltenes will precipitate first. Additional four components for oil-based mud, optionally mud contamination can be represented as the part of Saturates pseudo-component. The study

introduced the additional 3 or 4 pseudo-components for the effect of polydispersity of asphaltenes which are divided according to the solubility (ex. nC_{5-7} – asphaltenes soluble in pentane and insoluble in heptane). BIPs were set to zero between asphaltene pseudo-components.

PC-SAFT is so far the most widely used modification for asphaltene precipitation modelling. Since 2003 there are dozens of works in the literature that addresses the implementation of PC-SAFT for asphaltene phase behaviour modelling. The PC-SAFT modelling procedure (crude oil characterization method and parameter evaluation correlations) is described in the chapter "Methodology".

2.4.2.1 Binary interaction parameters (BIPs)

BIPs are temperature-independent parameters present in the dispersion term. They are used to improve prediction accuracy by correcting the calculation of intermolecular interactions between components. There are no established values of interaction parameters for PC-SAFT EoS. They are usually determined by fitting experimental VLE data at a corresponding temperature between two pure components. For pseudo-components, specific pure component within the pseudo-component is selected to perform the fitting. For example, Gonzalez et al. [68] used VLE for propane and decane to evaluate the BIPs between Light Alkanes and Saturates. Asphaltenes parameters were set to be equal to Aromatics parameters. Then, these Asphaltene parameters are adjusted to achieve the best match with experimental AOP. Pedersen et al. [16] mention that interaction parameters from cubic EoS can be reasonable initial estimates.

These parameters that require experimental data and computational time to be matched, constitute a significant shortcoming of PC-SAFT modelling. As was shown by Gonzalez [71], asphaltene precipitation onsets are sensitive to the values of interaction parameters – the change of one binary interaction parameter between Asphaltene and Saturates pseudo-components from 0.007 to 0.0024 resulted in the shift in AOP from 15244 psi to 9949 psi. The difficulties of finding the optimal set of interaction parameters were also reported by Zhang et al. [72].

There are several correlations presented in the literature for some binary systems. For example, Garcia-Sánchez et al. [73] developed the polynomial correlation for N_2 – *n*-alkane systems as a function of molecular weight of *n*-alkane. The equation was tested by modelling the P-X diagram for the N_2 – *n*-hexadecane system. There are also correlations for methanol-alkane systems [74] and CO_2, methane and ethane with high *n*-alkanes systems [75].

Stavrou et al. [76] proposed method for estimating BIPs between pure components based on Quantitative Structure Property Relationship model. For each type of interactions (i.e. dispersive, polar) there is separate descriptor, which is a function of SAFT parameters between binary pair. The resultant BIP is a summation of all descriptors multiplied to specific model coefficients.

Recently, a study [77] was conducted on the usage of an artificial neural network for the estimation of BIPs for PC-SAFT EoS. The algorithm uses two sets of input data – either 1) three SAFT parameters or 2) MW, specific gravity and the normal boiling point for each pair (the best results). The resultant algorithm was tested and demonstrated the good accuracy in the prediction of a bubble point and gas composition between several binary mixtures, as well as in the estimating the bubble point of a reservoir crude oil under nitrogen injection.

2.4.2.2 Comparison with the Cubic Equations of State

Several works were conducted to compare the PC-SAFT simulation of asphaltene phase equilibria with cubic EoS – another widely used in industry family of equations of state, thanks to its simplicity. This family originates from the van der Waals EoS and require critical temperature (T_c), critical pressure (P_c) and acentric factor (ω) for each component as input parameters. The BIPs are used to improve accuracy in calculations of intermolecular interactions.

The most widely used ones are SRK EoS [78] [79] and PR EoS [80] equations-of-state. This two has demonstrated good prediction of the phase behaviour of nonpolar gases. However, when it comes to liquids, the accuracy is considerably less. In the attempt to overcome this shortcoming, the Peneloux correction [81] to SRK EoS was introduced. It was noted that even with that corrections, cubic equations-of-state are not suitable for the modelling of complex structures, such as asphaltenes [5]. However, these EoS types remain a popular choice because of simplicity and computational efficiency.

Panuganti et al. [82] modelled the asphaltene precipitation envelope and bubble point curves of the Middle Eastern crude at different gas injection scenarios. As can be seen in Figure 21, the SRK with Peneloux correction failed to predict onsets at high gas injections accurately. The main disadvantage of the cubic EoS in the scope of asphaltene modelling is that it fails to accurately predict the behaviour of mixtures when the massive size difference between molecules is present. Additionally, cubic EoS is fit to the critical point of mixtures, where asphaltenes usually are not present due to the decomposition before reaching a critical point.

The simulation was carried on PVTSim (ver. 18). The higher accuracy of PC-SAFT was also displayed in another work in comparison with PR EoS and VR-SAFT [83].

On the other hand, Zhang et al. [72] used CPA EoS [84] to model asphaltene precipitation from six crudes with asphaltene concentration ranging from 0.5 to 3.6 wt%. The same crudes were modelled with PC-SAFT EoS using the "SARA-based" method by Ting [85] and Gonzalez [71]. The heavy end (C_{6+}) was divided into several pseudo-components using correlations of Lee and Riazi. The results indicated that this type of cubic EoS could be successfully implemented for asphaltene precipitation modelling. Furthermore, in some cases, CPA showed the superiority above PC-SAFT in predicting the precipitation amount and phase envelopes. Later, another comparison between CPA and PC-SAFT was performed by AlHammadi et al. [86] that have used the modifications by Panuganti et al. [87] for the PC-SAFT crude oil characterization. The results indicated that both EoS types showed adequate results in predicting the asphaltene phase envelope, with PC-SAFT being closer to experimental values and demonstrating greater accuracy in the prediction of GOR. Arya et al. [88] used CPA and PC-SAFT (with and without association term) to model phase envelopes for five different reservoir fluids and one model oil. CPA predictions resulted in the lowest deviation from experimental data both in BP and UAOP predictions.

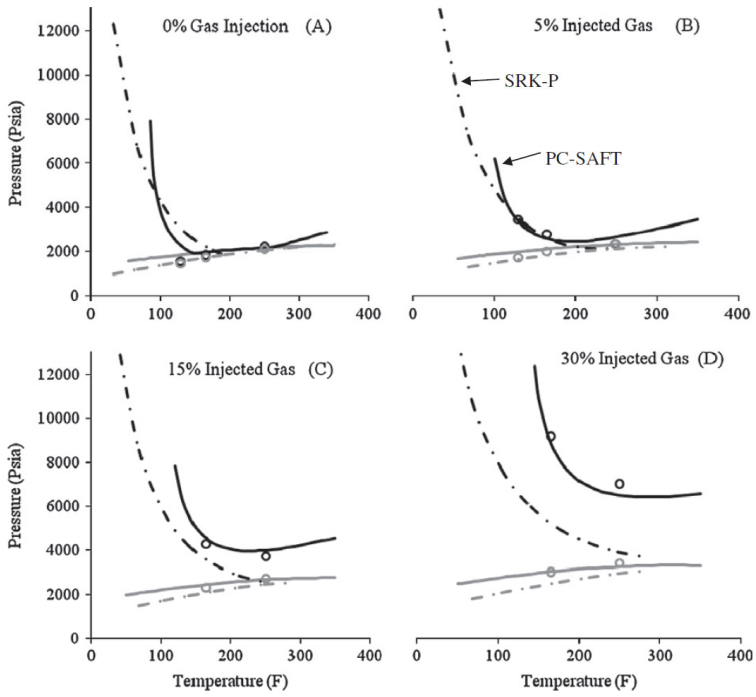

Figure 21 - The comparison between PC-SAFT and SRK with Peneloux correction predictions (gray line - bubble point, black line - AOP) [82].

3 METHODOLOGY

This chapter presents the methodology that was applied in order to achieve the stated goals of the work. Firstly, it states the modelling assumptions. Then the methodology that is most widely used for asphaltene phase behaviour modelling (the "SARA-based" method) will be explained in detail. Then, the modifications to this method will be introduced. Next, a brief explanation of algorithms that were written for MATLAB thermodynamic modelling will be given. Finally, the chapter gives the experimental data that was used for the research.

3.1 Modelling assumptions

For the asphaltene modelling, the general assumptions that were firstly formulated by Ting [25] are mostly similar in all works regarding the usage of PC-SAFT for asphaltene modelling and were also adopted by this work:

- The crude oil is a non-associating system.
- Asphaltene phase exists in crude in the form of nano-aggregates.
- Asphaltene precipitation is governed by Wan der Waals forces (particularly, London dispersion forces) and the negligible effect of polar interactions.
- Asphaltene precipitation is a thermodynamically reversible process.
- Above bubble-point pressure, the precipitation is modelled as LLE where one of the liquid phases is the asphaltene-rich dense phase. Below bubble-point pressure, since gas starts to liberate from crude oil, the precipitation is modelled as VLLE.

The accuracy of modelling is evaluated by calculating the MAPE between modelled and experimental values:

$$MAPE\ (\%) = \frac{1}{n}\sum_{i=1}^{n}\left|\frac{(A_i - F_i)}{A_i}\right| * 100\% \tag{17}$$

Where A_i and F_i are actual and predicted values respectively and n is the number of data points.

3.2 “SARA-based” method

The most popular method of crude oil characterization for PC-SAFT asphaltene precipitation modelling is so-called "SARA-based method" that was firstly introduced by Ting et al. [85] and later improved by Gonzalez [71], Panuganti et al. [82] and Punnapala & Vargas [7]. As the name implies, the method uses the results of SARA analysis.

By this method, PC-SAFT EoS models asphaltene phase behaviour by dividing crude oil into several pseudo-components and evaluating three SAFT parameters for each pseudo-component. The number of pseudo-components depends on the particular case and aims of modelling. Commonly, heavy oils (API lower than 30) have to be divided into more pseudo-components than light oils in order to predict phase behavior accurately. Asphaltene fraction is considered as a one pseudo-component. The number of pseudo-components depends on the specific conditions, aims of modelling, acceptable accuracy and computational time. For example, if precipitation under the gas injection is modelled, then all components of injected gas should be represented.

The list of experimental data that is required for monodisperse asphaltene precipitation modelling [7]:

- Compositional analysis of flashed gas and STO
- Density and average MW of STO
- GOR between STO and flashed gas
- SARA analysis
- Several AOPs at different temperatures (typically 3) and BPs of live oil.

The model generated using these data will predict the phase behaviour of the most unstable part of the asphaltene phase. It is necessary to divide the asphaltene fraction to several pseudo-components [89]. Tavakkoli et al. used four onset points by titration utilising four types of *n*-alkanes (C_5-C_8). These authors claim that their "indirect method" better describe asphaltene phase behaviour by taking into account the polydisperse nature of asphaltenes. The main disadvantage is that experiments and PC-SAFT parameters evaluations performed only at ambient conditions. Those data are then used to predict the behaviour of reservoir fluids, which can be unrepresentative [5].

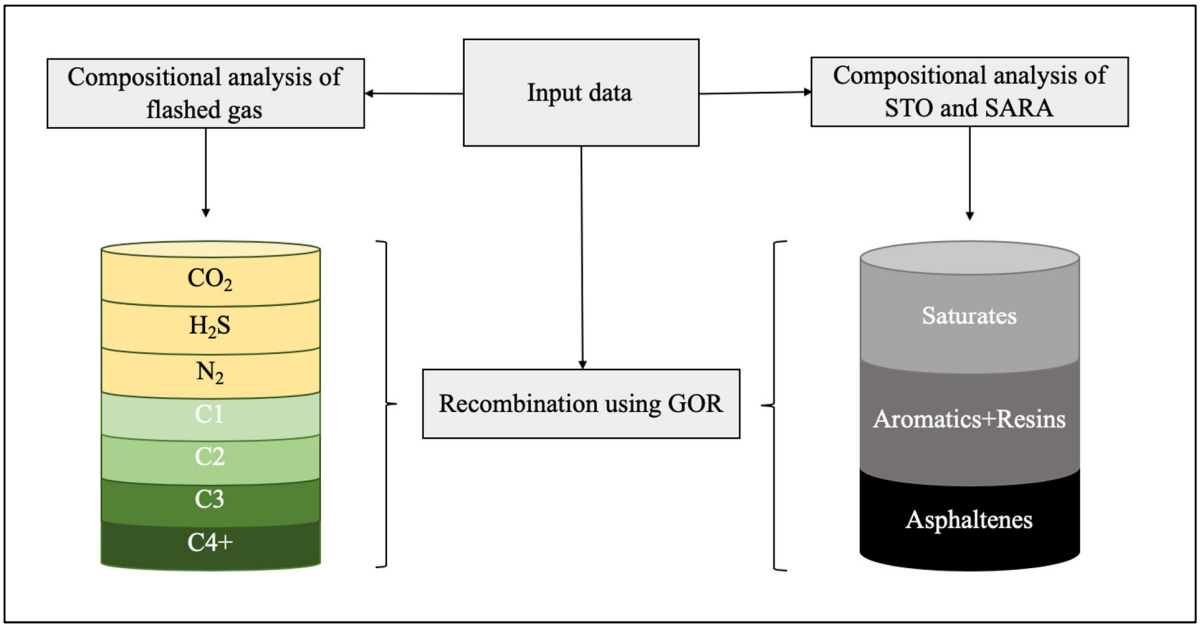

Figure 22 - "SARA-based" method crude oil characterization flowchart for this work

3.2.1 Flashed gas characterization

Light component's concentrations have a significant effect on asphaltene precipitation. For example, risk of asphaltene related problems during miscible gas injection processes. Because of these observations, gas fractions are treated as individually as possible, by representing all impurities such as N_2, CO_2, H_2S and also light hydrocarbons – methane, ethane, propane and one pseudo-component for gas fractions heavier than propane.

3.2.2 STO liquid characterization

Liquid phase is divided into three pseudo-components, representing saturates, aromatics, resins, and asphaltenes. Aromatics and Resins, cause of their similarity, are combined into the one pseudo-component. Asphaltenes are assumed to exist as pre-aggregated molecules, and the value of 1700 g/mol is taken as the molecular weight of such pre-aggregates [68] [70].

SARA analysis results are necessary for dividing the liquid into pseudo-components. The compositional analysis usually presented using the method by Katz and Firoozabadi [90] or by the later development of this method by Whitson [91] in terms of the SCN. It will contain the heavy end fraction, representing all components with the boiling cut equal and higher than certain SCN. For example, C_{30+} will represent all components equal and higher than C_{30}. Asphaltenes usually

considered to be only in the heavy end, according to their wt% by SARA. Aromatics, Resins and Saturates are considered to be distributed in both parts. The distribution performed by taking the certain SCN and manually picking and adding components in and below this SCN to either Saturates or Aromatics+Resins. Then wt% of these components are subtracted from the corresponding SARA analysis values of these pseudo-components. Components that are above this plus SCN are lumped to one plus fraction and MWs are divided according to this corrected SARA analysis values. For example, Ting [25] considered that in below C_{10} part, all nonpolar linear branched and cyclic components to be Saturates. All components that have one or more aromatic ring are lumped to Aromatics+Resins. Remaining composition is distributed in C_{10+} part according to the SARA. Asphaltenes are assumed to be present only in C_{10+} part. Panuganti et al. [82] considered that "below C_9" is a reasonable threshold choice for manual component lumping.

3.2.3 SAFT parameter evaluation

Parameters can be acquired by applying various correlations, based on the molecular weight of pseudo-components or well-established values (for pure components). Gross and Sadowski [62], for instance, calculated these parameters for 78 pure-components by fitting experimental vapour pressure and liquid molar volume data.

Parameters for C_1, C_2, C_3 and impurities such as CO_2, H_2S and N_2 are well established and can be found in original PC-SAFT work by Gross and Sadowski (Table 2). The parameters for the C_{4+} gas component can be obtained using the correlation for Saturates using the average molecular weight of a pseudo-component [85] (Table 3).

Table 2 - The constant PC-SAFT parameters for pure components [62].

Pure components	MW (g/mol)	m	σ (Å)	ϵ/k_{BT} (°K)
N_2	28.01	1.205	3.313	90.960
CO_2	44.01	2.073	2.785	169.210
H_2S	34.08	1.652	3.074	227.340
C_1	16.04	1.000	3.704	150.030
C_2	30.07	1.607	3.521	191.420
C_3	44.1	2.002	3.618	208.110

Table 3 - Correlations to evaluate PC-SAFT parameters for asphaltene modelling as a function of MW.

Ref.	Correlations of PC-SAFT parameters for non-associating pseudo-components of liquid phase					Comments
	Eq. #	Saturates	Eq.#	A+R	Asphaltenes	
[25]	(18)	$m = 0.0253MW + 0.9263$	(19)	$m = \gamma(0.0201MW + 0.7860) + (1-\gamma)(0.0139MW + 1.2988)$	Asphaltene parameter range For MW = 1700 g/mol: m – 25-35 σ – 3.389-4.239 ϵ/k_{BT} –414.77-658.01 For MW = 4000 g/mol: m – 56-80 σ – 3.902-4.271 ϵ/k_{BT} –449.55-760.18	Aromaticity parameter defined as follows: $\gamma = 1$ (PNA) $\gamma = 0$ (benzene, bi-phenyl, ter-phenyl) Asphaltene parameters fitted to experimental refractive indices at titration precipitation onsets. The initial guess is chosen such that parameters are in the region between *n*-alkanes and PNAs parameters correlations and solubility calculated is in the range reported for asphaltenes (19-24 $MPa^{0.5}$)
	(20)	$m\sigma = 0.1037MW + 2.7985$	(21)	$m\sigma = \gamma(0.0782MW + 2.466) + (1-\gamma)(0.0597MW + 4.2015)$		
	(22)	$\epsilon/k_{BT} = 32.81\ln(MW) + 80.398$	(23)	$\epsilon/k_{BT} = \gamma(40.65\ln(MW) + 112.4) + (1-\gamma)(119.41\ln(MW) - 230.21)$		
[71]	(24)	$m = 0.0257MW + 0.8444$	(25)	$m = \gamma(0.0101MW + 1.7296) + (1-\gamma)(0.0223MW + 0.751)$	Asphaltene parameter range (For MW = 1700 g/mol): m – 19-39 σ – 4.1-4.5 ϵ/k_{BT} –296-504	Range of correlations for aromatics and resins was expanded (to include more benzene derivatives as compared to Ting [25]) to more accurately calculate parameters for crudes with API gravity lower than 33. Asphaltene parameters fitted as previously.
			(26)	$\sigma = \gamma\left(4.6169 - \frac{93.98}{MW}\right) + (1-\gamma)\left(4.1377 - \frac{38.1483}{MW}\right)$		
	(27)	$\sigma = 4.047 - \frac{4.8013\ln(MW)}{MW}$	(28)	$\frac{\epsilon}{k_{BT}} = \gamma\left(508 - \frac{234100}{MW^{1.5}}\right) + (1-\gamma)(0.00436MW + 283.93)$		
[7]	(27)	$\sigma = 4.047 - \frac{4.8013\ln(MW)}{MW}$	(29)	$m = (1-\gamma)(0.0257MW + 0.8444) + \gamma(0.0101MW + 1.7296)$		Correlations for Saturates are the same as in the previous work by Gonzalez [71]. Aromaticity parameter was redefined as: $\gamma = 1$ (PNA) $\gamma = 0$ (Saturates) Asphaltene parameters are evaluated using correlations by tuning aromaticity (γ) and molecular weight (MW) of asphaltene pseudo-component to experimental onsets.
			(30)	$\sigma = (1-\gamma)\left(4.047 - \frac{4.8013\ln(MW)}{MW}\right) + \gamma\left(4.6169 - \frac{93.98}{MW}\right)$		
	(31)	$\ln\left(\frac{\epsilon}{k_{BT}}\right) = 5.5769 - \frac{9.523}{MW}$	(32)	$\frac{\epsilon}{k_{BT}} = \gamma\left(508 - \frac{234100}{MW^{1.5}}\right) + (1-\gamma)\left(\exp\left(5.5769 - \frac{9.523}{MW}\right)\right)$		

SAFT parameters for Saturates and Aromatics were noted to correlate linearly with molecular weight [62] [25]. Furthermore, parameters of components that have both aromatic rings and aliphatic chains (such as Resins and Asphaltenes) will be in the region between lines of *n*-alkane saturates and aromatics in graphs of parameters versus molecular weight and can be evaluated by adjusting so-called "aromaticity parameter" [25]. This fact led to the development of several correlations that are used in literature to calculate values of SAFT parameters for non-associating pseudo-components. These correlations are listed in Table 3 with corresponding references and comments.

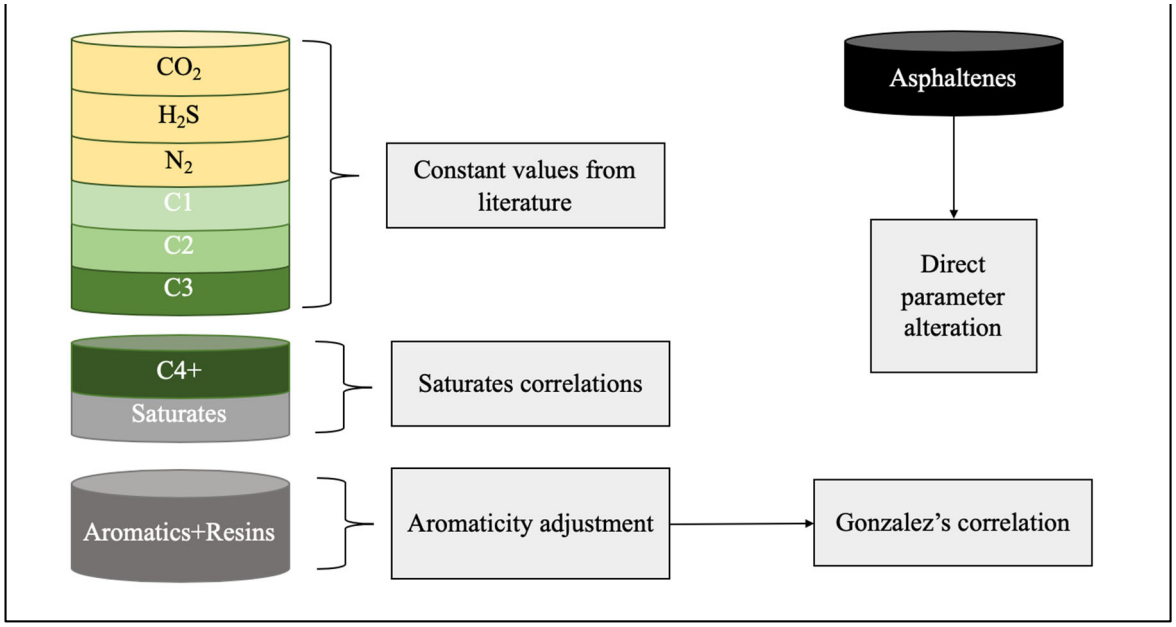

Figure 23 - Flowchart of PC-SAFT parameter evaluation process used by this work.

The procedure is as follows [7] [25] [5] [87] [71]:

1. Pure component parameters are obtained from the literature.
2. Pseudo-component parameters are evaluated using correlations.
3. The heavy gas pseudo-component and Saturates parameters are both calculated using the correlation for Saturates (Table 3).
4. A+R pseudo-component parameters are changed by adjusting "aromaticity parameter" until the minimal error is reached between model and experimental bubble point and density using correlations for A+R pseudo-component (Table 3). The one unknown in this case is aromaticity parameter (γ).
5. During the A+R, asphaltene parameters are set in the range of reported values from the literature, and its molecular weight is set as 1700 g/mol. Since asphaltene concentration is

usually low, and the light components mostly influence bubble point estimations, Asphaltene parameters have a negligible effect on the bubble point predictions.

6. Asphaltene parameters are directly adjusted [71] [68] or tuned using correlations from Punnapala & Vargas [7] as a function of aromaticity and MW of Asphaltene pseudo-component to minimize the error between calculated and experimental AOPs. If the correlations are used, liquid pseudo-component molar distribution has to be changed at each step because of changing MW.

The Gonzalez's [71] correlations for A+R was chosen by testing it against the performance of Punnapala's [7] correlations for each crude to determine the optimal one. For all three crudes, the minimal error between experimental and calculated data was lesser for Gonzalez's correlation [71]. Figure 24 demonstrates the tuning procedure by two correlations for Crude "A" made in this work with a step size of 0.005. The error is the equal-weighted MAPE of bubble point and STO density. For the Asphaltenes pseudo-component parameters, the method of directly changing asphaltene parameters has been chosen. As was mentioned, the alternative method suggests changing parameters by A+R correlations by adjusting aromaticity factor and molecular weight until the minimal error is reached between experimental and calculated AOP [7]. To simplify and increase the speed the process of method comparison, parameters fitted only to one AOP at the specific temperature, by changing one of the parameters and keeping others as constants. The initial guesses for this work are 33, 4.33 Å and 390°K for m, σ and ϵ/k_{BT} respectively, all in ranges reported in the literature (Table 3).

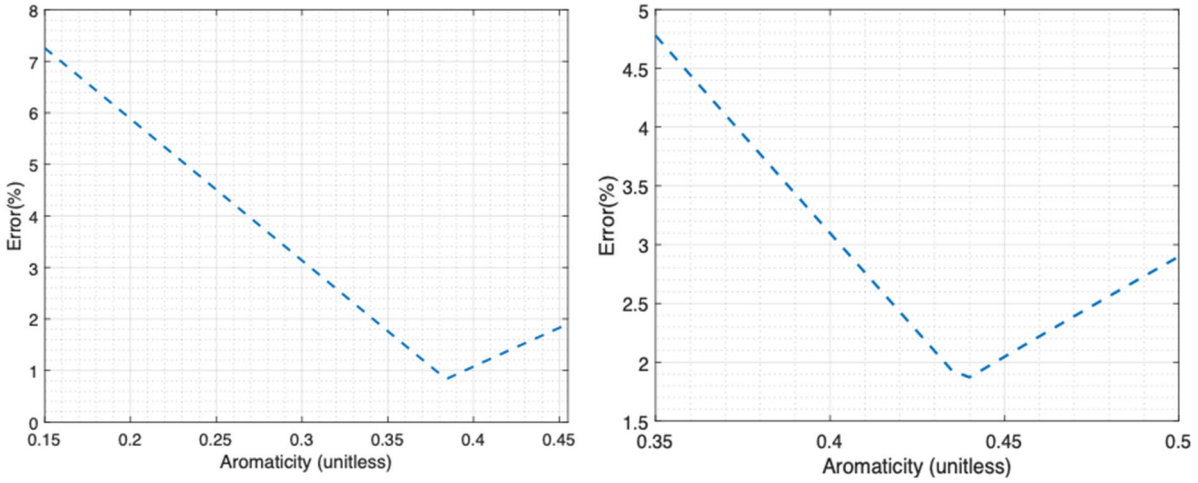

Figure 24 - A+R pseudo-parameter tuning for Crude "A" by Punnapala's correlations [7] (right) and Gonzalez's correlations [71] (left).

The constant set of BIPs are used for this method (from Panuganti et al. [82]):

Table 4 - The constant set of BIPs for the "SARA-based" method [82].

	N_2	CO_2	H_2S	C_1	C_2	C_3	C_{4+}	Saturates	A+R	Asphaltenes
N_2	0	0	0.09	0.03	0.04	0.06	0.075	0.14	0.158	0.16
CO_2		0	0.0678	0.05	0.097	0.1	0.12	0.13	0.1	0.1
H_2S			0	0.062	0.058	0.05	0.07	0.09	0.0015	0.0015
C_1				0	0	0	0.03	0.03	0.029	0.07
C_2					0	0	0.02	0.012	0.025	0.06
C_3						0	0.015	0.01	0.01	0.01
C_{4+}							0	0.005	0.012	0.01
Saturates								0	0.007	-0.004
A+R									0	0
Asphaltenes										0

3.3 The modification to the “SARA-based” method

The main disadvantage of the SARA analysis is the inconsistency of results depending on the method of performing the analysis. Panuganti et al. [87] reported the noticeable difference between results obtained through thin layer chromatography with flame ionization detection and HPLC for the same Middle East crude. Furthermore, the ratio of Saturates and A+R pseudo-components molecular weights in the plus fraction of STO is the assumed value. Tavakkoli and Vargas [5], for example, suggested using the value of 0.9 as a standard.

Since SARA analysis can be unavailable, this work suggests that Saturates and A+R can be lumped into one pseudo-component (S+A+R) to reduce the number of pseudo-components in the mixture and that the model can still reproduce the similar results as with “SARA-based” method. The EoS parameters for such joint pseudo-component have been searched in the region between the parameters of Saturates and Benzene derivatives. The following correlations. the combination of respective correlations from Gonzalez [71] is used in this work:

$$m = \lambda\,(0.0257MW + 0.8444) + (1 - \lambda)(0.0223MW + 0.751) \qquad \textbf{(33)}$$

$$\sigma = \lambda(4.047 - \frac{4.8013\ln(\mathrm{MW})}{\mathrm{MW}}) + (1-\lambda)\,(4.1377 - \frac{38.1483}{\mathrm{MW}}) \quad \textbf{(34)}$$

$$\frac{\epsilon}{k_{BT}} = \lambda(\exp\left(5.5769 - \frac{9.523}{MW}\right)) + (1-\lambda)\,(0.00436\mathrm{MW} + 283.93) \quad \textbf{(35)}$$

Aromaticity factor is replaced by an adjustable parameter λ to avoid confusion. When (λ = 1) it becomes the correlation for Saturates and when (λ = 0) – for Benzene derivatives. The step size of 0.005 is used. The original correlations can be seen in Table 2 (from Gonzalez [71]). Punnapala's correlations [7] are also can be used since they embrace the region between parameters of PNA and Saturates. The tuning procedure is similar to the one used for A+R pseudo-component, parameters were tuned to the bubble point and density value at the specific temperature. The example of parameter tuning at the bubble point and crude oil density at corresponding pressure and temperature can be seen in Figure 25 for Crude "B".

Since this S+A+R pseudo-component also will be fitted to the experimental data, no significant loss in accuracy is expected. This modification aims to gain several advantages in comparison with the "SARA-based" method:

- Less experimental data required. All non-Asphaltene STO components are lumped to the S+A+R pseudo-components. Because of this, only the asphaltene concentration and not the full SARA analysis is required. While asphaltene concentration can be obtained by the *n*-alkane titration, the determination of the concentration of saturates, aromatics and resins require additional equipment and chemicals (ex. alumina column, HPLC, trichloro-methane). So this is a viable alternative method when the full SARA analysis is not available.
- Simplified crude characterization – the division of STO into Asphaltenes and S+A+R is straightforward and require lesser calculations than the old method.
- Increased computational efficiency. More components in the mixture mean more time-consuming equilibrium calculations. PC-SAFT modelling requires a lot of bubble point pressure, density and AOP calculations during the model tuning. The decrease in the number of pseudo-components is expected to reduce the computational time of algorithms.

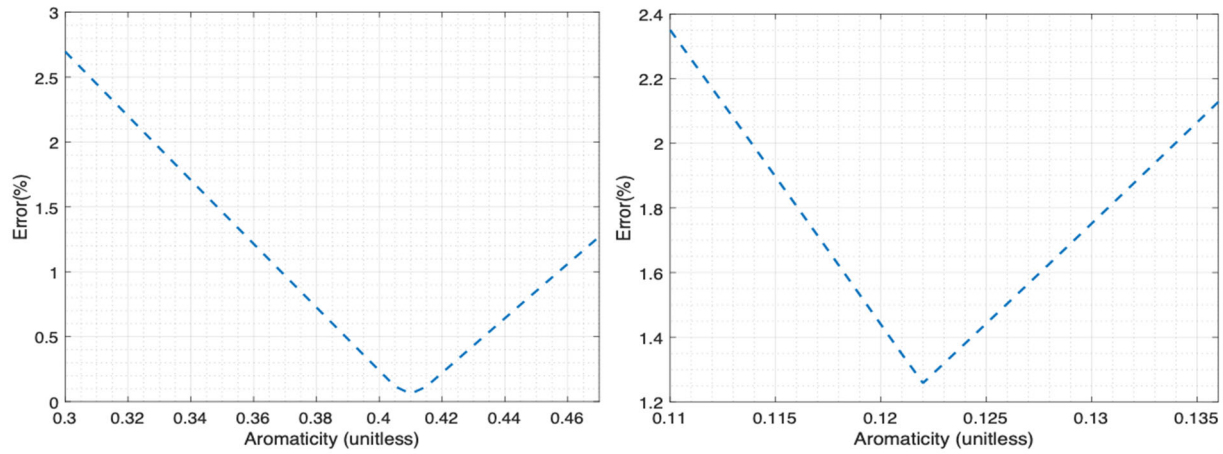

Figure 25 - S+A+R pseudo-component tuning for Crude "B" by Gonzalez's correlations for Saturate-Benzenes [71] (Eqs. 33-35) (left) and Punnapala's correlations [7] (right)

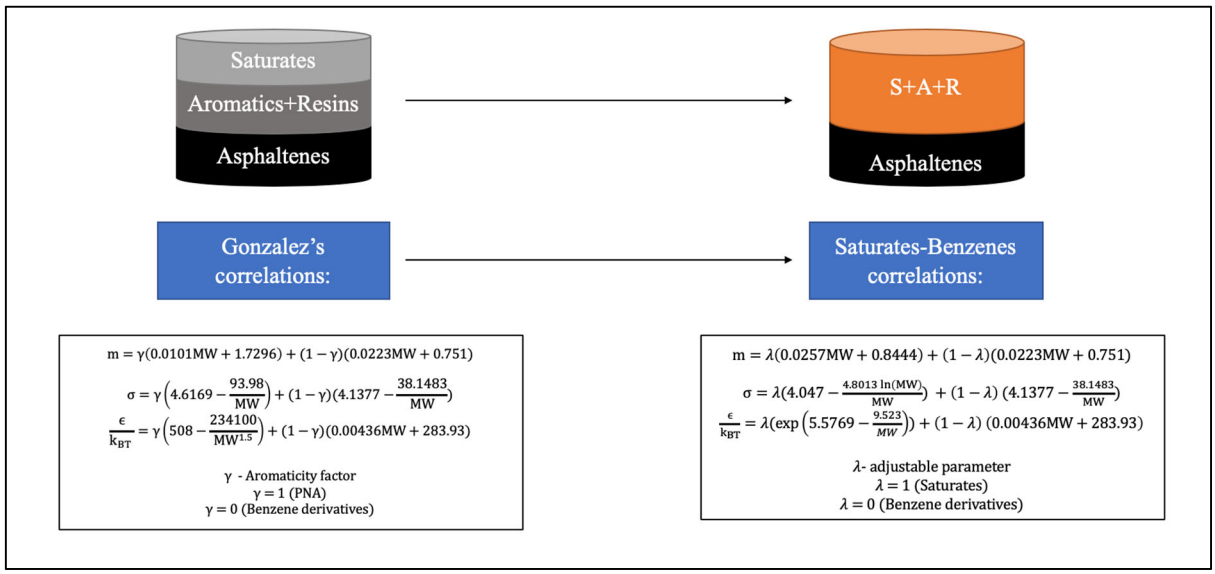

Figure 26 - The schematics of the modifications made by this work to the "SARA-based" method.

The following set of BIPs are used for this method which are almost similar to the set from Table 4. Since most of crudes has a predominant concentration of saturates, rather than aromatic hydrocarbons, BIPs for S+A+R pseudo-component are similar to the Saturate BIPs of "SARA-based" method, except for BIP between Asphaltenes and S+A+R that was adjusted to fit to the two Crude "A" AOPs:

Table 5 - The constant set of BIPs for the modified method

	N_2	CO_2	H_2S	C1	C2	C3	C4+	S+A+R	Asphaltenes
N_2	0	0	0.09	0.03	0.04	0.06	0.075	0.14	0.16
CO_2		0	0.0678	0.05	0.097	0.1	0.12	0.13	0.1
H_2S			0	0.062	0.058	0.05	0.07	0.09	0.0015
C_1				0	0	0	0.03	0.03	0.07
C_2					0	0	0.02	0.012	0.06
C_3						0	0.015	0.01	0.01
C_{4+}							0	0.005	0.01
S+A+R								0	-0.008
Asphaltenes									0

3.4 PVT parameter modelling methodology

Abutaqiya et al. [6] used PC-SAFT EoS for PVT parameters study and characterized the liquid phase by lumping all STO components into the one pseudo-component. The parameter evaluation for this liquid pseudo-component is similar to the procedure for A+R pseudo-component – single liquid pseudo component parameters are fitted to the experimental data. The EoS parameters for this pseudo-component are a function of the aromaticity factor which is adjusted from 0 to 1 until the minimal error has been reached between the predicted and experimental value of the certain parameter. The correlations from Punnapala & Vargas [7] (Eqs. 29, 30, 32) are used for the single liquid pseudo-component tuning. The reasonable accuracy in the prediction of various PVT parameters (such as density, FVF, the specific gravity of gas) was reported.

The similar methodology is adopted in this work. Crude "D" has no SARA data, neither it has reported problems with asphaltene precipitation. Single liquid pseudo-component (“Liquid”) parameters were fitted to the reported value of bubble-point pressure at the reservoir temperature. Then, this model was used for predicting densities and constructing graphs for other PVT parameters such as FVF of oil and gas, Z-factor and impurity concentrations in the liberated gas phase. Constant set of BIPs that is used for this method can be found in the work by Abutaqiya et al. [6].

3.5 Thermodynamic modeling framework

Once PC-SAFT parameters for all pseudo-components are evaluated and tuned, it is possible to predict various crude oil parameters such as bubble-point, density, precipitation onsets. As was mentioned previously, PC-SAFT EoS is present in a number of commercial simulators. However, in this work, MATLAB R2019b software was used for conducting phase equilibrium and modelling PVT parameters. MATLAB software combines computational capability with availability and gives more flexibility in comparison with commercial software. For the stated purposes, codes were written for:

- Gas/liquid densities calculations
- FVF of gas and oil, Z-factor calculations
- VLE/LLE/VLLE calculations
- PC-SAFT parameters optimization algorithms
- Viscosity predictions

3.5.1 Density calculations

The crude oil density is one of the crucial parameters both for asphaltene modelling and in general. In the conditions of the data scarcity, the density is the data type that most likely to be available. It serves both for the model validation and the model tuning purposes. The algorithm for liquid/gas density calculations is present in the original paper by Gross and Sadowski [62]. The number density of molecules (ρ) is expressed as:

$$\rho = \frac{6}{\pi}\,\eta\left(\sum_i X_i m_i d_i^3\right)^{-1} \qquad \textbf{(36)}$$

Where η is the reduced density, X_i, m_i and d_i is the molar fraction, segment number and temperature-dependent segment diameter of component i. The pressure (P) of a system of the interest at a fixed temperature is given as (in Pascals):

$$P = Zk_{BT}T\rho\,(10^{10}\frac{\dot{A}}{m})^3 \qquad \textbf{(37)}$$

Where Z is a compressibility factor and k_{BT} is the Boltzmann constant. Both Z and ρ are the function of the reduced density η. PC-SAFT calculates density iteratively by adjusting η until the calculated pressure is equal to the set system pressure. The Newton-Raphson

iteration algorithm is used for this purpose. The initial guess should be given to initiate the process. Gross and Sadowski [62] suggested using $\eta = 0.5$ for liquids and $\eta = 10^{-10}$ for gases.

Since crude oil composition is constant at the pressures above bubble-point, the algorithm is straightforward. At a fixed temperature, the only variable is the system pressure. However, at the pressures below bubble-point, light hydrocarbon fractions and some impurities start to liberate from crude, thus changing the values in the molar fraction vector. Because of this, VLE calculations should be performed at each step at the pressures below the bubble point. The resultant liquid composition is then used as a mixture composition, and density algorithm is performed.

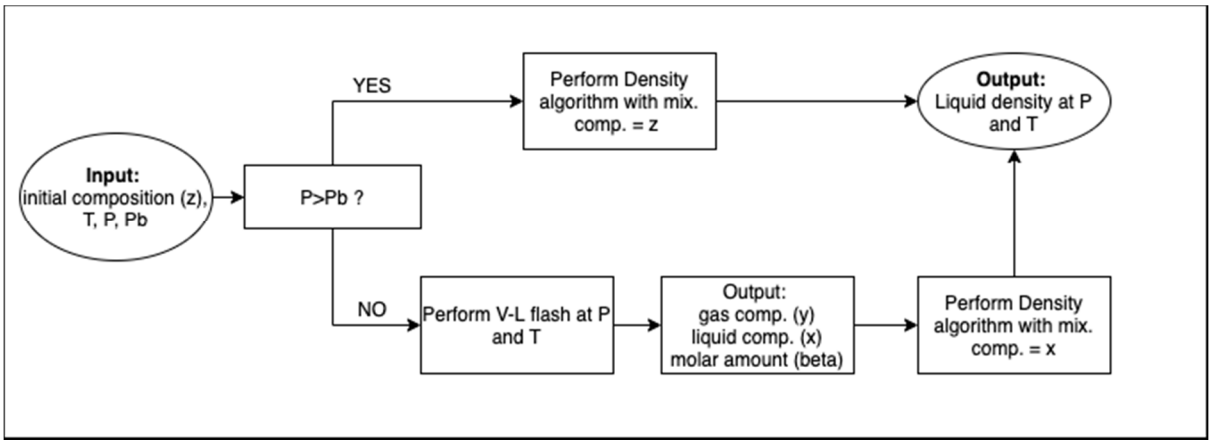

Figure 27 - Liquid density calculation algorithm implemented by this work

3.5.2 Flash calculations

The asphaltene precipitation is modelled as LLE above the bubble point pressure, where one of the liquid phases is the dense asphaltene-rich phase that may contain a certain amount of other components as well. Flash calculations are performed to assess the presence, amount and composition of two phases at given temperature and pressure. Typical schematic of a two-phase vapour-liquid flash is demonstrated in Figure 28.

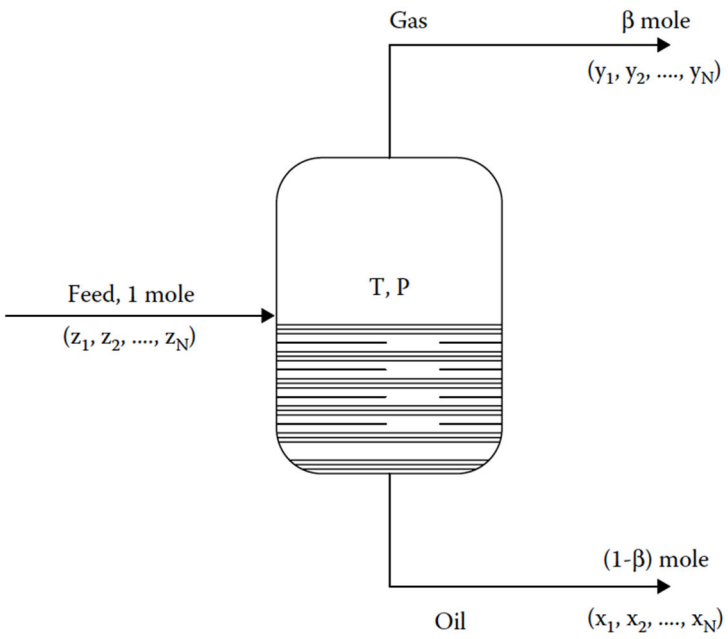

Figure 28 - Vapour-liquid P-T flash schematics [16].

The VLE/LLE algorithm is an iterative process that updates initial estimates for phase compositions and amounts until the equilibrium criteria are satisfied. The following relationship is valid for two phases in a thermodynamic equilibrium:

$$\frac{y_i}{x_i} = \frac{\varphi_i^x}{\varphi_i^y} \qquad i = 1,2,\dots Nc \tag{38}$$

Where x_i and y_i are the molar fractions of component *i* in corresponding phases and φ_i is a fugacity coefficient of component *i* in a corresponding phase. *Nc* represents the number of components in a mixture. The total initial composition of component i (z_i) and the mass balance constraint are expressed as:

$$z_i = \beta y_i + (1-\beta)x_i \qquad i = 1,2,\dots Nc \tag{39}$$

$$\sum_{i=1}^{nc}(y_i - x_i) = 0 \qquad i = 1,2,\dots Nc \tag{40}$$

Where β is a molar amount fraction of a phase *y*.

The flash calculation problem includes finding the roots of a Rachford-Rice objective function:

$$f(\beta) = \sum_{i=1}^{Nc} (y_i - x_i) = \frac{z_i(K_i - 1)}{1 + \beta(K_i - 1)} = 0 \quad \textbf{(41)}$$

Where K_i is an equilibrium constant that is expressed as:

$$K_i = \frac{y_i}{x_i} = \frac{\varphi_i^x}{\varphi_i^y} \quad \textbf{(42)}$$

The algorithm is adopted from the work of Zúniga-Hinojosa et al. [92]. It works by solving the Rachford-Rice equation in the inner loop and updating K_i values in the outer loop at each iteration. The schematics of the inner loop can be seen in Figure 29. Instead of Bisection/Newton-Raphson methods, MATLAB's "*fzero"* function is used to find the roots of the objective function. The schematics of the outer loop can be seen in Figure 30. The above procedure, depending on initial guesses for phase compositions and fugacity calculations, can be used both for liquid-liquid and vapour-liquid flash. As it can be seen from schematics (Figure 28), the resultant output will be the vector molar composition of two equilibrium phases (*x* and *y*) and their corresponding molar amount fractions. The fugacity coefficients, necessary to perform the equilibrium calculations, are calculated using PC-SAFT EoS by the algorithm provided in the original paper by Gross & Sadowski [62]. The algorithm requires initial guesses of phase compositions to initialize. The guesses can be made manually or can be made using correlations. The most popular choice for the vapour-liquid flash is Wilson's correlation [93]:

$$K_i = \left(\frac{P_{ci}}{P}\right) \exp\left[5.37(1 + \omega_i)\left(1 - \frac{T_{ci}}{T}\right)\right] \quad \textbf{(43)}$$

Where P_{ci}, T_{ci} and ω_i are critical pressure, critical temperature and acentric factor for the component *i* in the mixture. Below the bubble-point, where three phases can exist in the equilibrium, the algorithm is expanded to be vapour-liquid-liquid flash.

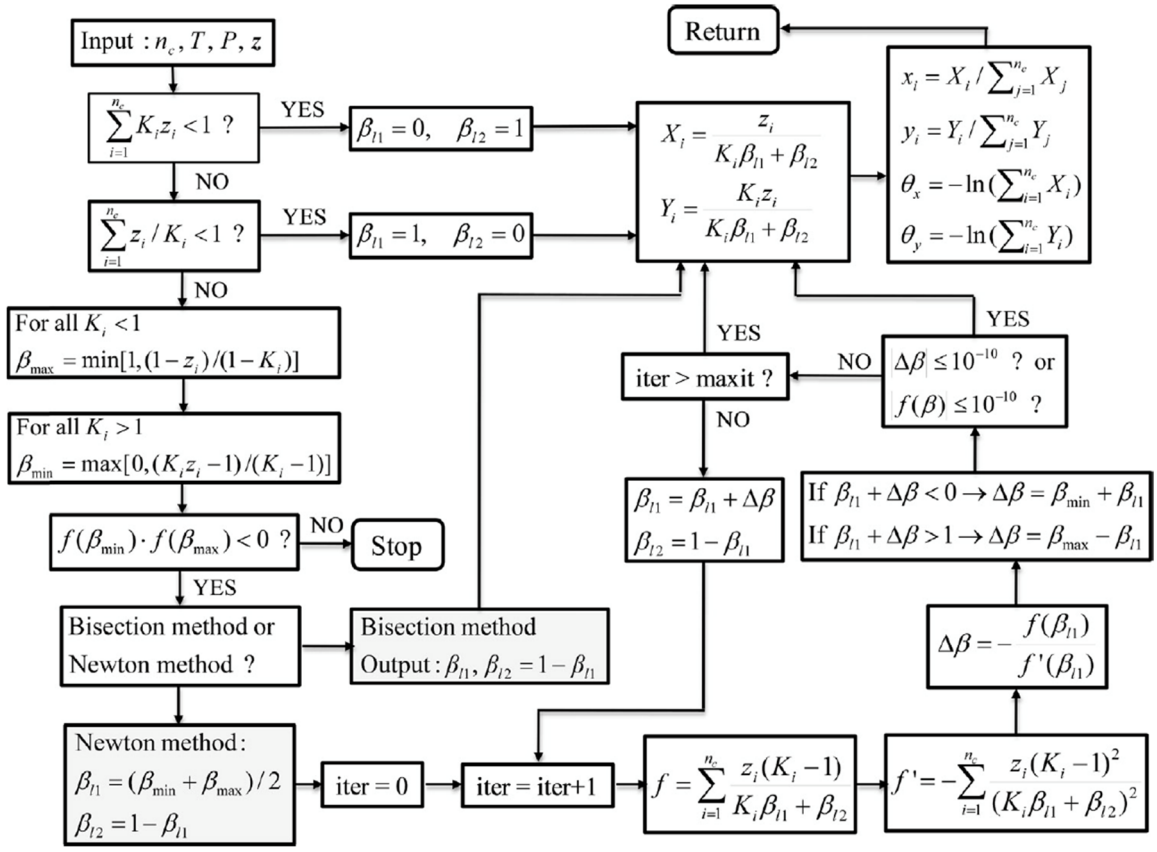

Figure 29 - Inner loop of the flash algorithm (Rashford-Rice routine). Adapted from [94] by [92].

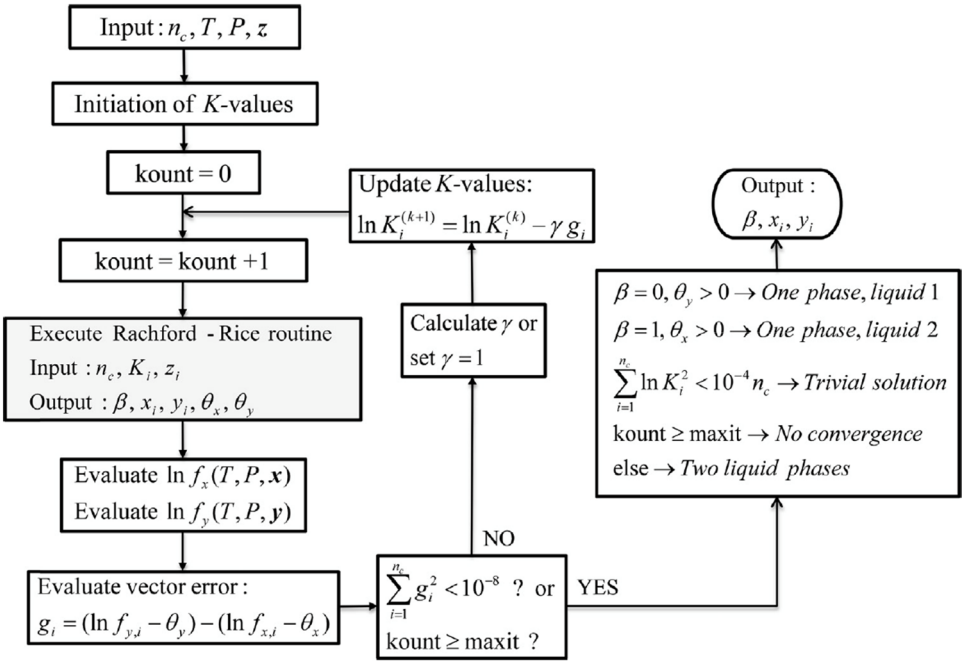

Figure 30 - Outer loop of the flash algorithm. Adapted from [94] by [92].

3.5.3 Viscosity model

The methodology adopted from Abutaqiya et al. [95] that used "General Friction Theory Viscosity Model" [96] to calculate dynamic viscosity of crude oils. The crude characterization is similar to that used for the PVT parameter modelling, with "Liquid" pseudo-component. The friction theory expresses viscosity [96] as follows:

$$\mu = \eta_o + \eta_f \tag{44}$$

Where η_f and η_o is a friction viscosity contribution and a diluted gas viscosity contribution. Diluted gas viscosity contribution is evaluated by expressions from Chung et al. [97]. The PC-SAFT Friction Theory is given as [96]:

$$\eta_f = \eta_a \left(\widetilde{k_a} \left(\frac{P_a}{P_c} \right) + \widetilde{k_{aa}} \left(\frac{P_a}{P_c} \right)^2 \right) + \eta_r \left(\widetilde{k_r} \left(\frac{P_r}{P_c} \right) + \widetilde{k_{rr}} \left(\frac{P_r}{P_c} \right)^2 \right) \tag{45}$$

η_a and η_r is viscosity scaling parameters and $\widetilde{k_a}$, $\widetilde{k_{aa}}$, $\widetilde{k_r}$, $\widetilde{k_{rr}}$ are reduced friction coefficients. P_r and P_a is a repulsive and an attractive pressure term respectively that are calculated using PC-SAFT EoS. P_c is a critical pressure of a component. The mixing rules that are used, as well as constants scaling parameters for a number of pure components and expressions for reduced coefficients, can be found in the original paper by Quiñones-Cisneros et al. [96]. For *n*-alkanes (C4+ pseudo-component), the following correlations with the segment number (m) are applied [96]:

$$\eta_a = -124.491 + \frac{5.88015}{m} + \frac{1023.46}{m^2} \tag{46}$$

$$\eta_r = 160.376 + \frac{44.6249}{m} - \frac{852.173}{m^2} \tag{47}$$

For "Liquid" pseudo-component, the following modification of above correlations are applied [95]:

$$\eta_a = K_c \left(-124.491 + \frac{5.88015}{m} + \frac{1023.46}{m^2} \right) \tag{48}$$

$$\eta_r = K_c \left(160.376 + \frac{44.6249}{m} - \frac{852.173}{m^2} \right) \tag{49}$$

Where K_c is an adjustable parameter that has to be tuned to the experimental viscosity data. Since the scaling parameters for H_2S are not provided, the model is fitted to three experimental data points of viscosity at different pressures.

3.6 Experimental crude oil data

A total of four crudes were selected for this work. Crude "A", "B" and "C" are used for the asphaltene phase behavior modelling, and Crude "D" was used for PVT and viscosity modelling. The following section contains general information about the above-mentioned crude oils.

3.6.1 Crude "A"

Crude "A" data is taken from Jamaluddin et al. [30]. The crude oil is light with API gravity of 32. The SARA analysis was performed by NIR spectroscopy. The field is reported to have problems with asphaltene precipitation.

Table 6 - Reservoir fluid characteristics of Crude "A" [30]

Measured depth (ft):	14134
Reservoir temperature (°F):	296
Reservoir pressure (psia):	3256
GOR (scf/STB):	900
API gravity:	32
SARA analysis (wt%):	
Saturates:	57.4
Aromatics:	30.8
Resins:	10.4
Asphaltenes:	1.4

Table 7 - Experimental AOPs and BPs of Crude "A" [30]

T (°F)	AOP (psi)	BP (psi)
190	5400	2500
230	4050	2700
260	3650	2900
300	3800	3060

Table 8 - Compositional analysis of Crude "A" [30]

Flashed gas			STO		
Components	MW (g/mol)	mol %	Components	MW (g/mol)	mol %
N_2	28.01	0.77	N_2	28.01	0
CO_2	44.01	17.67	CO_2	44.01	0
H_2S	34.08	5	H_2S	34.08	0
C_1	16.04	42.49	C_1	16.04	0
C_2	30.07	14.54	C_2	30.07	0.14
C_3	44.1	10.05	C_3	44.1	0.66
i-butane	58.12	1.13	*i*-butane	58.12	0.23
n-butane	58.12	4.11	*n*-butane	58.12	1.48
i-pentane	72.15	1.26	*i*-pentane	72.15	1.17
n-pentane	72.15	1.57	*n*-pentane	72.15	2.71
C_6	86.18	0.92	C_6	86.18	5.32
C_7	100.21	0.37	C_7	100.21	7.38
C_8	114.23	0.1	C_8	114.23	8.62
C_9	128.2	0.02	C_9	128.2	7.67
C_{10}	142.29	0.01	C_{10}	142.29	6.49
C_{11}	156.31	0.01	C_{11}	156.31	5.31
C_{12+}	167.11	0.01	C_{12+}	337.98	52.82

3.6.2 Crude “B” & Crude “C”

Crude “B” and Crude “C” taken from one source [98]. This paper presents the results of experimental AOP and bubble-point determination for recombined crude oils. Crude "B" has a very little asphaltene concentration (0.2 wt%), and it is a highly light crude with API gravity of 37.4 from Kuwait. Crude "C" is a light crude with API gravity of 32.7 from the Gulf of Mexico. AOPs were determined with a reported accuracy of ± 250 psi and BPs – with an accuracy of ± 50 psi.

Table 9 - SARA analysis results of Crude "B" and Crude "C" [98]

SARA analysis (wt %)	Crude “B”	Crude “C”
Saturates:	66.6	70.6
Aromatics:	27	22.5
Resins:	5.3	2.5
Asphaltenes:	0.2	2.5

Table 10 - Experimental AOPs and BPs of Crude “B” and Crude “C” [98]

	Crude “B”		Crude “C”	
T (°F)	AOP (psi)	BP (psi)	AOP (psi)	BP (psi)
167	8000	2700	8750	2950
212	7000	2900	6750	3100
257	5500	3100	5750	3200

Table 11 - The compositional analysis of Crude "B" [98]

		Flashed gas		STO	
Components	MW (g/mol)	wt %	mol %	wt %	mol %
H_2S	44.01	2.106	1.284	0	0
CO_2	34.08	0	0	0	0
N_2	28.01	0.23	0.22	0	0
C_1	16.04	37.324	62.436	0	0
C_2	30.07	17.323	15.461	0	0
C_3	44.1	16.903	10.287	0.199	0.858
i-C_4	58.12	2.897	1.338	0.086	0.282
n-C_4	58.12	9.276	4.283	0.468	1.531
i-C_5	72.15	2.93	1.09	0.41	1.08
n-C_5	72.15	4.377	1.628	0.869	2.291
C_6	84	3.66	1.169	2.46	5.573
Mcyclo-C_5	84.16	0.17	0.054	0.167	0.377
Benzene	78.11	0.07	0.024	0.074	0.181
Cyclo-C_6	84.16	0.078	0.025	0.159	0.359
C_7	96	1.446	0.404	3.243	6.427
Mcyclo-C_6	98.19	0.02	0.005	0.401	0.776
Toluene	92.14	0.134	0.039	0.416	0.859
C_8	107	0.624	0.157	4.128	7.339
C_2-benzene	106.17	0.029	0.007	0.252	0.452
m- and *p*-Xylene	106.17	0.028	0.007	0.67	1.2
o-Xylene	106.17	0.053	0.013	0.282	0.505
C_9	121	0.187	0.041	4.288	6.743
C_{10}	134	0.097	0.019	5.834	8.283

C_{11}	147	0.024	0.004	5.352	6.927
C_{12}	161	0.007	0.001	4.83	5.708
C_{13}	175	0.002	0	4.598	4.999
C_{14}	190	0.002	0	4.104	4.11
C_{15}	206	0.004	0.001	4.107	3.794
C_{16}	222	0	0	3.723	3.191
C_{17}	237	0	0	3.383	2.716
C_{18}	251	0	0	3.168	2.401
C_{19}	263	0	0	3.2	2.315
C_{20}	275	0	0	2.972	2.056
C_{21}	291	0	0	2.776	1.815
C_{22}	305	0	0	2.554	1.593
C_{23}	318	0	0	2.323	1.39
C_{24}	331	0	0	2.12	1.219
C_{25}	345	0	0	1.978	1.091
C_{26}	359	0	0	1.884	0.999
C_{27}	374	0	0	1.823	0.927
C_{28}	388	0	0	1.726	0.847
C_{29}	402	0	0	1.654	0.783
C_{30+}	548.62	0	0	17.322	6.007
MW total	-	-	26.837	-	190.26
mol %	-	-	64.268	-	35.732

Table 12 - The compositional analysis of Crude "C" [98]

		Flashed gas		STO	
Components	MW (g/mol)	wt %	mol %	wt %	mol %
H_2S	44.01	0.884	0.522	0	0
CO_2	34.08	0	0	0	0
N_2	28.01	0.496	0.46	0	0
C_1	16.04	42.439	68.668	0	0
C_2	30.07	12.49	10.782	0	0
C_3	44.1	14.571	8.578	0.185	0.869
i-C_4	58.12	3.157	1.41	0.096	0.341
n-C_4	58.12	9.466	4.228	0.446	1.592
i-C_5	72.15	3.698	1.33	0.494	1.418
n-C_5	72.15	4.593	1.652	0.851	2.445
C_6	84	3.982	1.231	2.273	5.61
Mcyclo-C_5	84.16	0.526	0.162	0.448	1.104
Benzene	78.11	0.078	0.026	0.075	0.199
Cyclo-C_6	84.16	0.482	0.149	0.479	1.181
C_7	96	1.498	0.405	2.889	6.239
Mcyclo-C_6	98.19	0.513	0.136	1.159	2.446
Toluene	92.14	0.099	0.028	0.285	0.642
C_8	107	0.551	0.134	3.692	7.153
C_2-benzene	106.17	0.03	0.007	0.199	0.389
m- and *p*-Xylene	106.17	0.018	0.004	0.549	1.072
o-Xylene	106.17	0.014	0.003	0.225	0.44
C_9	121	0.283	0.061	3.413	5.848
C_{10}	134	0.106	0.02	4.483	6.936
C_{11}	147	0.023	0.004	3.767	5.313
C_{12}	161	0.005	0.001	3.444	4.435
C_{13}	175	0	0	3.651	4.325
C_{14}	190	0	0	3.266	3.564
C_{15}	206	0	0	3.483	3.506
C_{16}	222	0	0	3.074	2.871

C_{17}	237	0	0	2.969	2.598
C_{18}	251	0	0	2.965	2.449
C_{19}	263	0	0	2.821	2.224
C_{20}	275	0	0	2.512	1.894
C_{21}	291	0	0	2.444	1.741
C_{22}	305	0	0	2.285	1.553
C_{23}	318	0	0	2.164	1.411
C_{24}	331	0	0	2.059	1.29
C_{25}	345	0	0	1.949	1.171
C_{26}	359	0	0	1.889	1.091
C_{27}	374	0	0	1.861	1.032
C_{28}	388	0	0	1.799	0.961
C_{29}	402	0	0	1.807	0.932
C_{30+}	587.73	0	0	27.55	9.718
MW total	-	-	25.958	-	207.32
mol %	-	-	60.984	-	39.016

3.6.3 Crude “D”

Crude “D”, in contrast to other that was used for this study, does not have a reported problem with asphaltene precipitation. It is a Kazakhstan light crude (API gravity of 40.91) with the high sulfur content (13 mol %). This crude was selected to assess the ability of PC-SAFT EoS to model liquid densities and viscosities.

Table 13 - General data of Crude "D"

Reservoir temperature (°F):	223
GOR (scf/STB):	2675.91
API:	40.91
BP (psi):	3739.1

Table 14 - The composition of Crude "D"

Components	mol %	MW (g/mol)
Flashed gas		
H_2S	16.46	34.08
CO_2	3.64	44.01
N_2	1.1	28.01
C_1	54.84	16.04
C_2	10.8	30.07
C_3	5.89	44.1
C_{4+}	7.27	69.587
STO		
STO	1	180

Table 15 - Experimental densities and viscosities at the reservoir pressure of Crude "D"

P (psi)	Viscosity (cP)	Density (g/cc)
10760.4	0.173	0.6308
9514.5	0.148	0.6096
7514.4	0.137	0.5983
6515.1	0.126	0.5852
5514.3	0.115	0.5693
4515.0	0.104	0.5488
3814.5	0.096	0.5297
3739.1	0.096	0.5271
3514.3	0.114	0.5377
2515.0	0.176	0.5783
2014.6	0.203	0.6009
1514.2	0.237	0.6245
1015.3	0.292	0.6472
514.9	0.39	0.6726
265.4	0.473	0.684
14.5	0.641	0.7371

4 RESULTS AND DISCUSSIONS

4.1 Asphaltene Phase Behavior Modelling

This work models Crude “A”, “B” and “C” using both the “SARA-based” and the modified method. The characterization for Crude “A” can be seen in Table 16. As can be seen, the parameters for gas phase components are the same, and a difference is in the division of liquid phase into three and two pseudo-components respectively. Molecular weight for asphaltene pre-aggregates was set as 1700 g/mol, and the ratio of molecular weights of C_{12+} Saturates and Aromatics+Resins were assumed to be 0.9 (as was recommended in the literature [5]). A+R/S+A+R parameters were tuned to the bubble point at 230°F and STO density.

Table 16 - Characterization of crude oil "A" by the "SARA-based" method and the modified method

Recombined fluid			PC-SAFT parameters		
Components	MW (g/mol)	X (mol/mol)	m	σ (Å)	ϵ/k_{BT} (°K)
N_2	28.01	0.004957	1.205	3.313	90.960
CO_2	44.01	0.113759	2.073	2.785	169.210
H_2S	34.08	0.03219	1.652	3.074	227.340
C_1	16.04	0.273551	1.000	3.704	150.030
C_2	30.07	0.093609	1.607	3.521	191.420
C_3	44.1	0.064702	2.002	3.618	208.110
C_{4+}	67.69	0.061032	2.584	3.748	229.572
“SARA-based” method					
Saturates	183.53	0.258275	5.561	3.911	250.890
A+R (γ = 0.385)	349.88	0.097245	7.287	4.152	357.363
Asphaltenes	1700	0.00068	33	4.2378	390
The modified method					
S+A+R (λ = 0.13)	229.033	0.35552	5.972	3.966	280.841
Asphaltenes	1700	0.00068	33	4.1845	390

Two methods were checked for their accuracy by modelling BP and AOP at experimental data points. One experimental data point of BP was used to model tuning (at 230°F), and others were used to evaluate the predictive capabilities between predicted and experimental data. Also, this crude was used to alter Asphaltene – S+A+R BIP for the modified method. The results for both methods can be seen in Table 17 and Figure 31.

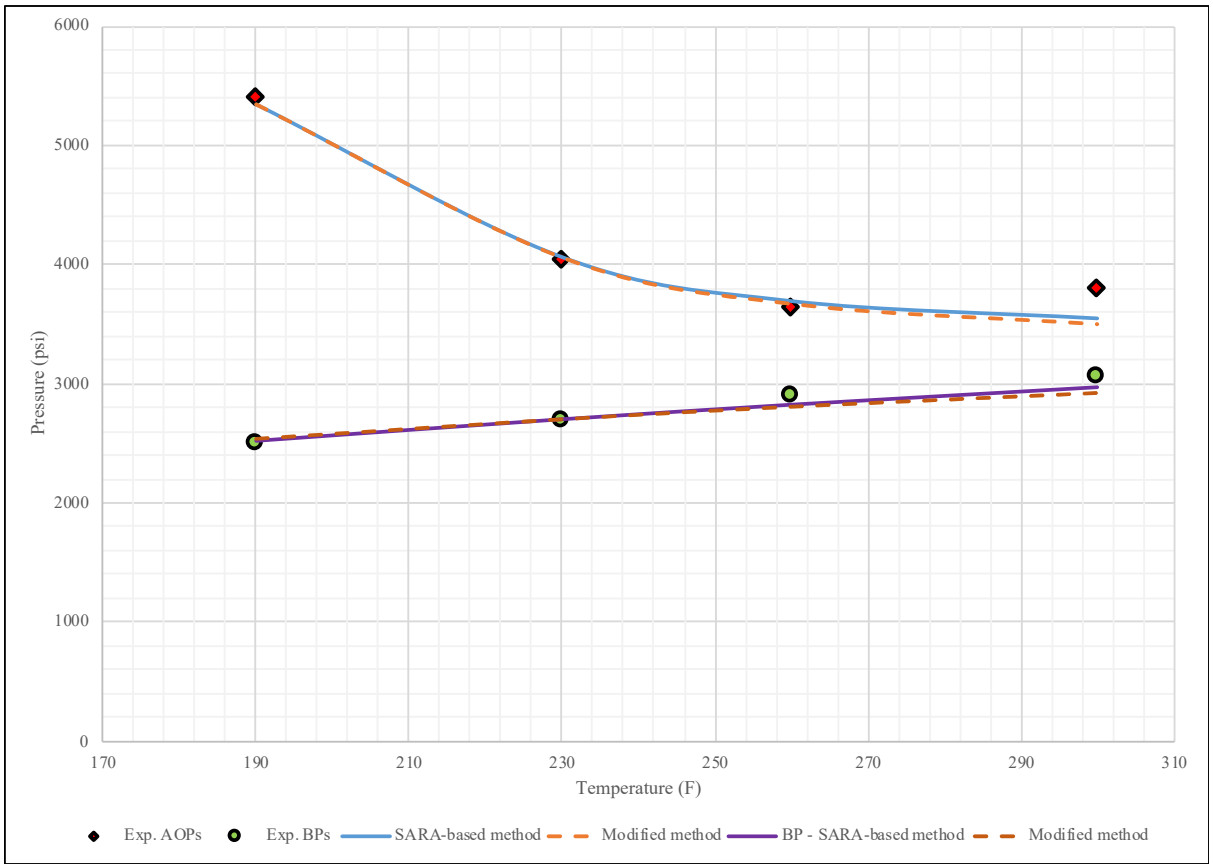

Figure 31 - Modelling at experimental data points [30] for both methods for Crude “A”.

Table 17 - Results of modelling at experimental data points [30] by both methods for Crude “A”

T	Exp. BP	Exp. AOP	BP	AOP	BP – APE	AOP – APE
(°F)	(psi)	(psi)	(psi)	(psi)	(%)	(%)
The modified method						
190	2500	5400	2543.2	5344.4	1.728	1.030
230	2700	4050	2703.1	4053.5	fitting point	fitting point
260	2900	3650	2805.9	3662.9	3.245	0.353
300	3060	3800	2918.8	3492.2	4.614	8.100
				MAPE (%):	**3.161**	**3.196**
The “SARA-based” method						
190	2500	5400	2524.2	5338.8	0.968	1.133
230	2700	4050	2700.2	4052.2	fitting point	fitting point
260	2900	3650	2819.9	3685.5	2.762	0.973
300	3060	3800	2963.6	3539.2	3.150	6.863
				MAPE (%):	**2.293**	**2.990**

As can be seen, both methods showed comparable results in modelling BPs and AOPs. The slope of the BP line was found to be slightly more horizontal than the actual experimental data slope, which leads to errors, especially at the higher temperature. The asphaltene parameter σ was altered in order to achieve fit to the experimental data point. It was observed that the increase in this parameter decreases the AOP. It should be noted that usually at least three data points of AOP are required to fit the model for each of the EoS parameters. One parameter alteration here used only as a simplification to speed up the process and due to the unavailability of more than three AOPs for Crude “B” and “C”. Since initial guesses were good enough, it was possible to generate curve with acceptable accuracy that fits to three AOPs (in case of Crude “A”) and no further model fitting was performed except for BIP alteration on the Crude “A” (at the fitting point and at AOP of 190°F). Models can possibly be improved for both methods by tuning them to the more experimental data points of the AOP.

The modified method was used to generate the P-T phase diagram for crude "A" (Figure 32). The upper AOP line, the bubble point line and the lower AOP line are generated over the temperature range from 190°F to 470°F. Upper AOP line is the line at below which asphaltene-

rich phase starts to split from crude oil. The precipitation continues and reaches its maximum at the bubble point pressure. Below the bubble point pressure, gas-phase starts to liberate, making the asphaltene-rich phase more soluble in crude oil. At the lower AOP, the incipient phase stops to precipitate, and asphaltenes are completely reintegrated into the crude. The process can be observed in the generated contour maps of asphaltene and gas-phase precipitation intensity (Figure 33 and Figure 34).

The phase diagram suggests that there is a particular value of temperature, below which the full reintegration of the asphaltene-rich phase is not possible regardless of change in pressure. Lower AOP curve is reaching zero at a temperature of 240°F. It can be essential for industrial applications since although the reservoir is assumed to be isothermal, the temperature conditions will go down drastically when crude flows in wells and surface facilities.

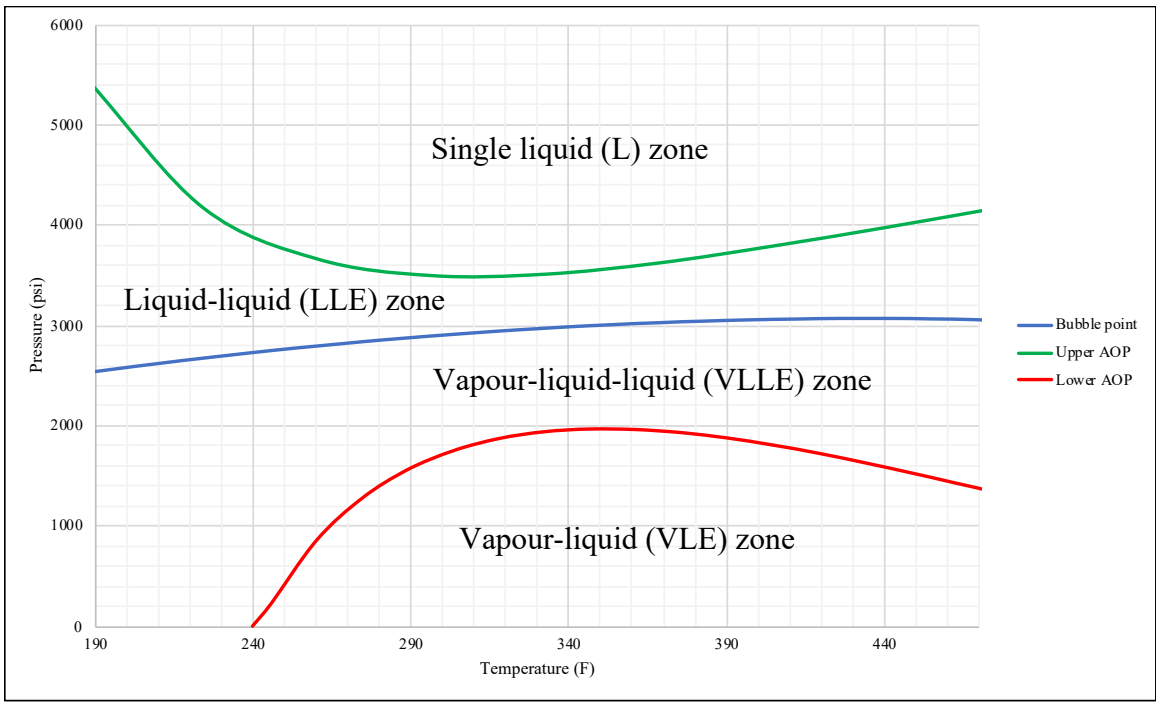

Figure 32 - Phase Diagram for Crude "A"

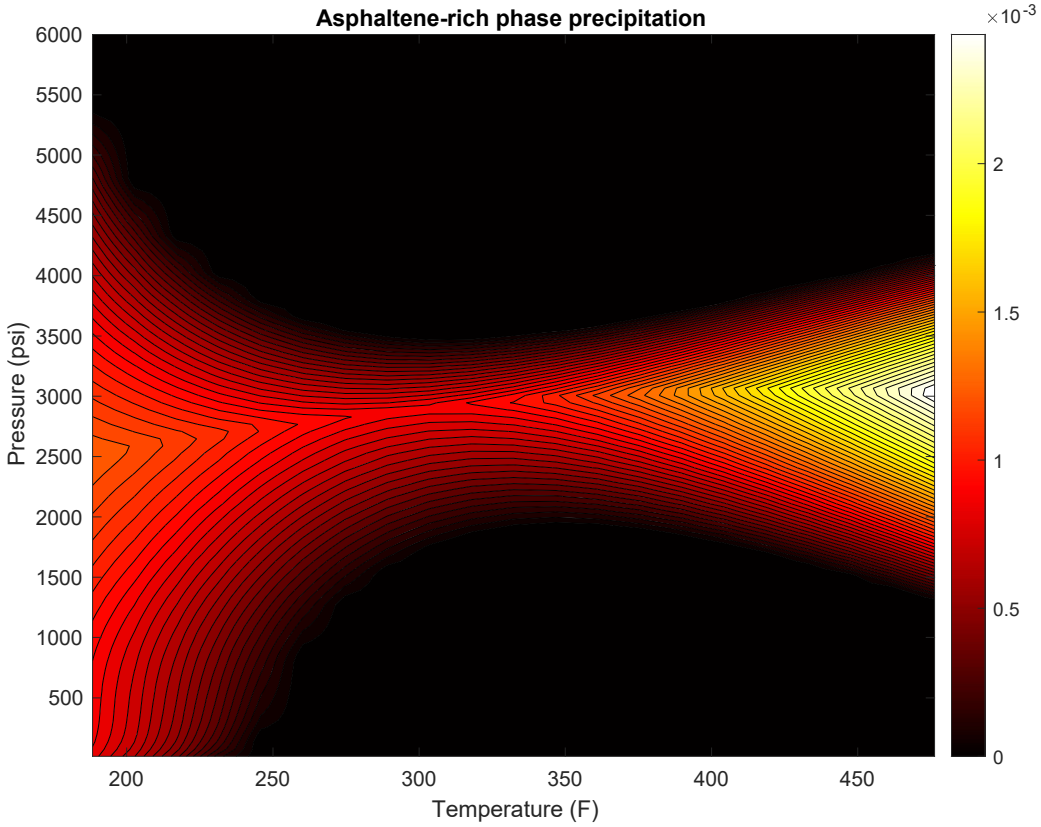

Figure 33 - Contour map of asphaltene phase precipitation for Crude "A" in terms of the fraction of total molar amount.

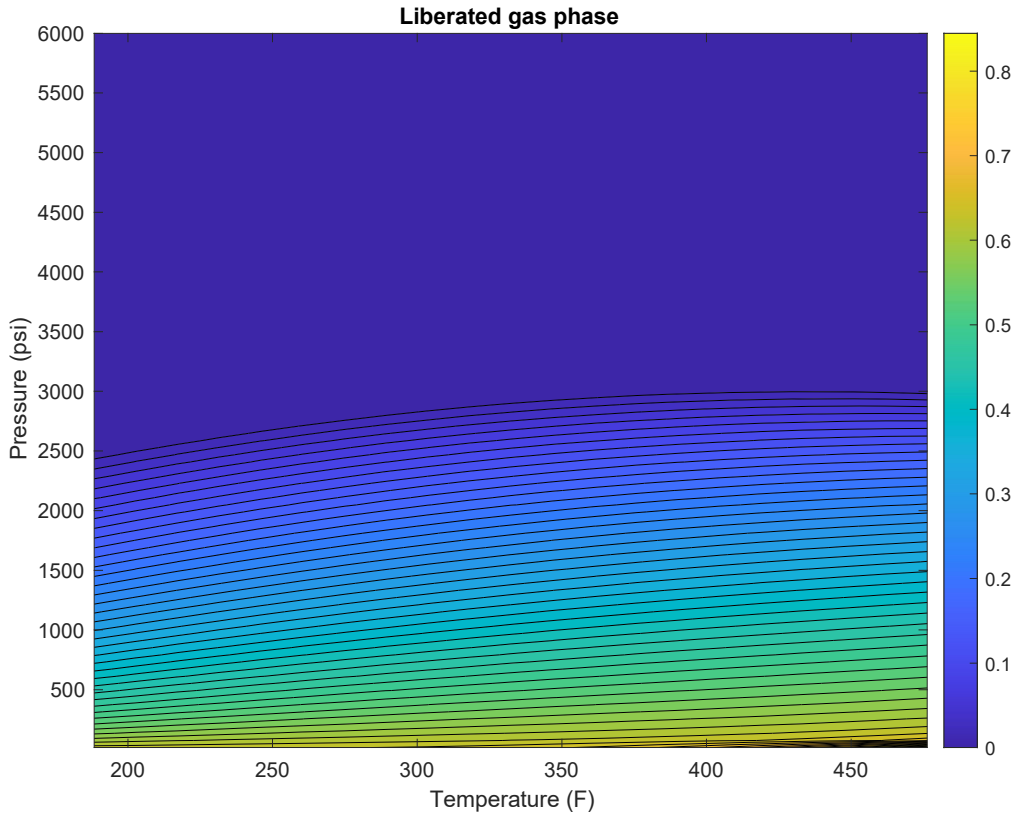

Figure 34 - Contour map of gas-phase precipitation for Crude "A" in terms of the fraction of total molar amount.

Crude “B” was similarly modelled using both the “SARA-based” and the modified methods. The results can be seen in Table 18. A+R/S+A+R parameters were tuned to the bubble point at 212°F and density at corresponding bubble point pressure. The results of the comparative modelling can be seen in Figure 35 and Table 19. The asphaltene parameter ϵ/k_{BT} was altered in order to achieve fit to the experimental data point. It was observed that the increase in this parameter increases the AOP. The results demonstrate that both models gave almost similar results in fitting to experimental AOPs and predicting BPs. PC-SAFT models were successful in modelling of AOP at the higher temperature. However, at the lower temperature AOP, the curve rapidly deviates upward and results in huge errors at the low-temperature AOP.

The same behavior is observed in Crude "C" modelling (Figure 37 and Table 21). As was mentioned, both crudes are from the same source. It was attempted to alter segment number (*m*) to fit the AOP. It was observed that the increase in this parameter increases the AOP. However, the value exceeded the range reported in the literature (Table 2). Asphaltene parameter ϵ/k_{BT} was altered in order to achieve fit to the experimental data point instead.

Table 18 - Characterization of crude oil "B" by the "SARA-based" method and the modified method

Recombined fluid			PC-SAFT parameters		
Components	MW (g/mol)	X (mol/mol)	m	σ (Å)	ϵ/k_{BT} (°K)
N_2	28.01	0.0014	1.205	3.313	90.960
CO_2	44.01	0.0083	2.073	2.785	169.210
C_1	16.04	0.4013	1.000	3.704	150.030
C_2	30.07	0.0994	1.607	3.521	191.420
C_3	44.1	0.0661	2.002	3.618	208.110
C_{4+}	67.974	0.0663	2.591	3.749	229.706
The “SARA-based” method					
Saturates	174.215	0.2616	5.321	3.905	250.194
A+R (γ = 0.34)	232.925	0.0956	5.312	4.055	338.394
Asphaltenes	1700	0.00008	33	4.33	406.37
The modified method					
S+A+R (λ = 0.41)	189.92	0.3572	5.289	3.928	271.05
Asphaltenes	1700	0.00008	33	4.33	414.06

This work was not able to find a set of parameters that can give a good fit to the low-temperature AOP. Changing Asphaltene pseudo-component parameters, molecular weight and its BIPs with other components had no or little effect on the curve steepness at the lower temperatures. It was noted, however, that for different molecular weights there are different sets of parameters that can reproduce the same curve. This observation can be explained by the fact that the EoS parameters are directly dependent on the molecular weight of a pseudo-component. A wide range of molecular weights of asphaltene pre-aggregates can be set and give similar results. In this work, MWs of 600 g/mol, 1000 g/mol and 2000 g/mol was checked for the Crude "B" and for each case it was possible to tune a set of parameters that reproduce the curve in Figure 35.

Such erratic behavior of PC-SAFT asphaltene phase behavior models at the lower temperatures has also been noted by several authors in the literature. Ting et al. [67] noted the PC-SAFT model deviation from experimental data at lower temperatures for the asphaltenes-toluene-methane mixtures. Authors suggested that inclusion of asphaltene polydispersity can solve the problem. The similar problem was mentioned by Arya et al. [88]. Abutaqiya et al. [99] named the temperature at which the slope of the AOP curve is reaching infinity the Minimum Upper Critical Solution Temperature. Authors also mention that all SAFT-based models tend to have such low-temperature behaviour [99].

Recently, AlHammadi et al. [100] encountered a similar trend of AOP curve with several crudes. Authors note that generally, the experimental onsets follow the specific pattern, with an abrupt increase of AOP values at low temperatures. However, some crudes demonstrate atypical behavior with the onset curve increasing linearly with a decrease in temperature. The experimental AOPs of Crude “B” and Crude “C”, as can be seen in Figure 35 and Figure 37, demonstrate precisely such kind of trends. They explained the erratic behavior of the model by the nature of experimental procedures that are used for AOP detection. The slow aggregation of asphaltenes at low temperatures and not sufficient equilibration time during the experiments cause the onset of asphaltene precipitation to be spotted at lower pressures and the actual onset to be bypassed [100].

Table 19 - Results of modelling at experimental data points [98] for both methods for Crude "B"

T (°F)	Exp. BP (psi)	Exp. AOP (psi)	BP (psi)	AOP (psi)	BP – APE (%)	AOP – APE (%)
The modified method						
167	2700	8000	2780.3	13416	2.974	67.700
212	2900	7000	2902.9	7003	fitting point	fitting point
257	3100	5500	2990.6	5597	3.529	1.764
				MAPE (%):	**3.252**	**34.732**
The "SARA-based" method						
167	2700	8000	2764.3	16950	2.381	111.875
212	2900	7000	2901.7	7001	fitting point	fitting point
257	3100	5500	3007.2	5461	2.994	0.709
				MAPE (%):	**2.688**	**56.292**

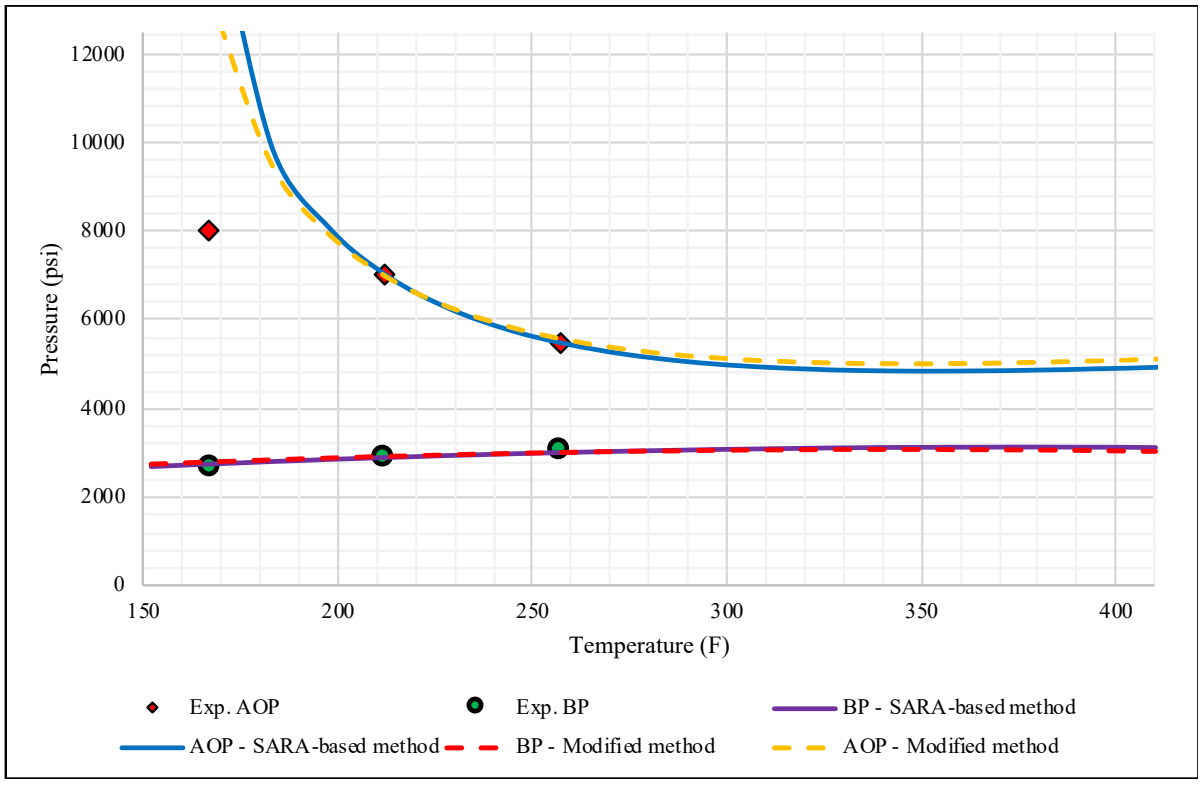

Figure 35 - Modelling at experimental data points [98] by both methods for Crude "B"

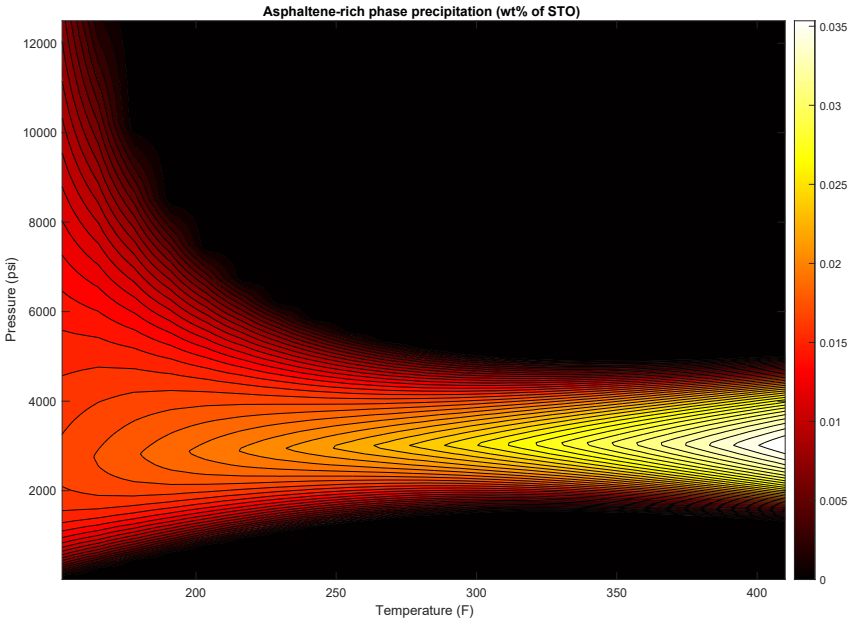

Figure 36 - The contour map of asphaltene phase precipitation for Crude “B” (wt% of STO)

Table 20 - Characterization of crude oil "C" by the "SARA-based" method and the modified method

Recombined fluid			PC-SAFT parameters		
Components	MW (g/mol)	X (mol/mol)	m	σ (Å)	ϵ/k_{BT} (°K)
N_2	28.01	0.0028	1.205	3.313	90.960
CO_2	44.01	0.0032	2.073	2.785	169.210
C_1	16.04	0.4188	1.000	3.704	150.030
C_2	30.07	0.0658	1.607	3.521	191.420
C3	44.1	0.0523	2.002	3.618	208.110
C_{4+}	68.773	0.0670	2.612	3.751	230.081
“SARA-based” method					
Saturates	194.32	0.2978	5.838	3.917	251.61
A+R (γ = 0.645)	230.321	0.0911	4.706	4.125	385.614
Asphaltenes	1700	0.0012	33	4.33	385.8
Modified method					
S+A+R (λ = 0.295)	202.755	0.3890	5.503	3.941	275.171
Asphaltenes	1700	0.0012	33	4.33	401.1

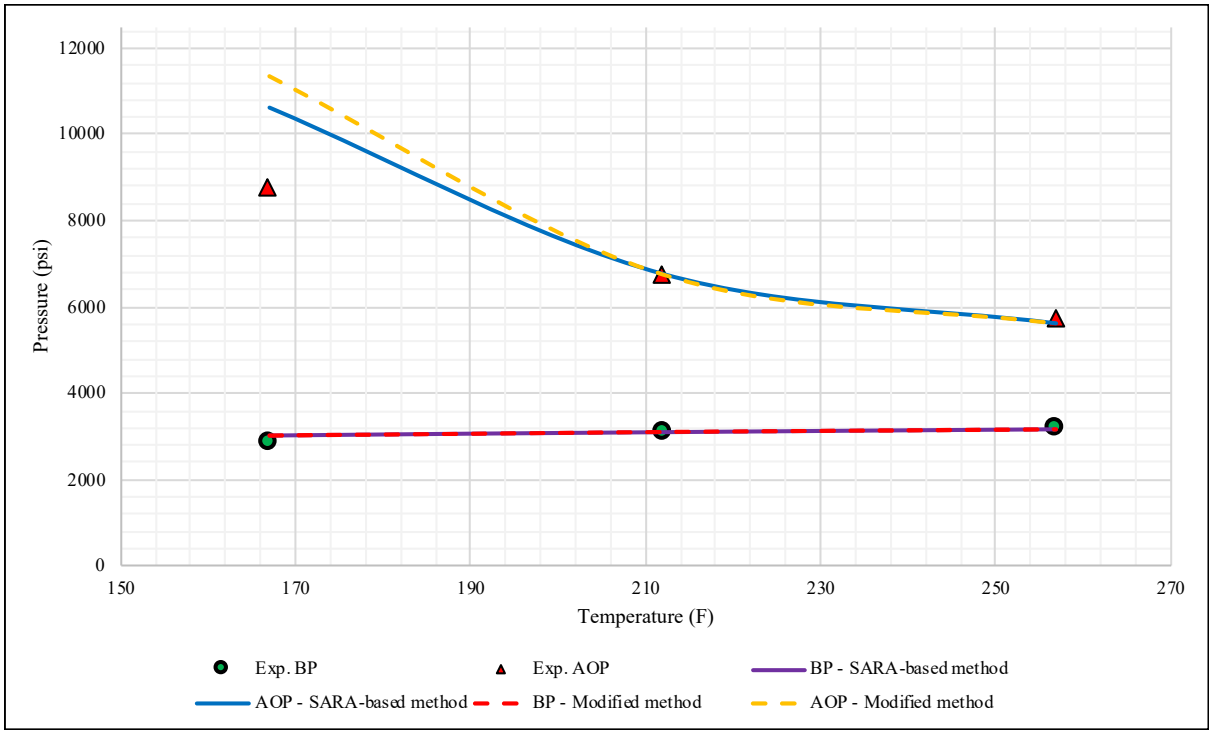

Figure 37 - Predictions at experimental data points [98] by both methods for Crude "C"

Table 21 - Results of modelling at experimental data points [98] for both methods for Crude "C"

T (°F)	Exp. BP (psi)	Exp. AOP (psi)	BP (psi)	AOP (psi)	BP – APE (%)	AOP – APE (%)
The modified method						
167	2900	8750	3033.4	11361	4.6	29.840
212	3100	6750	3109.9	6753	fitting point	fitting point
257	3200	5750	3166.3	5617	1.053	2.313
				MAPE (%):	**2.827**	**16.077**
"SARA-based" method						
167	2900	8750	3010.7	10608	3.817	21.234
212	3100	6750	3098.7	6754	fitting point	fitting point
257	3200	5750	3168.1	5606	0.997	2.504
				MAPE (%):	**2.407**	**11.869**

4.2 Advantages of the modified method

While it was shown that both methods gave comparable results of the modelling. The modified method does not require full SARA analysis as "SARA-based" method. The concentration of asphaltene fraction and MW of STO is enough to characterize the liquid pseudo-components.

Since full SARA analysis can be unavailable, the modified method can serve as a viable alternative to perform the asphaltene phase behavior modelling.

Another difference is the computational time required to perform the simulation. Figure 38 demonstrates the decrease in CPU time when the modified method was applied instead of the "SARA-based" method. Generally, the convergence of equilibrium algorithms depends on the quality of initial guesses and individual complexity of crude oil systems. This fact explains the varying results for different crudes. For both methods, the same starting parameters were set (such as initial guesses, P-T conditions, tolerance constraints) for each case. Despite the variations in results for each case, generally, the increase in computational efficiency was achieved for all three crudes. Saturates and A+R pseudo-components are of high molar concentration and lumping of such components substantially decreased the time of convergence of algorithms.

The effect is not significant when two- or three-flash algorithms are applied since they are usually very fast to converge. However, when AOP and BP algorithms are applied to generate P-T curves in a wide range of temperatures, the significant amount of time is saved not only during the predictions but especially during the model tuning processes (since the model tuning include a large number of BP and AOP calculations). The computational efficiency is especially crucial when generating precipitation contour maps (such as in Figure 33 and Figure 36) because such algorithms include the initiation of thousands of three- and two-phase flash calculations at different pressures and temperatures.

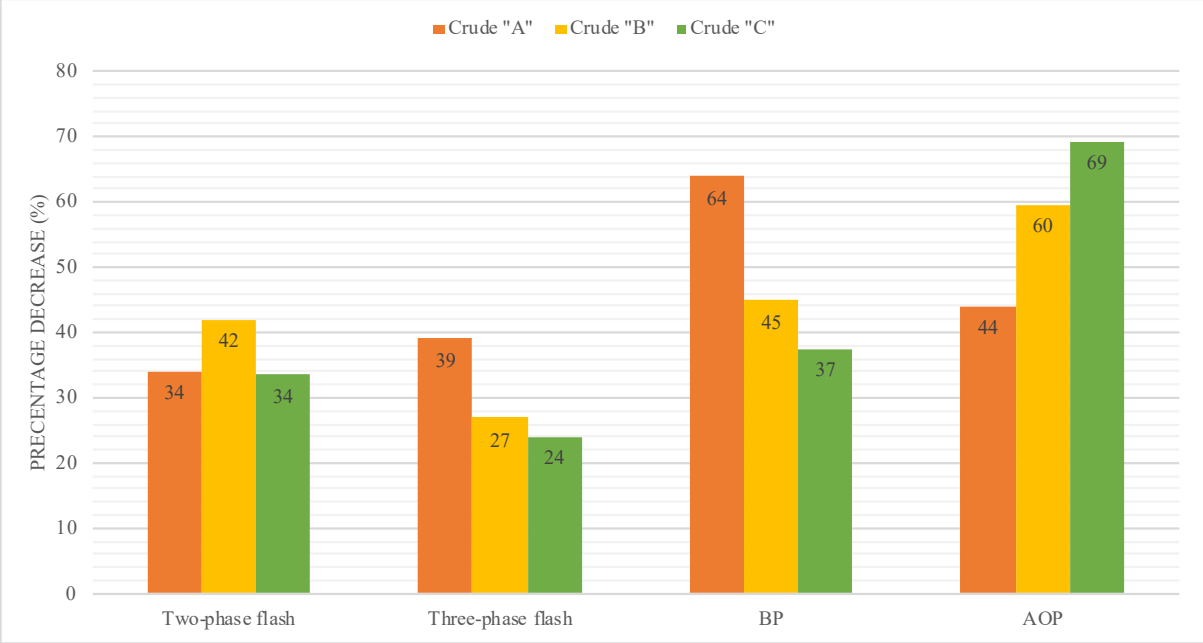

Figure 38 - Decrease in the CPU time during the modified method modelling in comparison with the "SARA-based" method for four different algorithms

4.3 PVT parameter modelling

Crude “D” was selected to evaluate the ability of PC-SAFT to model PVT parameters of crude oil. The significant difference in the modelling method is that the liquid phase was characterized by lumping all STO components into one “Liquid” pseudo-component. Flashed gas composition is characterized in a conventional way. The characterized crude parameters are shown in Table 22. Experimental data and PC-SAFT model prediction results are shown in Table 23 and Figure 39.

Table 22 - Characterization for Crude “D”

Recombined fluid			PC-SAFT parameters		
Components	MW	X	m	σ	ϵ/k_{BT}
	(g/mol)	(mol/mol)		(Å)	(°K)
H_2S	34.08	0.1338	1.652	3.074	227.340
CO_2	44.01	0.0296	2.073	2.785	169.210
N_2	28.01	0.0089	1.205	3.313	90.960
C_1	16.04	0.4458	1.000	3.704	150.030
C_2	30.07	0.0878	1.607	3.521	191.420
C_3	44.10	0.0479	2.002	3.618	208.110
C4+	69.59	0.0591	2.633	3.754	230.454
Liquid ($\gamma = 0.125$)	180	0.1870	5.2301	3.9318	270.6877

The usual procedure is to fit the aromaticity parameter to the bubble point and density of crude. However, in this work, “Liquid” pseudo-component parameters were tuned to the reservoir

bubble point (BP = 3739.1 psi) only. All the density data points are used for model validation. This was done in order to evaluate the ability of PC-SAFT to model densities in a fully predictive way. The correlations from Punnapala & Vargas are used for the "Liquid" pseudo-component tuning [7].

The results show a good match with experimental data with a MAPE of 2.36%. The predicted curve slightly overpredicts densities at and below the bubble point. Crude "D" has its liquid STO composition and MW from the same sample on which density and viscosity measurements were made. However, due to the unavailability of the gas composition data for this sample, the gas composition is taken from the average gas composition across all samples of this crude. This may be the reason why the model gives such high deviations from experimental data below the bubble point.

Table 23 - Density prediction results for Crude "D" at the reservoir temperature

Experimental data			**Model predictions**	
	Pressure	Density	Density	APE
#	(psi)	(g/cc)	(g/cc)	(%)
1	10760.4	0.6308	0.622	1.388
2	9514.5	0.6096	0.612	0.406
3	7514.4	0.5983	0.594	0.780
4	6515.1	0.5852	0.583	0.394
5	5514.3	0.5693	0.571	0.251
6	4515.0	0.5488	0.557	1.434
7	3814.5	0.5297	0.545	2.934
8	3739.1	0.5271	0.544	3.274
9	3514.3	0.5377	0.556	3.457
10	2515.0	0.5783	0.603	4.232
11	2014.6	0.6009	0.624	3.880
12	1514.2	0.6245	0.646	3.417
13	1015.3	0.6472	0.669	3.340
14	514.9	0.6726	0.695	3.330
15	265.4	0.684	0.710	3.790
16	14.5	0.7371	0.726	1.455
			MAPE (%):	**2.36**

Once the model is tuned and validated, it is possible to model several PVT parameters (from Figure 40 to Figure 43). The modelling of density and other PVT parameter are straightforward and require a very little of computational time. The most relatively time-consuming the algorithm is a liquid-vapor flash calculation below the bubble-point. Another

advantage is that the PVT modelling requires a little experimental data since it does not need SARA analysis at all.

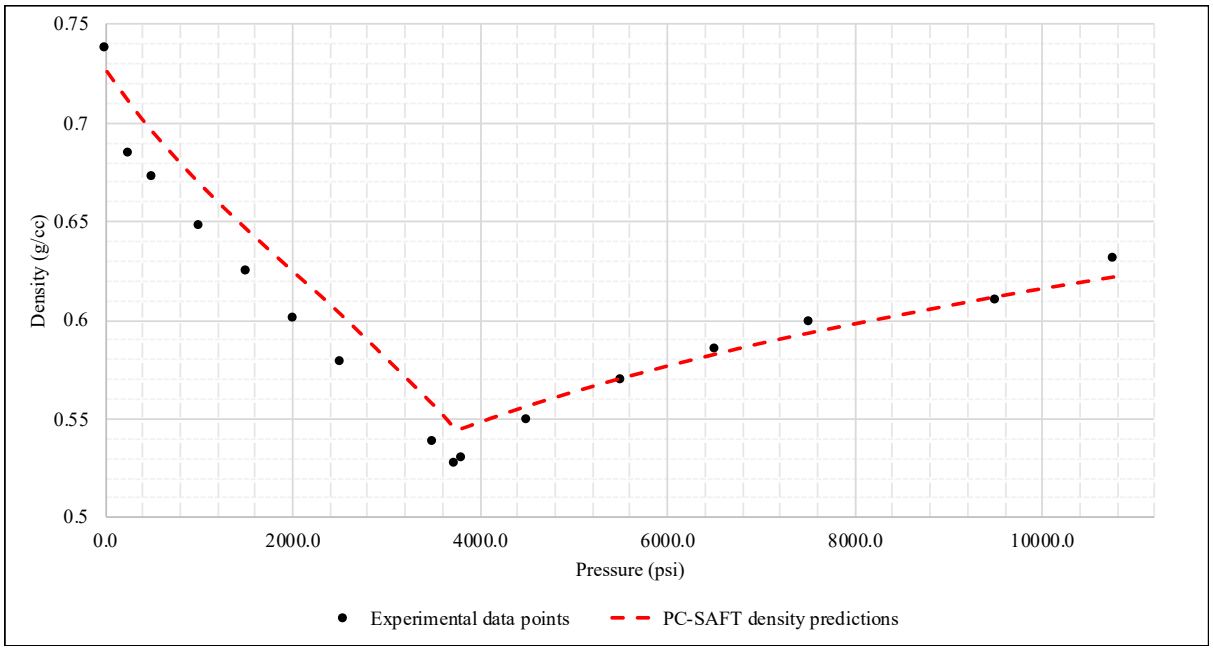

Figure 39 - Density predictions for Crude "D"

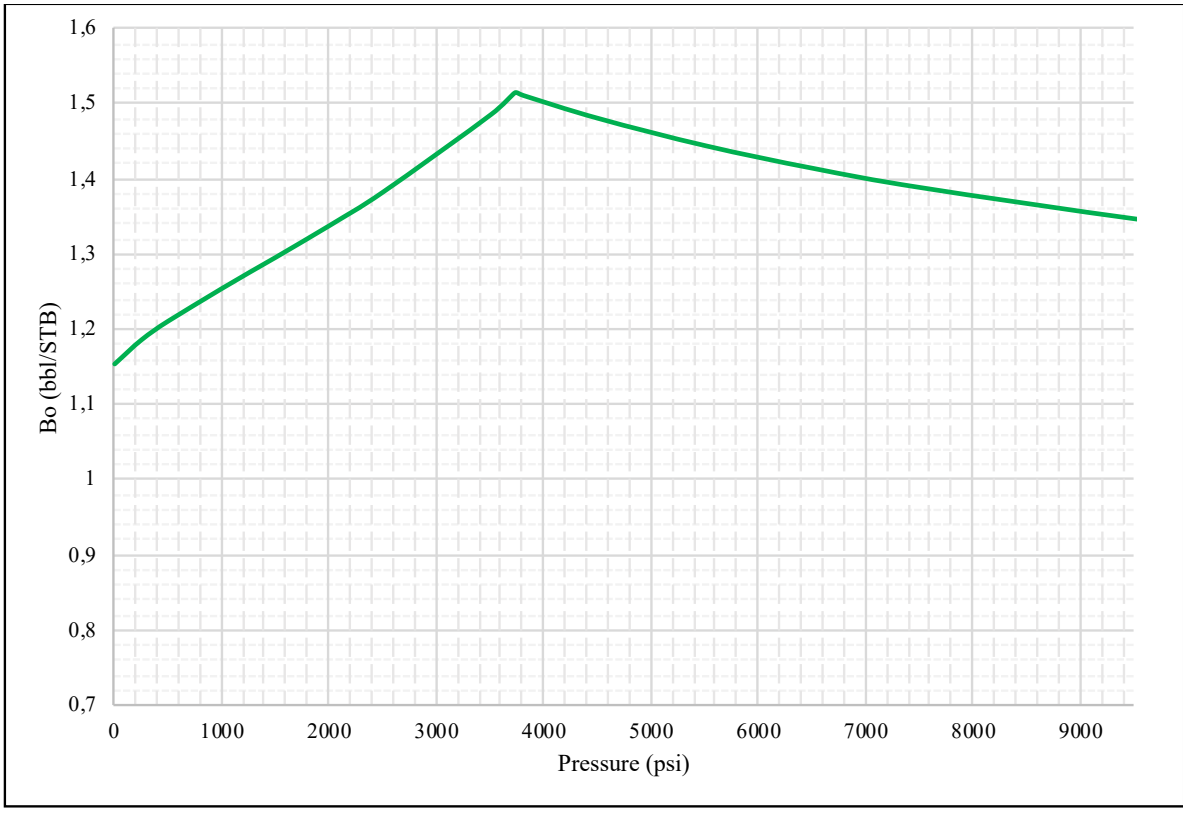

Figure 40 - Oil formation volume factor predictions for Crude "D"

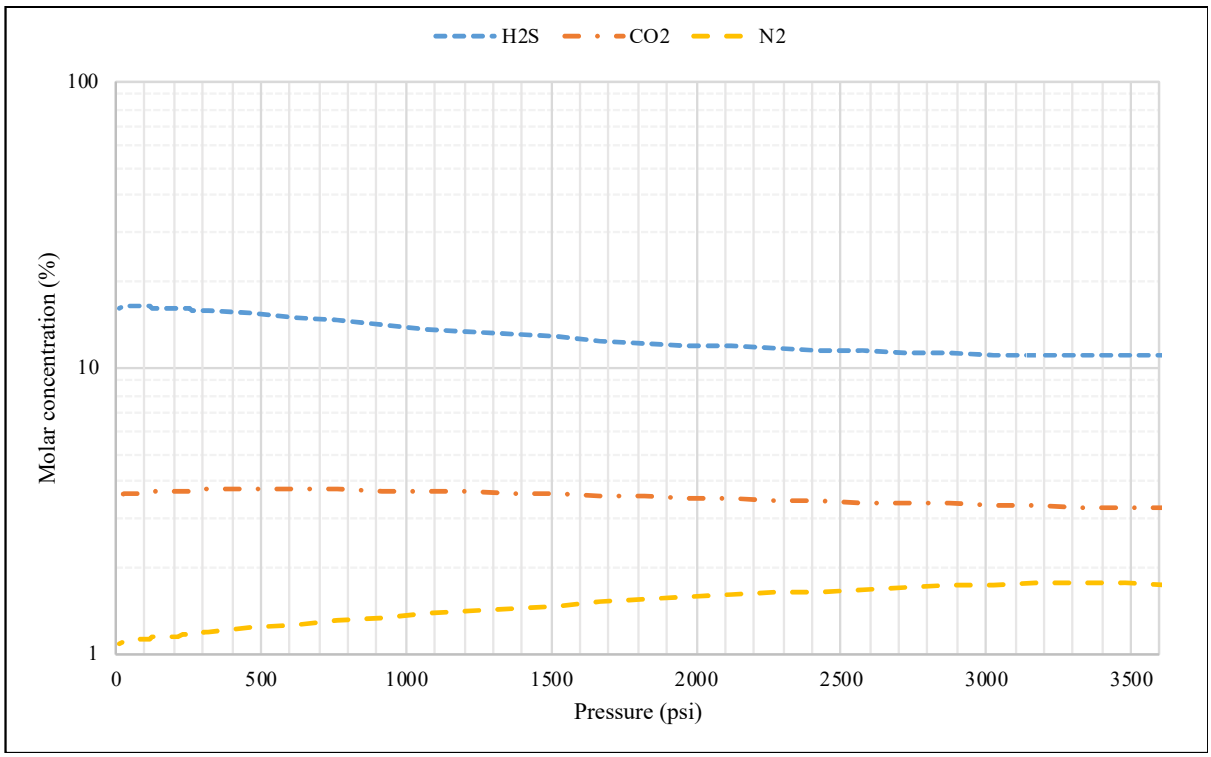

Figure 41 - The molar concentrations of several non-hydrocarbon components in the gas phase for Crude “D”

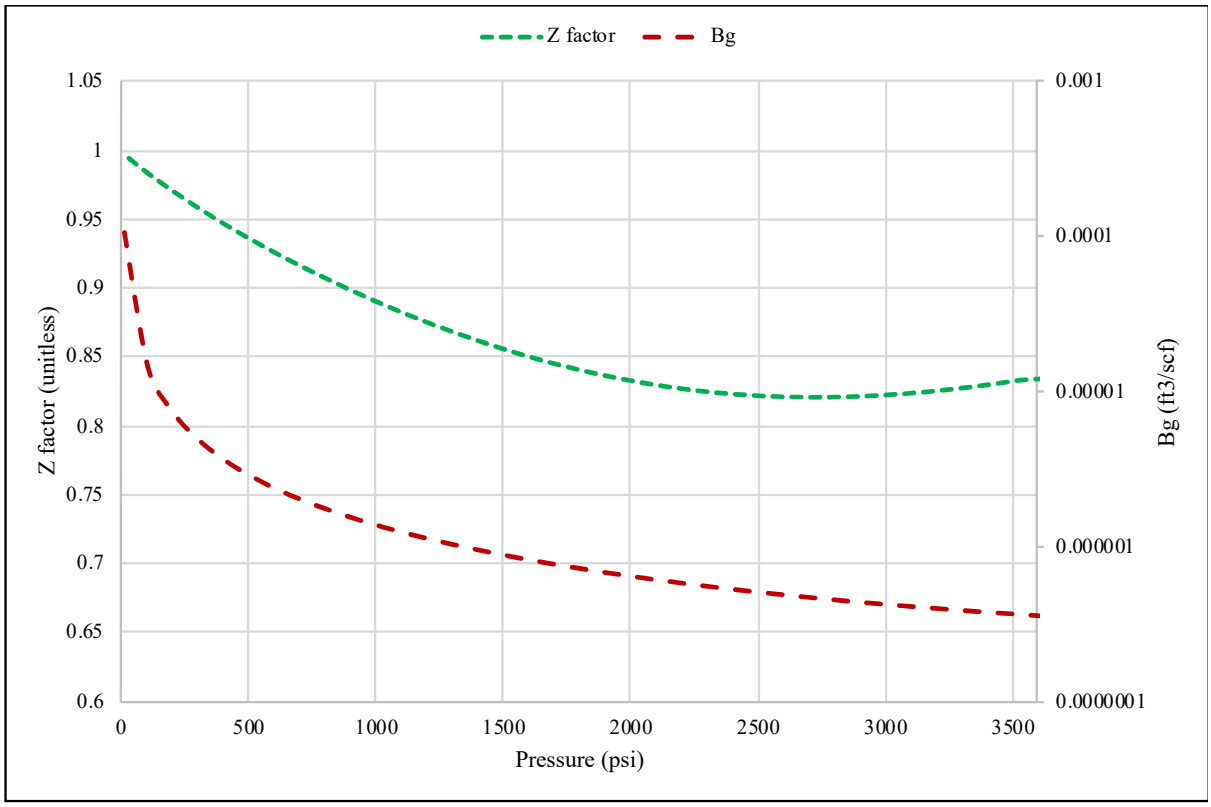

Figure 42 - Predicted gas parameters for Crude "D"

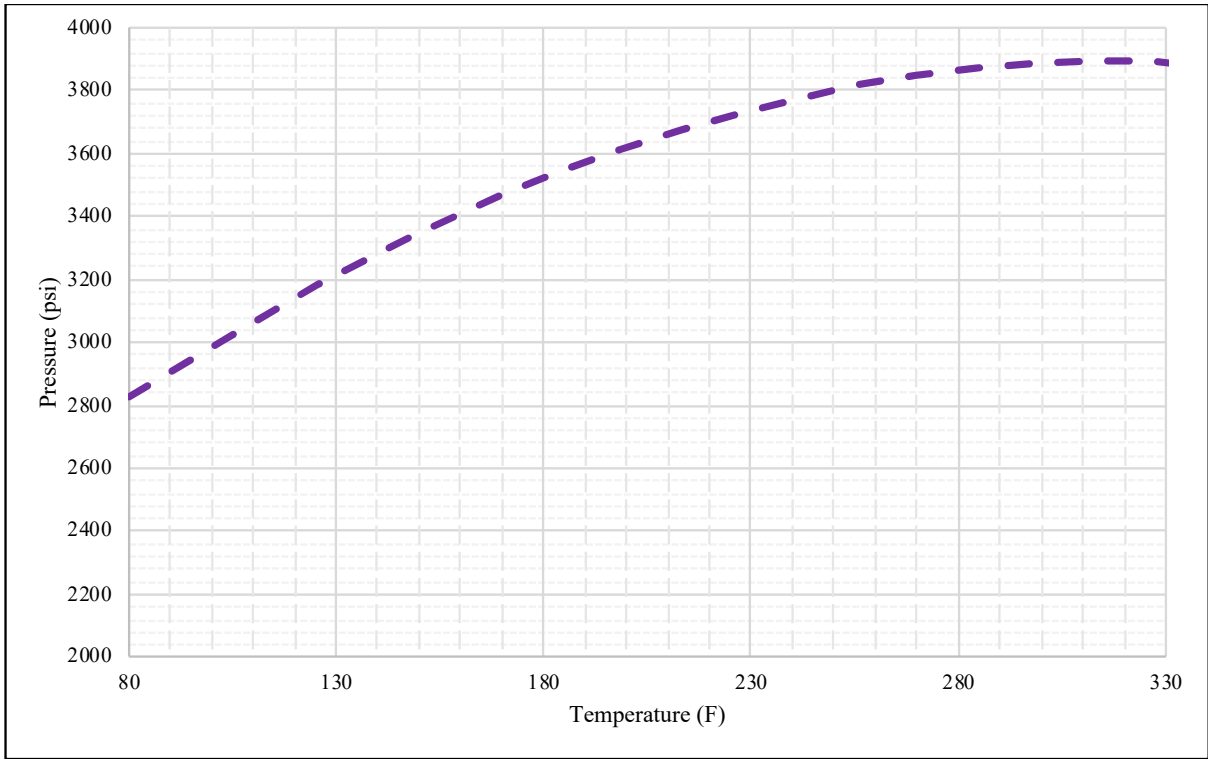

Figure 43 - Predicted bubble point pressure line for Crude "D"

4.4 Viscosity modelling

The modelling parameters used can be seen in Table 24. The results are demonstrated in Table 25 and Figure 44.

Table 24 - Parameters for the viscosity modelling for Crude "D"

Recombined oil			Viscosity model scaling parameters	
Components	MW	X	η_a	η_r
	(g/mol)	(mol/mol)	(μP)	(μP)
H_2S	34.08	0.1338	16.5936	-466.0333
CO_2	44.01	0.0296	-16.1322	119.251
N_2	28.01	0.0089	2.28277	57.7935
C_1	16.04	0.4458	8.15957	48.741
C_2	30.07	0.0878	9.04189	49.9325
C_3	44.10	0.0479	1.29954	65.0437
C_{4+}	69.59	0.0591	25.3704	300.2453
Liquid (K_c = 0.5514)	180	0.1870	-48.141	109.6164

Table 25 - Results of the viscosity model for Crude “D”

Experimental data			Model predictions	
	Pressure	Viscosity	Viscosity	APE
#	(psi)	(cP)	(cP)	(%)
1	10760.4	0.173	0.173	fitting point
2	9514.5	0.148	0.159	7.703
3	7514.4	0.137	0.138	0.438
4	6515.1	0.126	0.127	0.635
5	5514.3	0.115	0.116	0.783
6	4515.0	0.104	0.105	0.769
7	3814.5	0.096	0.097	0.937
8	3739.1	0.096	0.096	fitting point
9	3514.3	0.114	0.104	9.211
10	2515.0	0.176	0.146	17.273
11	2014.6	0.203	0.175	13.596
12	1514.2	0.237	0.217	8.608
13	1015.3	0.292	0.279	4.315
14	514.9	0.39	0.390	fitting point
15	265.4	0.473	0.481	1.628
16	14.5	0.641	0.611	4.758
			MAPE (%):	**5.445**

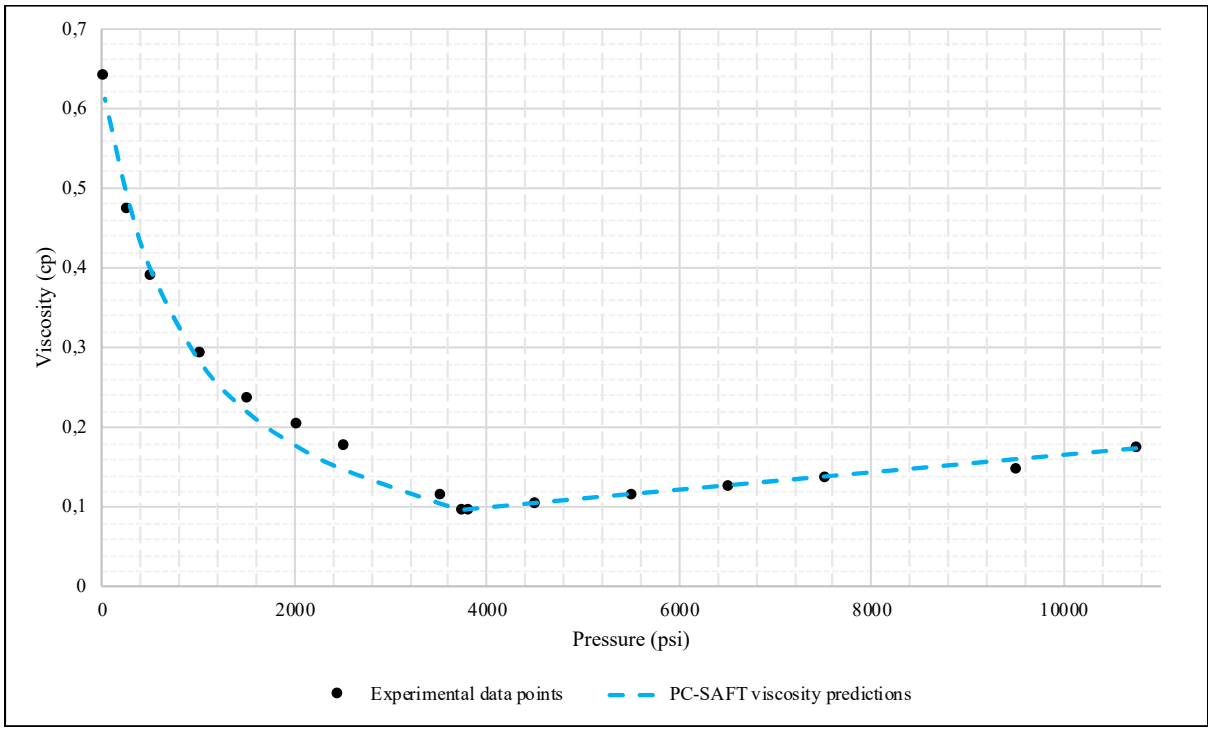

Figure 44 - Viscosity predictions for Crude "D"

The results indicate MAPE of 5.445% across all data points. The region with the most significant deviation from the experimental data is four points below the bubble point pressure. Regularly, only one point will be required to fit the model to obtain the parameter K_c. However, all crudes that were modelled in the literature [95] was sulfurless (or with a very little H_2S content). Crude "D", on the contrary, has a significant H_2S content of about 13 mol %. Because of this, η_a and η_r parameter values for H_2S were not found in the literature, and the model was fitted at three experimental data points – for K_c, $\eta_{a\,(H2S)}$ and $\eta_{r\,(H2S)}$.

Despite the acceptable results, more study is necessary for establishing the adequacy of the predictive capabilities of PC-SAFT for the crude oil dynamic viscosity predictions with high-sulfur crudes. The accuracy of the model significantly depends on the selected data points for the fitting, and three values of viscosities at different pressures can be not available. Furthermore, the accuracy of the model is not tested at changing temperature conditions due to the lack of experimental data.

5 CONCLUSIONS AND RECOMMENDATIONS

Three crude oils were used for the modelling of asphaltene phase equilibria using PC-SAFT Equation of State by applying two different methods of modelling. “SARA-based” method is existing in the literature and is widely used for the purpose of thermodynamic modelling of asphaltene phase behavior. This thesis suggested modifications aimed to improve computational efficiency and reduce the number of experimental data that is necessary for the modelling by the “SARA-based” method. The work is then compared the results of the modelling by both methods as well as the computational time necessary to execute modelling algorithms. Additionally, the ability of PC-SAFT EoS in the modelling of PVT parameters and dynamic viscosity of crude was evaluated. The accuracy of models was evaluated by calculating the MAPE between predicted and experimental data. The following conclusions were derived:

1. PC-SAFT EoS was able to accurately model AOPs at higher temperatures (MAPE of 2.99% for Crude “A”) but demonstrated the serious deviations from experimental data at lower temperatures (Crude “B” and “C”). Several studies in the literature have noted such kind of issues with PC-SAFT EoS, and the cause of this phenomena is the subject of ongoing discussions. BP predictions gave good accuracy in all cases.
2. The modified method demonstrated comparable results with the “SARA-based” method in modelling of AOPs.
3. The improvement of computational speed by the modified method was evaluated in terms of percentage decrease of CPU time in comparison with the “SARA-based” method. The time of performance of four different algorithms was recorded and compared. The results showed the improvement of computational efficiency (from 24% to 69% CPU time decrease) for all three crudes.
4. Density and viscosity predictions for Crude “D” gave acceptable results, with MAPE of 2.36% and 5.45% respectively. The work demonstrated the ability of PC-SAFT to model some other PVT parameters.

Overall, it was shown that the number of liquid pseudo-components could be decreased without compromising the modelling abilities and with a considerable increase in computational efficiency. The modified method can serve as a viable alternative when the full “SARA” analysis is not available. PC-SAFT was found to be able to give acceptable AOP modelling results even with one experimental data point fitting. However, due to the wide

ranges of parameters and MWs that can reproduce similar curves, it is imperative to have as much as possible AOP data for the model validation and/or correction for the accurate modelling of experimental results.

Several issues can be further investigated. The following recommendations are suggested for future studies:

1. The tendency of AOP curve to deviate upwards at lower temperatures can be further investigated. Some authors consider such deviations are a drawback of PC-SAFT EoS and made several attempts to modify the EoS itself [101] [99] or its crude oil characterization procedure [100]. On the other hand, the experimental procedures for the AOP determination are not perfect and can lack sufficient accuracy [100]. Crudes “B” and “C” can be remodeled according to the above-mentioned solutions to check their efficiency.
2. Development of accurate correlations for BIPs for asphaltene-crude oil systems will be the valuable modification of the PC-SAFT modelling procedure. Such improvements have the potential to greatly simplify the modelling process and, simultaneously, considerably increase its accuracy.
3. The procedure of the asphaltene EoS parameter estimation techniques can take a long time to perform and can be further improved. The method by Punnapala & Vargas [7] require performing search at wide range of MWs and aromaticity factors with a recommended step size of 25 g/mol and 0.005 respectively [5].
4. The modified method was not checked with the Asphaltenes parameter fit method from Punnapala & Vargas [7] by adjusting aromaticity and MW of Asphaltene pseudo-component.
5. Viscosity modelling procedure needs to be further examined for crudes with high sulfur content.

REFERENCES

[1] J. G. Speight, "Petroleum Asphaltenes - Part 1: Asphaltenes, Resins and the Structure of Petroleum," *Oil & Gas Science and Technology,* pp. 467-477, 2004.

[2] M. A. Kelland, Production Chemicals for the Oil and Gas Industry, New York: CRC Press: Taylor & Francis Group, 2014.

[3] D. C. Thomas , H. L. Becker and R. A. Del Real Soria, "Controlling Asphaltene Deposition in Oil Wells," *SPE Production & Facilities,* vol. 10, no. 02, 1995.

[4] K. Gharbi, K. Benyounes and M. Khodja, "Removal and prevention of asphaltene deposition during oil production: A literature review.," *Journal of Petroleum Science and Engineering,* vol. 158, pp. 351-360, 2017.

[5] F. M. Vargas and M. Tavakkoli, Ashpaltene Deposition: Fundamentals, Prediction, Prevention, and Remediation, CRC Press, Taylor & Francis Group, 2018.

[6] M. I. L. Abutaqiya, S. R. Panuganti and F. M. Vargas, "Efficient Algorithm for the Prediction of Pressure−Volume−Temperature Properties of Crude Oils Using the Perturbed-Chain Statistical Associating Fluid Theory Equation of State," *Industrial & Engineering Chemistry Research,* vol. 56, pp. 6088-6102, 2017.

[7] S. Punnapala and F. M. Vargas, "Revisiting the PC-SAFT characterization procedure for an improved asphaltene precipitation prediction," *Fuel,* vol. 108, pp. 417-429, 2013.

[8] L. Dominique and J.-F. Argillier, "Interfacial behavior of asphaltenes," *Advances in Colloid and Interface Science,* vol. 233, pp. 83-93, 2016.

[9] Energy Institute, "IP 143: Determination of asphaltenes (heptane insolubles) in crude petroleum and petroleum products". REF/ISBN: IP143-2939444.

[10] A. A. El-Bassoussi, M. H. M. Ahmed, S. M. El Sayed, J. S. Basta and E.-S. K. Attia, "Characterization of Some Local Petroleum Residues by Spectroscopic Techniques," *Petroleum Science and Technology,* vol. 28, no. 5 , pp. 430-444, 2010.

[11] M. A. Fahim, T. A. Al-Sahhaf and A. S. Elkilani, "Prediction of Asphaltene Precipitation for Kuwaiti Crude Using Thermodynamic Micellization Model," *Industrial & Engineering Chemistry Research,* vol. 40, no. 12, pp. 2748-2756, 2001.

[12] K. J. Leontaritis and G. A. Mansoori , "Asphaltene Flocculation During Oil Production and Processing: A Thermodynamic Colloidal Model," in *SPE International Symposium on Oilfield Chemistry*, San Antonio, Texas , 1987 .

[13] K. J. Leontaritis and G. Mansoori, "Fast crude-oil heavy-component characterization using combination of ASTM, HPLC, and GPC methods," *Journal of Petroleum Science and Engineering,* vol. 2, no. 1, pp. 1-12, 1989.

[14] G. Andreatta, C. C. Goncalves, G. Buffin, N. Bostrom, C. M. Quintella, F. Arteaga-Larios, E. Perez and O. C. Mullins, "Nanoaggregates and Structure-Function Relations in Asphaltenes," *Energy & Fuels,* vol. 19, pp. 1282-1289, 2005.

[15] O. C. Mullins, S. S. Betancourt, E. M. Cribbs, F. X. Dubost, J. L. Creek, A. B. Andrews and L. Venkataramanan, "The Colloidal Structure of Crude Oil and the Structure of Oil Reservoirs," *Energy & Fuels,* vol. 21, pp. 2785-2794, 2007.

[16] K. S. Pedersen, P. L. Christensen and J. A. Shaikh, Phase Behavior of Petroleum Reservoir Fluids, New York: CRC Press: Taylor & Francis Group, 2014.

[17] D. M. Barrera, D. P. Ortiz and H. W. Yarranton, "Molecular Weight and Density Distributions of Asphaltenes from Crude Oils," *Energy & Fuels,* vol. 27, no. 5, pp. 2474-2487, 2013.

[18] E. Ghloum, "Effect of inhibitors on asphaltene precipitation for Marrat Kuwaiti reservoirs," *Journal of End-to-End-testing,* vol. 36, no. 8, pp. 827-835, 2010.

[19] S. Fakher, M. Ahdaya, M. Elturki and A. Imqam, "Critical review of asphaltene properties and factors impacting its stability in crude oil," *Journal of Petroleum Exploration and Production Technology,* 2019.

[20] O. C. Mullins, "The Modified Yen Model," *Energy & Fuels ,* vol. 24, pp. 2179-2207, 2010.

[21] O. C. Mullins , "The Asphaltenes," *Annual Review of Analytical Chemistry,* 2011.

[22] O. C. Mullins and E. Y. Sheu, Eds., Structures and Dynamics of Asphaltenes, New York : Springer Science+Business Media, LLC, 1998.

[23] M. Mousavi, T. Abdollahi, F. Pahlavan and E. H. Fini, "The influence of asphaltene-resin molecular interactions on the colloidal stability of crude oil," *Fuel,* vol. 183, pp. 262-271, 2016.

[24] B. Zhao and J. M. Shaw, "Composition and Size Distribution of Coherent Nanostructures in Athabasca Bitumen and Maya Crude Oil," *Energy & Fuels,* vol. 21, pp. 2795-2804, 2007.

[25] D. Ting, "Thermodynamic Stability and Phase Behavior of Asphaltenes in Oil and of Other Highly Asymmetric Mixtures - PhD Thesis," *Rice University ,* 2003.

[26] M. Tavakkoli, A. Chen and F. M. Vargas, "Rethinking the modeling approach for asphaltene precipitation using the PC-SAFT Equation of State," *Fluid Phase Equilibria,* vol. 416, pp. 120-129, 2016.

[27] Z. Novosad and T. G. Costain, "Experimental and Modeling Studies of Asphaltene Equilibria for a Reservoir Under CO2 Injection," in *SPE 65th Annual Technical Conference and Exhibition*, New Orleans, 1990.

[28] K. J. Leontaritis and G. Mansoori, "Asphaltene deposition: a survey of field experiences and research approaches," *Journal of Petroleum Science and Engineering,* vol. 1, pp. 229-239, 1988.

[29] S. L. Kokal and G. S. Sayegh, "Asphaltenes: The Cholesterol of Petroleum," in *SPE Middle East Oil Show* , Bahrain, 1995.

[30] A. K. Jamaluddin , N. Joshi, F. Iwere and O. Gurpinar, "An Investigation of Asphaltene Instability Under Nitrogen Injection," in *SPE International Petroleum Conference and Exhibition* , Villahermosa, Mexico , 2002.

[31] S. Negahban, J. N. M. Bahamaish, N. Joshi , J. Nighswander and A. K. M. Jamaluddin, "An Experimental Study at an Abu Dhabi Reservoir of Asphaltene Precipitation Caused by Gas Injection," *SPE Production & Facilities,* vol. 20, no. 2, 2005.

[32] P. Zanganeh, S. Ayatollahi, A. Alamdari, A. Zolghadr, H. Dashti and S. Kord, "Asphaltene Deposition during CO2 Injection and Pressure Depletion: A Visual Study," *Energy & Fuels ,* vol. 26, pp. 1412-1419, 2011.

[33] A. Kalantari-Dahaghi, V. Gholami, J. Moghadasi and R. Abdi, "Formation Damage Through Asphaltene Precipitation Resulting From CO2 Gas Injection in Iranian Carbonate Reservoirs," *SPE Production & Operations,* vol. 23, no. 02, 2008.

[34] S. Soroush, P. Pourafshary and M. Vafaie-Sefti, "A Comparison of Asphaltene Deposition in Miscible and Immiscible Carbon Dioxide Flooding in Porous Media," in *SPE EOR Conference at Oil and Gas West Asia* , Muscat, Oman , 2014.

[35] H. K. Sarma, "Can We Ignore Asphaltene in a Gas Injection Project for Light-Oils?," in *SPE International Improved Oil Recovery Conference in Asia Pacific* , Kuala Lumpur , 2003.

[36] L. C. C. Marques, J. B. Monteiro and G. Gonza´lez, "Asphaltenes Flocculation in Light Crude Oils: A Chemical Approach to the Problem," *Journal of Dispersion Science and Technology,* vol. 28, pp. 391-397, 2007.

[37] S. R. Panuganti, M. Tavakkoli, F. M. Vargas, D. L. Gonzalez and W. G. Chapman, "SAFT model for upstream asphaltene applications," *Fluid Phase Equilibria,* vol. 359, pp. 2-16, 2013.

[38] C. E. Haskett and M. Tartera, "A Practical Solution to the Problem of Asphaltene Deposits-Hassi Messaoud Field, Algeria," *Journal of Petroleum Technology,* vol. 17, no. 04, 1965.

[39] V. A. Branco, G. Mansoori, L. C. Xavier, S. J. Park and H. Manafi, "Asphaltene flocculation and collapse from petroleum fluids.," *Journal of Petroleum Science and Engineering,* vol. 32, no. 2-4, pp. 217-230, 2001.

[40] J. F. Yanes, F. X. Feitosa, F. R. Carmo and H. B. Sant'Ana, "Paraffin effects on the stability and precipitation of crude oil asphaltenes: Experimental onset determination and phase behavior approach.," *Fluid Phase Equilibria,* vol. 474, pp. 116-125, 2018.

[41] J. L. Creek, "Freedom of Action in the State of Asphaltenes: Escape from Conventional Wisdom," *Energy & Fuels,* vol. 19, pp. 1212-1224, 2005.

[42] R. Kaminsky and C. Radke, "Asphaltenes, Water Films, and Wettability Reversal," *SPE Journal,* vol. 2, no. 04, pp. 485-493, 1997.

[43] G. Piro, L. Canonico, G. Galbariggi, L. Bertero and C. Carniani, "Asphaltene Adsorption Onto Formation Rock: An Approach to Asphaltene Formation Damage Prevention," *SPE Production & Facilities,* vol. 11, no. 03, pp. 156-160, 1996.

[44] S. A. Shedid and A. Y. Zekri, "Formation Damage Caused By Simultaneous Sulfur and Asphaltene Deposition," *SPE Productions & Operations,* vol. 21, no. 01, 2006.

[45] M. Madhi, R. Kharrat and T. Harmoule , "Screening of inhibitors for remediation of asphaltene deposits: Experimental and modeling study. ," *Petroleum,* vol. 4, no. 2, pp. 168-177, 2018.

[46] A. S. Al-Ghazi and J. Lawson, "Asphaltene Cleanout Using VibraBlaster Tool," in *SPE Saudi Aramco Section Technical Symposium* , Dhahran, Saudi Arabia , 2007.

[47] R. Thawer, D. C. A. Nicoli and G. Dick, "Asphaltene Deposition in Production Facilities," *SPE Production Engineering,* vol. 5, no. 04, 1990.

[48] A. I. Victorov and A. Firoozabadi , "Thermodynamic Micellization Model of Asphaltene Precipitation from Petroleum Fluids," *AIChE Journal ,* vol. 42, no. 6, 1996.

[49] H. Pan and A. Firoozabadi, "Thermodynamic Micellization Model for Asphaltene Precipitation From Reservoir Crudes at High Pressures and Temperatures," *SPE Production & Facilities,* vol. 15, no. 01, 2000.

[50] T. A. Al-Sahhaf, M. A. Fahim and A. S. Elkilani, "Retardation of asphaltene precipitation by addition of toluene, resins, deasphalted oil and surfactants," *Fluid Phase Equilibria,* Vols. 194-197, pp. 1045-1057, 2002.

[51] W. G. Chapman, K. E. Gubbins, G. Jackson and M. Radosz, "New Reference Equation of State for Associating Liquids," *Industrial & Engineering Chemistry Research,* vol. 29, no. 8, pp. 1709-1721, 1990.

[52] W. G. Chapman, G. Jackson and K. E. Gubbins, "Phase equilibria of associating fluids," *Molecular Physics: An International Journal at the Interface Between Chemistry and Physics,* vol. 65, no. 5, pp. 1057-1079, 1988.

[53] W. G. Chapman, K. E. Gubbins, G. Jackson and M. Radosz, "SAFT: Equation-of-State Solution Model for Associating Fluids," *Fluid Phase Equilibria,* vol. 52, pp. 31-38, 1989.

[54] E. A. Müller and K. E. Gubbins, "Molecular-Based Equations of State for Associating Fluids: A Review of SAFT and Related Approaches," *Industrial & Engineering Chemistry Research,* vol. 40, pp. 2193-2211, 2001.

[55] N. F. Carnahan and K. E. Starling, "Equation of State for Nonattracting Rigid Spheres," *The Journal of Chemical Physics,* vol. 51, no. 2, pp. 635-636, 1969.

[56] R. L. Cotterman, B. J. Schwarz and J. M. Prausnitz, "Molecular Thermodynamics for Fluids at Low and High Densities," *AICHE Journal,* vol. 32, no. 11, pp. 1787-1798, 1986.

[57] G. Jackson, W. G. Chapman and K. E. Gubbins, "Phase equilibria of associating fluids," *Molecular Physics: An International Journal at the Interface Between Chemistry and Physics,* vol. 65, no. 1, pp. 1-31, 1988.

[58] A. Gil-Villegas, A. Galindo, P. J. Whitehead, S. J. Mills, G. Jackson and A. N. Burgess, "Statistical associating fluid theory for chain molecules with attractive potentials of variable range," *The Journal of Chemical Physics,* vol. 106, no. 10, p. 4168, 1997.

[59] J. A. Barker and D. Henderson, "Perturbation Theory and Equation of State for Fluids. II. A Successful Theory of Liquids," *The Journal of Chemical Physics,* vol. 47, p. 4714, 1967.

[60] E. A. Müller, K. E. Gubbins, D. M. Tsangaris and J. J. de Pablo, "Comment on the accuracy of Wertheim's theory of associating fluids," *The Journal of Chemical Physics,* vol. 103, no. 3, pp. 3668-3869, 1995.

[61] F. M. Vargas, M. Garcia-Bermudes, M. Boggara, S. Punnapala, M. Abutaquiya, N. Mathew, S. Prasad, A. Khaleel, M. Al Rashed and H. Al Asafen, "On the Development of an Enhanced Method to Predict Asphaltene Precipitation," *SPE Offshore Technology Conference,* 2014.

[62] J. Gross and G. Sadowski, "An Equation of State Based on a Perturbation Theory for Chain Molecules.," *Industrial & Engineering Chemistry Research, 40(4),* p. 1244–1260, 2001.

[63] G. A. Mansoori, N. F. Carnahan, K. E. Starling and T. W. Leland, "Equilibrium Thermodynamic Properties of the Mixture of Hard Spheres," *The Journal of Chemical Physics ,* vol. 54, no. 4, pp. 1523-1525, 1971.

[64] T. Boublík, "Hard-Sphere Equation of State," *The Journal of Chamical Physics,* vol. 53, pp. 471-472, 1970.

[65] S. S. Chen and A. Kreglewski, "pplications of the Augmented van der Waals Theory of Fluids. I. Pure Fluids," *Berichte der Bunsengesellschaft für physikalische Chemie,* vol. 81, no. 10, pp. 1048-1052, 1977.

[66] L. Yelash, M. Müller, W. Paul and K. Binder, "A global investigation of phase equilibria sing the perturbed-chain statistical associating-fluid-theory approach," *The Journal of Chemical Chemistry,* vol. 123, no. 1, 2005.

[67] D. Ting, G. J. Hirasaki and W. G. Chapman, "Modeling of Asphaltene Phase Behavior with the SAFT Equation of State," *Petroleum Science and Technology,* vol. 21, no. 3-4, pp. 647-661, 2003.

[68] D. L. Gonzalez, D. Ting, G. J. Hirasaki and W. G. Chapman, "Prediction of Asphaltene Instability under Gas Injection," *Energy & Fuels,* vol. 19, pp. 1230-1234, 2005.

[69] D. L. Gonzalez, F. M. Vargas, G. J. Hirasaki and W. G. Chapman, "Modeling Study of CO2-Induced Asphaltene Precipitation," *Energy & Fuels,* vol. 22, pp. 757-762, 2008.

[70] D. L. Gonzalez, G. J. Hirasaki, J. Creek and W. G. Chapman, "Modeling of Asphaltene Precipitation Due to Changes in Composition Using the Perturbed Chain Statistical Associating Fluid Theory Equation of State," *Energy & Fuels,* vol. 21, pp. 1231-1242, 2007.

[71] D. L. Gonzalez, "Modeling of Asphaltene Precipitation and Deposition Tendency using the PC-SAFT Equation of State," *PhD Thesis,* 2008.

[72] X. Zhang , N. Pedrosa and T. Moorwood, "Modeling Asphaltene Phase Behavior: Comparison of Methods for Flow Assurance Studies," *Energy & Fuels ,* vol. 26, p. 2611−2620, 2011.

[73] F. Garcia-Sánchez, G. Eliosa-Jiménez, G. Silva-Oliver and R. Vázquez-Román, "Vapor–liquid equilibria of nitrogen–hydrocarbon systems using the PC-SAFT equation of state," *Fluid Phase Equilibria ,* vol. 217 , p. 241–253, 2004.

[74] M. Yarrison and W. G. Chapman, "A systematic study of methanol + n-alkane vapor–liquid and liquid–liquid equilibria using the CK-SAFT and PC-SAFT equations of state," *Fluid Phase Equilibria,* vol. 226, pp. 195-205, 2004.

[75] M. Ma, S. Chen and J. Abedi, "Binary interaction coefficients of asymmetric CH4, C2H6, and CO2 with high n-alkanes for the simplified PC-SAFT correlation and prediction," *Fluid Phase Equilibria,* vol. 405, pp. 114-123 , 2015.

[76] M. Stavrou, A. Bardow and J. Gross, "Estimation of the binary interaction parameter kij of the PC-SAFT Equation of State based on pure component parameters using a QSPR method," *Fluid Phase Equilibria,* vol. 416, pp. 138-149 , 2016.

[77] A. Fateme , Z. Abbasi and R. B. Boozarjomehry, "Estimation of PC-SAFT binary interaction coefficient by artificial neural network for multicomponent phase equilibrium calculations," *Fluid Phase Equilibria,* vol. 510, 2020.

[78] O. Redlich and J. N. S. Kwong, "On the Thermodynamics of Solutions. V. An Equation of State. Fugacities of Gaseous Solutions.," *Chemical Reviews,* vol. 44 , no. 1, pp. 233-244, 1949.

[79] G. Soave, "Equilibrium constants from a modified Redkh-Kwong equation of state," *Chemical Engineering Science,* vol. 27, pp. 1197-1203, 1972.

[80] D.-Y. Peng and D. B. Robinson, "A New Two-Constant Equation of State," *Industrial & Engineering Chemistry Fundamentals,* vol. 15, no. 1 , pp. 59-64, 1976.

[81] A. Péneloux , E. Rauzy and R. Fréze, "A consistent correction for Redlich-Kwong-Soave volumes," *Fluid Phase Equilibria,* vol. 8, no. 1 , pp. 7-23, 1982.

[82] S. R. Panuganti, F. M. Vargas, D. L. Gonzalez, A. S. Kurup and W. G. Chapman, "PC-SAFT characterization of crude oils and modeling of asphaltene phase behavior," *Fuel,* vol. 93, pp. 658-669, 2012.

[83] Y. H. Dehaghani, M. Assareh and F. Feyzi, "Asphaltene precipitation modeling with PR and PC-SAFT equations of state based on normal alkanes titration data in a Multisolid approach," *Fluid Phase Equilibria,* vol. 420, pp. 212-220, 2018.

[84] G. M. Kontogeorgis, E. C. Voutsas, I. V. Yakoumis and D. P. Tassios, "An Equation of State for Associating Fluids," *Industrial & Engineering Chemistry Research,* vol. 35, no. 11, pp. 4310-4318, 1996.

[85] D. Ting, G. J. Hirasaki and W. G. Chapman, "Modeling of Asphaltene Phase Behavior with the SAFT Equation of State," *Petroleum Science and Technology,* vol. 21, pp. 647-661, 2003.

[86] A. A. AlHammadi, F. M. Vargas and W. G. Chapman, "Comparison of Cubic-Plus-Association and Perturbed-Chain Statistical Associating Fluid Theory Methods for Modeling Asphaltene Phase Behavior and Pressure−Volume−Temperature Properties," *Energy & Fuels,* vol. 29, no. 5, pp. 2864-2875, 2015 .

[87] S. R. Panuganti , M. Tavakkoli, F. M. Vargas, D. L. Gonzalez and W. G. Chapman, "SAFT model for upstream asphaltene applications," *Fluid Phase Equilibria,* vol. 359, pp. 2-16, 2013.

[88] A. Arya, X. Liang, N. von Solms and G. M. Kontogeorgis, "Modeling of Asphaltene Onset Precipitation Conditions with Cubic Plus Association (CPA) and Perturbed Chain Statistical Associating Fluid Theory (PC-SAFT) Equations of State," *Energy & Fuels ,* vol. 30 , p. 6835−6852, 2016.

[89] M. Tavakkoli, A. Chen and F. M. Vargas, "Rethinking the modeling approach for asphaltene precipitation using the PC-SAFT Equation of State," *Fluid Phase Equilibria,* vol. 416, pp. 120-129, 2016.

[90] D. L. Katz and A. Firoozabadi, "Predicting Phase Behavior of Condensate/Crude-Oil Systems Using Methane Interaction Coefficients," *Journal of Petroleum Technology,* vol. 30, no. 11, pp. 1649-1655, 1978.

[91] C. H. Whitson, "Characterizing Hydrocarbon Plus Fractions," *Society of Petroleum Engineers Journal,* vol. 23, no. 04, pp. 683-694, 1983.

[92] M. A. Zúniga-Hinojosa, D. N. Justo-García, M. A. Aquino-Olivos, L. A. Román-Ramírez and F. García-Sánchez, "Modeling of asphaltene precipitation from n-alkane diluted heavy oilsand bitumens using the PC-SAFT equation of state," *Fluid Phase Equilibria,* vol. 376, pp. 210-224, 2014.

[93] G. A. Wilson, "A modified Redlich-Kwong EOS. Application physical data calculation.," in *American Institute of Chemical Engineers 65th National Meeting, Paper No. 15C*, Clevelend, OH, 1968.

[94] O. Sabbagh, "M.Sc. Thesis," Calgary, AB, Canada, University of Calgary, 2004.

[95] M. I. Abutaqiya, J. Zhang and F. M. Vargas, "Viscosity modeling of reservoir fluids using the Friction Theory with PC-SAFT crude oil characterization," *Fuel,* vol. 235, p. 113–129, 2019.

[96] S. E. Quiñones-Cisneros, C. K. Zéberg-Mikkelsen, J. Fernández and J. García, "General Friction Theory Viscosity Model for the PC-SAFT Equation of State," *AIChE Journal,* vol. 52, no. 4, p. 1600–1610, 2006.

[97] T. H. Chung , M. Ajlan and L. L. LeeKenneth , "Generalized multiparameter correlation for nonpolar and polar fluid transport properties," *Industrial & Engineering Chemistry Research,* vol. 27, no. 4, pp. 671-679, 1988.

[98] M. Sullivan, E. J. Smythe , S. Fukagawa, C. Harrison, H. Dumont and C. Borman, "A Fast Measurement of Asphaltene Onset Pressure," *SPE Reservoir Evaluation & Engineering,* 2020.

[99] M. I. Abutaqiya, C. J. Sisco and F. M. Vargas, "A Linear Extrapolation of Normalized Cohesive Energy (LENCE) for fast and accurate prediction of the asphaltene onset pressure," *Fluid Phase Equilibria,* vol. 483, pp. 52-69, 2019.

[100] A. A. AlHammadi and A. M. AlBlooshi, "Role of Characterization in the Accuracy of PC-SAFT Equation of State Modeling of Asphaltenes Phase Behavior," *Industrial & Engineering Chemistry Research,* vol. 58, p. 18345−18354, 2019.

[101] W. A. Cañas-Marín, D. L. Gonzalez and B. A. Hoyos, "A theoretically modified PC-SAFT equation of state for predicting asphaltene onset pressures at low temperatures," *Fluid Phase Equilibria,* vol. 495, pp. 1-11, 2019.

[102] H. Zhao, P. Morgado, A. Gil-Villegas and C. McCabe, "Predicting the Phase Behavior of Nitrogen + n-Alkanes for Enhanced Oil Recovery from the SAFT-VR Approach: Examining the Effect of the Quadrupole Moment," *The Journal of Physical Chemistry B,* vol. 110, no. 47, pp. 24083-24092, 2006.

[103] F. M. Vargas, D. L. Gonzalez, G. J. Hirasaki and W. G. Chapman, "Modeling Asphaltene Phase Behavior in Crude Oil Systems Using the Perturbed Chain Form of the Statistical

Associating Fluid Theory (PC-SAFT) Equation of State," *Energy & Fuels,* vol. 23, pp. 1140-1146, 2009.

[104] F. M. Vargas, D. L. Gonzalez, J. L. Creek, J. Wang, J. Buckley, G. J. Hirasaki and W. G. Chapman, "Development of a General Method for Modeling Asphaltene Stability," *Energy & Fuels,* vol. 23, pp. 1147-1154, 2009.